catalysts

MDPI

Review

Metal-Catalysed A^3 Coupling Methodologies: Classification and Visualisation

Jonathan Farhi [1], Ioannis N. Lykakis [2] and George E. Kostakis [1,*]

[1] Department of Chemistry, School of Life Sciences, University of Sussex, Brighton BN1 9QJ, UK; jonathan.farhi@emory.edu
[2] Department of Chemistry, Aristotle University of Thessaloniki, University Campus, 54124 Thessaloniki, Greece; lykakis@chem.auth.gr
* Correspondence: g.kostakis@sussex.ac.uk

Abstract: The multicomponent reaction of aldehydes, amines, and alkynes, known as A^3 coupling, yields propargylamines, a valuable organic scaffold, and has received significant interest and attention in the last years. In order to fully realise the potential of the metal-based catalytic protocols that facilitate this transformation, we summarise substrates, in situ and well-characterised synthetic methods that provide this scaffold and attempt a monumental classification considering several variables (Metal, Coordinating atom(s), Ligand type and name, in-situ or well-characterised, co-catalyst, catalyst and ligand Loading (mol%), solvent, volume, atmosphere, temperature, microwave, time, yield, selectivity (e.e. d.r.), substrate name, functionality, loading (amines, aldehydes, alkynes), and use of molecular sieves). This pioneering work creates a valuable database that contains 2376 entries and allows us to produce graphs and better visualise their impact on the reaction.

Keywords: A^3 coupling; catalysis; multicomponent reaction; propargylamines; amines; alkynes; synthetic methodologies

check for updates

Citation: Farhi, J.; Lykakis, I.N.; Kostakis, G.E. Metal-Catalysed A^3 Coupling Methodologies: Classification and Visualisation. *Catalysts* **2022**, *12*, 660. https://doi.org/10.3390/catal12060660

Academic Editors: Antonia Iazzetti and Alessia Ciogli

Received: 19 May 2022
Accepted: 5 June 2022
Published: 15 June 2022

Publisher's Note: MDPI stays neutral with regard to jurisdictional claims in published maps and institutional affiliations.

Copyright: © 2022 by the authors. Licensee MDPI, Basel, Switzerland. This article is an open access article distributed under the terms and conditions of the Creative Commons Attribution (CC BY) license (https://creativecommons.org/licenses/by/4.0/).

1. Introduction

Creating molecular complexity from readily available starting materials and catalysts is a long-standing and ongoing goal for synthetic chemists [1]. Synthetic methodologies that use more than two substrates and a metal-based catalyst, a subcategory of the well-known multicomponent reactions, involve complicated, possibly domino, organic transformations and yield valuable organic scaffolds in one step. These methodologies are inexpensive, produce minimal waste, and are atom- and energy-efficient, all significant advantages over traditional catalytic industrial protocols. Moreover, many such industrial protocols employ fossil fuels and well-characterised but expensive catalysts—considering the pressing need to transition to "green" processes, a modular and selective polycomponent reaction starting from readily available material is highly desirable.

At present, the catalysts used in these reactions are most often generated in situ. These protocols have several disadvantages: high catalyst loadings (over 10 mol%) are required, the identity and role of the catalyst are vague, and reaction monitoring is inaccessible. Likewise, some protocols require elevated temperatures that may cause the formation of metal nanoparticles.

The reactivity, selectivity, and stability of traditional homogenous metal catalysts are all highly dependent on the ligand environment and the interplay between the metal, ligand(s), and reagents. Thus, ligand design is paramount when aiming to improve a catalyst's performance [2,3]. For example, the number and nature of the coordinating heteroatoms in a ligand affect rate and selectivity while the ligand's rigidity imposes regioselectivity [4]. It is unclear whether these principles apply to polycomponent reactions promoted by well-characterised species. Several studies on well-characterised catalysts, i.e., those in which the active species is known, suggest that these catalysts [5–13]:

1. Facilitate the organic transformations in low loadings (1% or less), almost an order of magnitude less than the in situ protocols; thus,
2. Exclude nanoparticle formation;
3. Give access to "clean" products and obviate the necessity for ICP-MS studies to trace metal elements;
4. Permit (pre-)catalyst and/or substrate monitoring, thus establishing a thorough mechanistic investigation; and
5. Most importantly, give access to meaningful trial experiments.

Trial experiments include:

- Addition of radical traps to identify or exclude radical paths;
- Variation of reaction conditions (O_2, or N_2/Ar atmosphere) to exclude the influence of atmospheric oxygen;
- Substrate alteration defines reaction incompetence and provides meaningful information to establish a reasonable catalytic cycle.

Compared to in situ based protocols, these significant advantages make evident the need to invest in multicomponent approaches catalysed by well-characterised compounds.

One multicomponent reaction is the A^3 coupling (Scheme 1), named for its three components: an aldehyde, an alkyne and an amine. This versatile reaction constitutes the most straightforward paradigm for a multicomponent reaction. It combines two unique catalytic concepts: C-H activation of the alkyne moiety and use or in situ formation of imines or enamines. Furthermore, the ideally chiral propargylamines (PA) formed by this reaction are essential precursors in organic synthesis for various products, including isoindolines [14], oxazolidines [15], pyridines [16,17], and alkaloids [18–20] (Scheme 2). Due to this importance, it is necessary to understand the catalyst's role and develop protocols to yield the final product in high enantiomeric excess. This review explores advances in the A^3 coupling using metal salts and in situ well-characterised compounds.

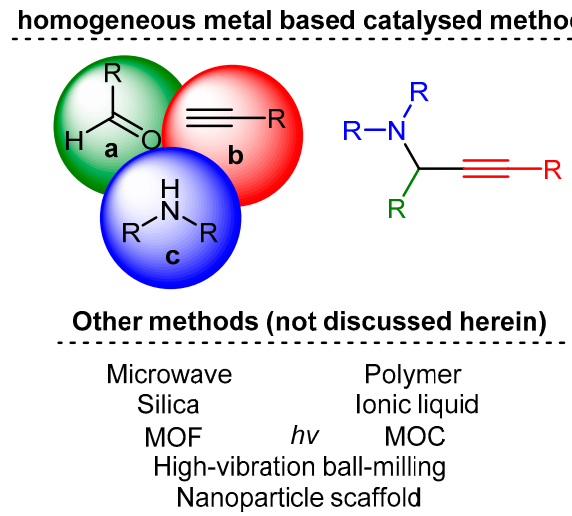

Scheme 1. The A^3 coupling reaction.

The C-H activation has gained significant interest and represents one of the eighth main research milestones [21–23]. Similarly, imines and enamines are essential components for several organic transformations and organic scaffolds of high interest [24–29]. The A^3 coupling reaction forms a new C-C σ bond via C-H activation of a terminal alkyne and yields PAs in one step with one water molecule as a by-product. Late transition metal catalysts effectively catalyse the A^3 reaction. Mechanistic studies have identified the in situ formation of a π complex between the metal salt and the triple bond of the alkyne component. This intermediate partly shifts electron density from the alkyne to the metal cation, weakening the C-H *sp* bond, thus allowing proton removal by a weak base. The deprotonation of the π complex results in σ activation and formation of the acetylide,

which can be subsequently added to the imine [30,31]. Initial reports on the A^3 coupling reaction demonstrated that the reaction could be catalysed by silver [32], gold [33], and copper [34] via a one-pot synthesis. Other studies demonstrated various metals, including cadmium [35], cobalt [36], iron [37], mercury [38], indium [39], manganese [35], nickel [40], tin [35], zirconium [41], and zinc [42–46] facilitate the A^3 coupling. These reactions often require an inert atmosphere, high temperatures, and long reaction times. Moreover, while several plausible reaction mechanisms have been proposed, in situ conditions make it difficult to analyse the catalytic mechanism effectively: for example, some hypotheses assume a monomeric active species [47–51], while others claim the active species is a paddlewheel dimer that would make the formation of a catalytic monomer difficult [20,52]. In contrast, other studies have suggested the existence of a dicopper catalyst instead of the monomeric species [53]. A more comprehensive understanding of the A^3 catalytic mechanism would facilitate asymmetric synthesis developments and advance other reactions involving alkyne activation via a metal catalyst.

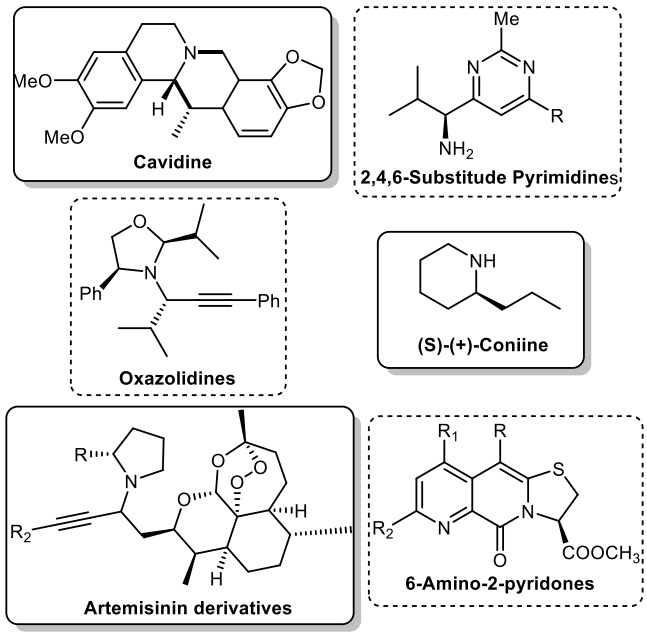

Scheme 2. Natural and building blocks synthesised from PAs.

Notably, PAs can be formed at elevated temperatures without a metal catalyst [54], whilst various other methodologies successfully yield PAs. Protocols that involve polymers [55–57], silica [58,59], metal-organic cages [60], metal-organic frameworks (MOFs) [61,62], high-vibration ball-milling [63], photoredox [64], ionic liquids [65], microwaves [48], and nanoparticles [66,67] have been reported. Recent studies have developed a library of organic ligands that can bind in situ with a metal salt to produce various PAs in high yields and enantiomeric excess. While the scope of these reactions may be limited to a specific subset of components such as aromatic amines, a clear trend has emerged regarding useful metal salts and ligands: remarkably, a copper salt and an atropoisomer with a high barrier to rotation [68]. These atropoisomeric co-catalysts often have several non-covalent stabilising interactions that activate the imine and metal acetylide, including π-stacking rings [20,52,68–71], hydrogen bonding [72], and a combination of hard-soft interactions [68,72].

Several reviews discuss the role of the metal salts and organic ligands [73–79] and address catalyst design parameters. These include operational stability and a partially saturated coordination environment fulfilled by ligands bearing two or three heteroatoms. Given the extensive interest, the reaction gained, and the population of the reported paradigms, this review aims to approach the A^3 reaction and these multi-component protocols with a different perspective. In this work, we attempt a monumental classification

of the reported protocols that discuss the A^3 coupling. This classification considers several variables (temperature, catalyst, loading, yield, *ee*, type of ligand, etc.) It contains 2376 entries, which allows us to produce two-dimensional graphs and better visualise each parameter's effect on the reaction. In short, this review achieves the following:

- Summarises substrates (Section 2) and methodologies that involve metal salts without (Section 3) and with (Section 4) ligands and well-characterised compounds (Section 5), reported until the first week of January 2021;
- Provides a database of 2376 entries with different variables: catalyst, coordinating atoms and type, ligand name, type and code, in situ or well-characterised, temperature, co-catalyst, catalyst loading, solvent, volume, atmosphere (open-air, N_2, O_2, Ar), temperature, time, yield, stereoselectivity, *ee* and dr values, name and type of amines, alkynes and aldehydes, and last, the use of molecular sieves. We have to note that this classification discards the laboratory's geographical information, which may impact reaction conditions. All these entries contain solely homogeneous catalysts, whereas reactions related to MOF, MCM, ball mill, and MW protocols are excluded from the list;
- Within the database, 634 (26%) entries correspond to well-characterised compounds and 1786 (74%) to in situ protocols, justifying the need for more data for the well-characterised;
- Classifies the ligands used in terms of their polydentate (bi-, tri-, etc.) and type of heteroatoms (N/N, O/N, P/N, N/N/N, etc.);
- Provides two-dimensional graphs (yield, *ee*, loading) and heatmaps to visualise their effect on yielding PAs and *ee*;
- Visualises the comparison of well-characterised and in situ based protocols;
- Concludes the findings, pros, and cons of this classification and visualisation.

To the best of our knowledge, the current classification is the first of its nature and may apply to other polycomponent reactions. In these reactions, the formation of the product is affected by several parameters; therefore, it is impossible to set rules and guides. We envisage that this type of classification, by simplifying variables comparison and visualisation, contributes to understanding the catalytic efficacy and mechanism, and the impact of the surrounding chemical environment created by ligand, metal, and solvent and other parameters.

2. Amines, Aldehydes and Alkynes

Our classification yielded 126 different amines, 120 different aldehydes, and 133 different alkynes The database with the classification (Supplementary Material) can be found online. The number of classified entries corresponds only to 0.12% of the almost two million possibilities (2,010,960). Aldehydes are mainly classified into aromatic (87 out 120) and aliphatic (31 out of 120), amines to primary aliphatic (14 out of 69) and aromatic (42 out of 69), secondary (52 out of 126), whilst alkynes to aromatic (73 out of 133) or aliphatic (58 out of 133). Notably, the alkyne group contains propiolic acid derivatives (19 substrates, entries 32–35, 61–65, 111–120) that in situ form the corresponding alkyne, with(out) a catalyst. All substrates were numbered based on the date of deposition of each article in our database; thus, the classification did not follow a chronological order (Scheme 3). We are aware that this classification may confuse the reader of this review since some substrates will not follow the appropriate numbering. However, our effort to improve this listing has not been successful because other variables should be taken into account and altered simultaneously; therefore, we decided to retain the current numbering. In addition, phenylacetylene (80%), piperidine (22%), and benzaldehyde (35%) are the most popular substrates

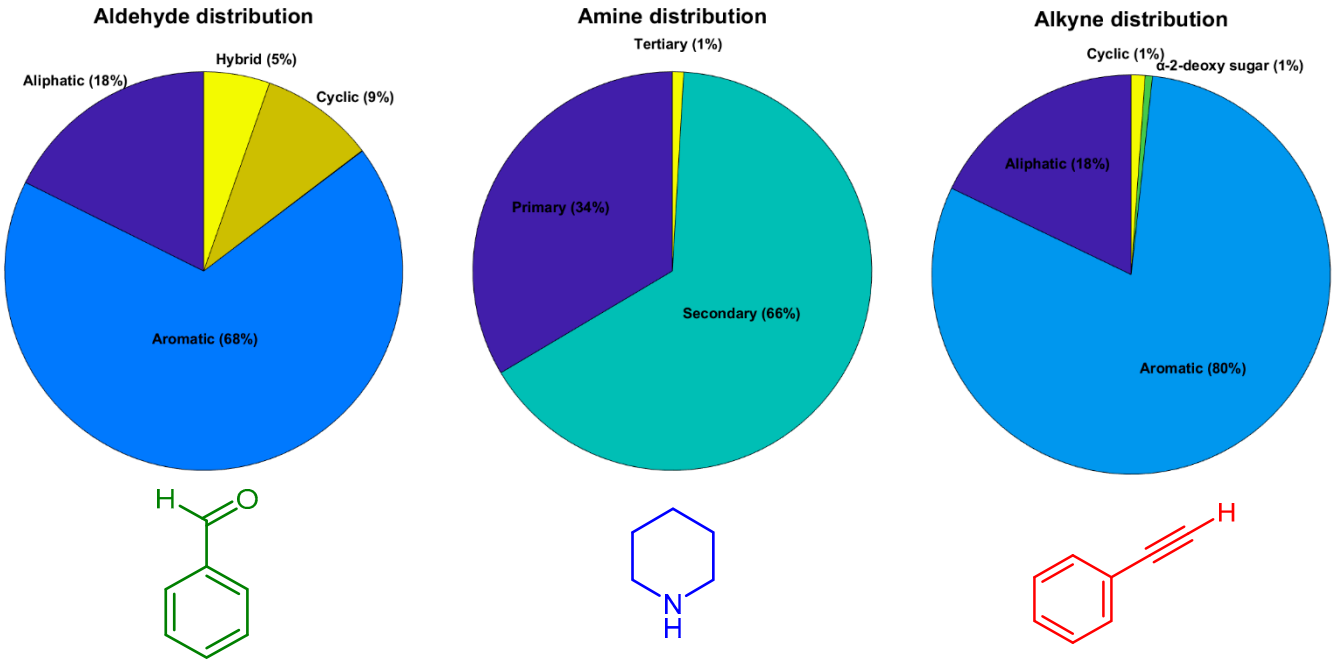

Scheme 3. (**upper**) Total distribution of aldehydes (**left**), amines (**middle**), and alkynes (**right**). (**lower**) The three most popular entries benzaldehyde (aldehydes, 35%, **left**), piperidine (amines, 22%, **middle**), and phenylacetylene (alkynes, 80%, **right**).

3. A^3 Coupling with Metal Salts

The initial investigations of the transition-metal catalysed A^3 coupling reaction to form PAs involved common metal salts such as copper, silver, and gold, with copper being the metal of choice due to its low cost.

3.1. Copper Salts

The initial investigations of the A^3 coupling reaction incorporated Cu(I) salts. In an initial study by Li [34], a combination of two different metal sources, CuBr and $RuCl_3$, was used to add phenylacetylene to an imine formed from aniline and aromatic or aliphatic aldehyde derivatives (Scheme 4). Notably, the reaction involved acetylide addition to an imine, a more challenging substrate than the more electronegative iminium made via secondary amines. To the best of our knowledge, this work remains one of the most efficient A^3 coupling protocols involving aniline.

Similarly, Iqbal and co-workers reported a procedure using solely CuCl to synthesise quinoline derivatives [80]. In the reported method, an aniline or other substituted arylamines (e.g., 4-methoxy aniline), aromatic aldehyde, and alkyne were sequentially added and reacted at 70 °C for up to 10 h, yielding a PA intermediate that subsequently cyclised into the functionalised quinoline product (Scheme 5). The proposed in situ generated Cu-acetylide intermediate reacts with the imine leading to the formation of the corresponding PA. After a propargyl–allenyl isomerisation cyclisation process, the desired quinoline derivative was formed under copper-catalysed conditions (mechanism not shown).

In the same year, CuBr was used to catalyse the addition of alkynes to enamines, producing Pas [52]. Various alkynes were used while the enamine substrate was kept relatively constant: secondary amine (dibenzylamine, diallylamine) and aliphatic aldehyde. Authors proposed that the enamine tautomerises to an iminium, which subsequently reacts with the activated alkyne (Scheme 6). It is worth noting that in the presence of *R*-(+)-Quinap (5.5 mol%) in toluene and at room temperature within 24 h, the corresponding enantiomeric PAs were synthesised in high yields and good to high enantiomeric excess, % *ee* (Scheme 6), these results will be discussed in detail in the related chapter.

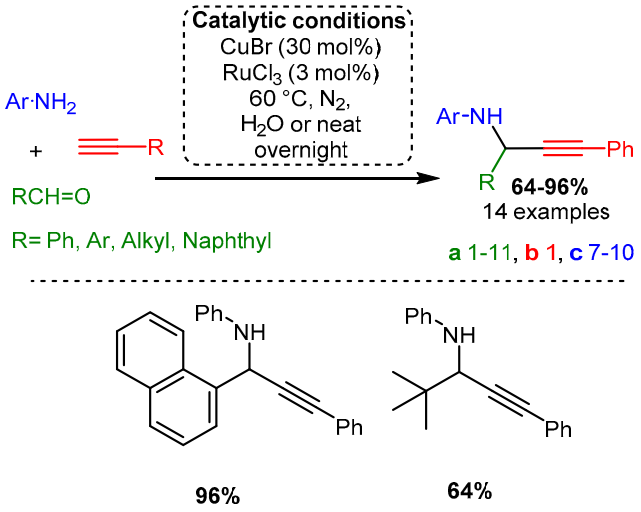

Scheme 4. (**Upper**): catalytic conditions and representative PAs with a range of yields and number of entries. (**Lower**): highest and lowest yielding PA. Coloured entries corresponding to the starting materials are provided whenever possible to facilitate correlation with the provided database. The following Schemes have a similar structure, and explanations will be provided if necessary.

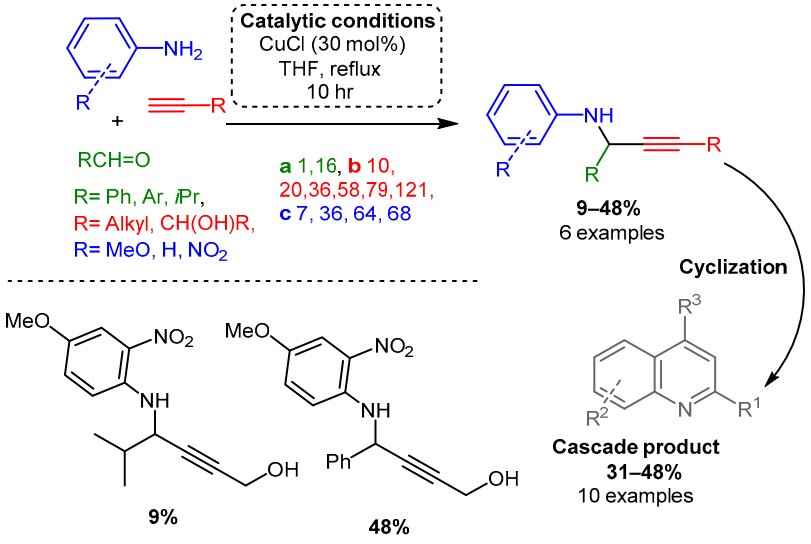

Scheme 5. Cyclisation cascade to form quinoline derivatives via PA intermediates.

The use of scaffolds containing secondary and tertiary amines were exploited to diastereoselectively synthesise PAs using a CuBr catalyst without an atropoisomer or other ligand [81]. High yields were achieved with aliphatic and aromatic alkynes and aldehydes. The proposed mechanism involved a diamine component complexing with the CuBr dimer to form a restrictive catalytic site, similar to the ligands discussed later in this review. In a later step, these PAs were converted to allenes using a CuI catalyst. Of note, the same substrates produced PAs with high yields and diasteromeric ratio (dr) when ZnI was incorporated under reflux conditions (Scheme 7).

Similarly, the combination of two different Cu(II) salts and amino alcohol as the amine component facilitated a cascade reaction that led to the formation of chiral oxazolidines [83]. In the optimised reaction, the combination of $CuBr_2$ and $CuCl_2$, each 10% loading, with the presence of the chiral plenylglycinol as the precursor and in solvent-free conditions, resulted in the target products in good yields (up to 90%) and excellent diastereomeric ratio (dr > 20/1) with a wide range of substrates (Scheme 9).

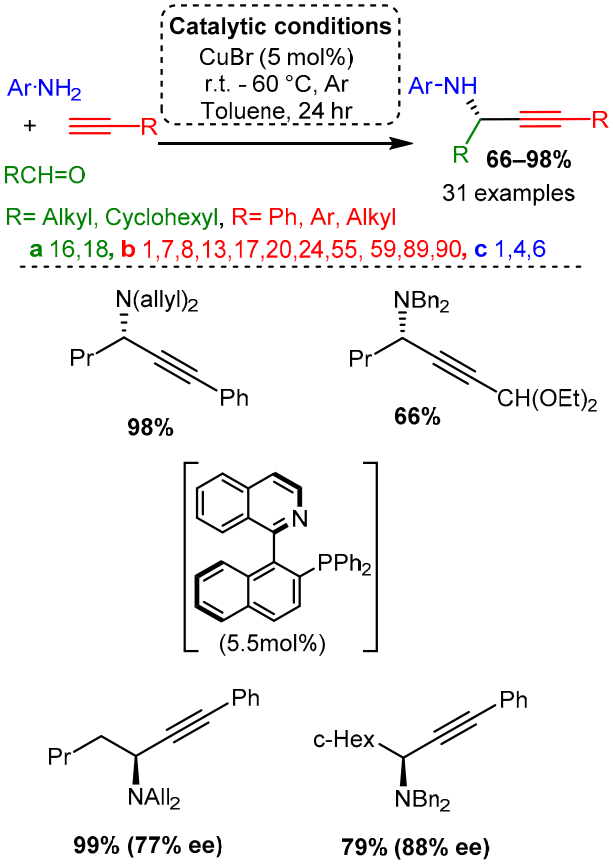

Scheme 6. PA access from premade enamines and synthesis of optically pure enantiomers.

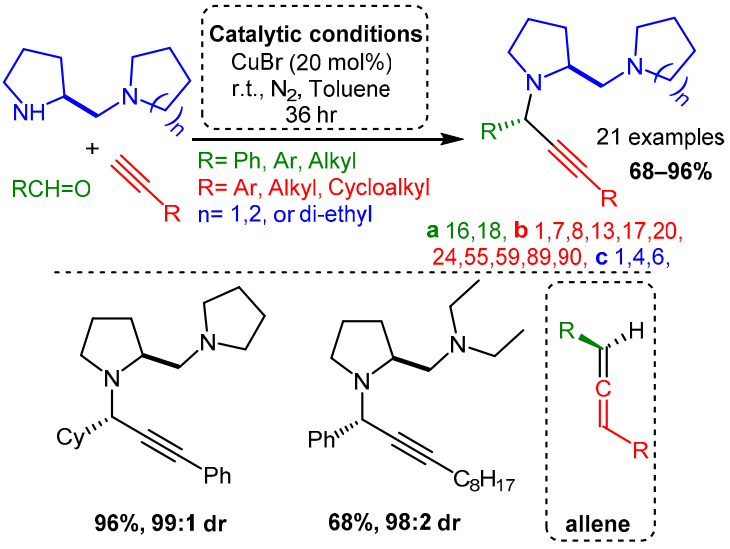

Scheme 7. Diastereoselective control of PA product using diamine substrates Post catalysis, the PAs could be converted to the corresponding allenes (bottom right).

The unique structural features of cyclic PAs incorporating scaffolds with two terminal amines and formaldehyde were exploited using a microwave-assisted CuCl catalyst in 1,4-dioxane to form functionalised, N-containing heterocycles [82]. While the substrates for this reaction were restricted due to the cyclisation cascade, the produced substituted heterocycles demonstrate the applicability of the A^3 coupling reaction, especially when considering the chemoselectivity of the unsymmetrical dialkynylation (Scheme 8).

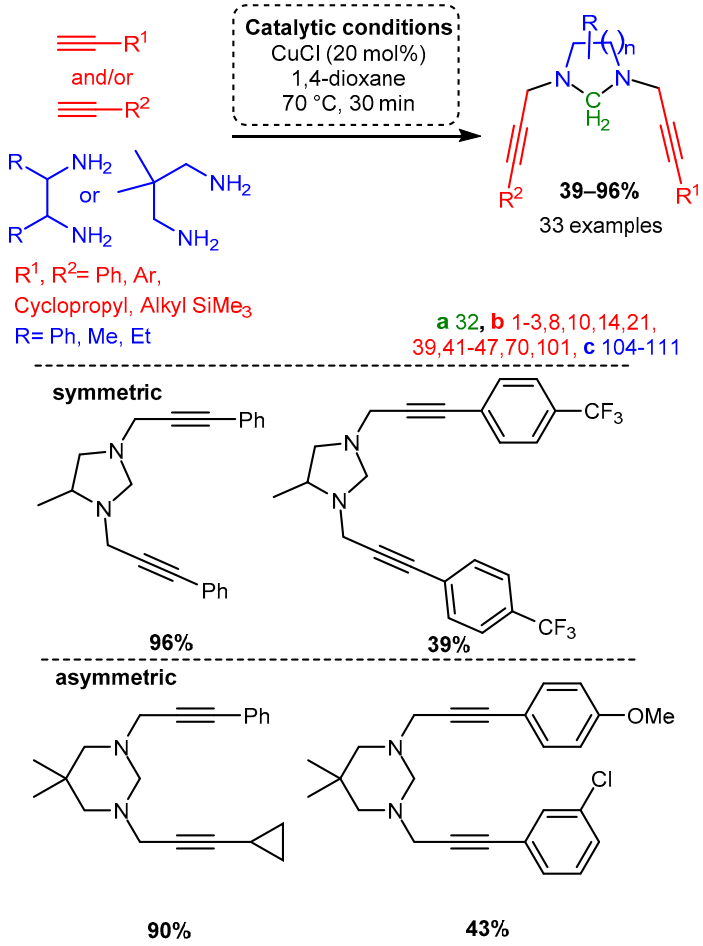

Scheme 8. Formation of cyclic divalent PAs from diamines with the appropriate component choice. Chemoselective alkynylation forms unsymmetrical products.

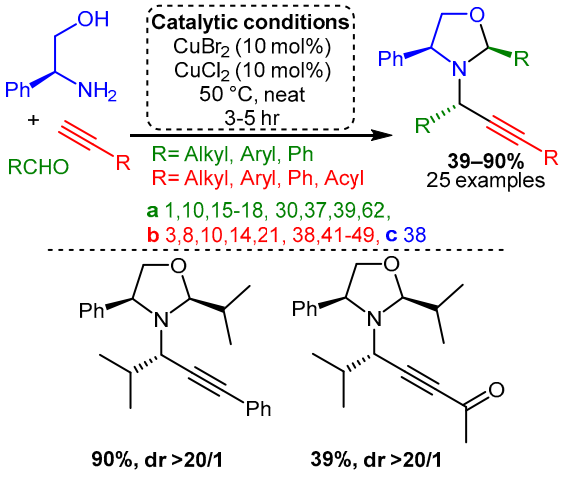

Scheme 9. Formation of monocyclic oxazolidines from chiral amino alcohols.

Dos Santos and co-workers demonstrated that different alkynols could be used as a substrate with a CuCl catalyst to produce the corresponding hydroxy-PAs. The resulting hydroxy-PAs were achieved in moderate to high yields and could be converted in subsequent steps to alkaloids under a simple reduction process and intramolecular cyclisation [18] (Scheme 10).

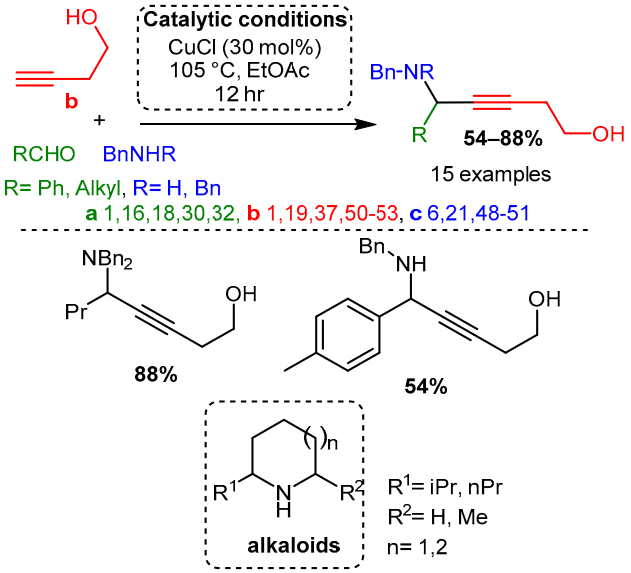

Scheme 10. A^3 coupling with alkynols and further formation of alkaloids after a reductive/cyclisation cascade reaction.

Similarly, the use of propynal derivatives with a CuI catalyst yields 3-amino-1,4-diynes [84]. Interestingly, when subjected to the A^3 coupling (propynal, amine, alkyne), asymmetric 3-amino-1,4-diynes were accessed in moderate to high yields (Scheme 11).

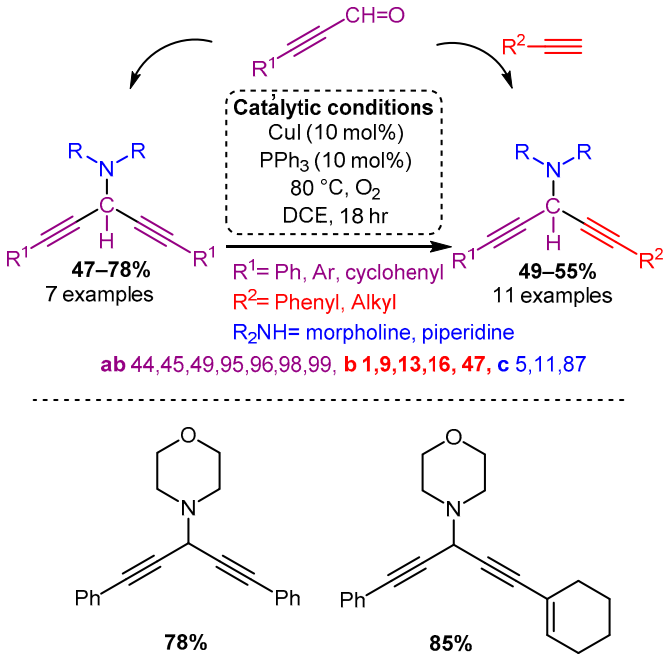

Scheme 11. The use of propargyl derivatives allows access to symmetric and asymmetric 3-amino-1,4-diynes.

Using propiolic acid and its derivatives, PAs can be formed following a decarboxylative coupling path. This variation of the A^3 coupling could be achieved at elevated temperatures without a metal-based catalyst but only when formaldehyde was incorporated as the aldehyde component [54] and with various aromatic and aliphatic aldehydes when CuI is involved as a catalyst [85] (Schemes 12 and 13).

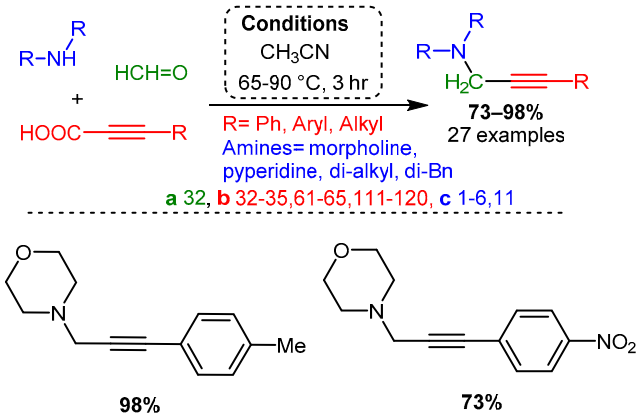

Scheme 12. The A^3 decarboxylative coupling without catalyst.

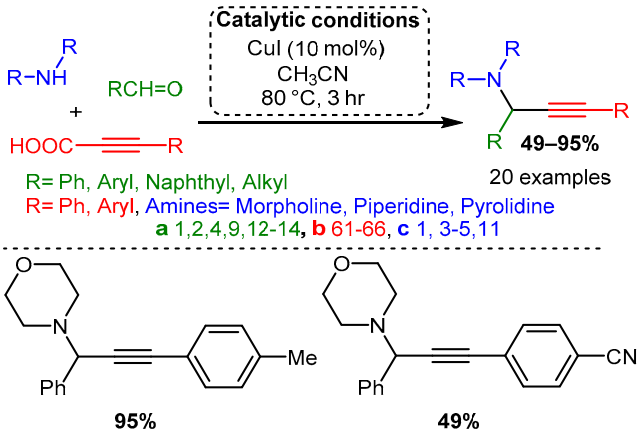

Scheme 13. The A^3 decarboxylative coupling in the presence of CuI.

The apparent advantage of this method is the increased stability of the alkynyl carboxylic acids. However, the applicability of this offshoot of the A^3 coupling still needs to be explored.

The Cu(I) salts presented thus far have catalysed the A^3 coupling reaction with various substrates. High yields have been achieved with more challenging substrates, such as primary amines and aliphatic alkynes, and creative choice of substrates has even allowed access to highly diastereoselective reactions. Nevertheless, many of these experiments are limited in scope; for example, the copper/ruthenium catalytic system presented by Li, while notable for its use of aniline derivates, limited the other substrates to phenylacetylene and aldehydes without α-hydrogens [83].

Many more recent studies have shifted attention to Cu(II) salts due to their ease of handling and lower costs, although their use without a chiral ligand has not been extensively explored. Larsen reported a $Cu(OTf)_2$ catalyst for the A^3 coupling of the electron-deficient (tosylated) nitrogen sources with alkyl, aryl, and heteroaryl aldehydes. This catalyst was able to catalyse the A^3 variant, the ketone–alkyne–amine coupling reaction (KA2), which substitutes a ketone for an aldehyde [86] (Scheme 14). While initial screenings used a pre-formed imine component, it was later found that the three-component, one-pot reaction provided a higher yield (63% vs. 79%) and at a rate 20 times faster (results not shown). This observation suggests that the reaction proceeds via imine protonation to form an iminium intermediate instead of imine-copper coordination. To gain insights into the identity and function of the catalyst, a mixed catalyst study was performed. The addition of Cu(I) salts, the assumed catalytic species, did not increase the rate while doubling the concentration of $Cu(OTf)_2$ doubled the reaction rate. These results cast doubt on the assumed Cu(I) active species and highlight the importance of the counterion in affecting the chemical environment to allow for effective catalysis.

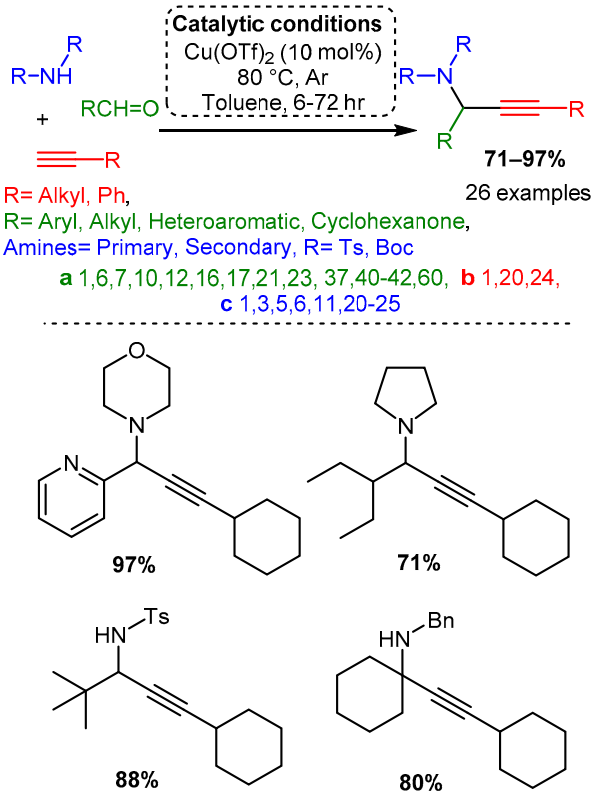

Scheme 14. Larsen et al. [86] used a Cu catalyst to catalyse the A^3 coupling reaction with electron-deficient amines.

Delpiccolo and co-workers employed a variety of substrates using a $Cu(OTf)_2$ catalyst [87]. An aliphatic alkyne and cyclic secondary amine were used with differently substituted aromatic aldehydes. These data indicate that a small substituent at the *ortho* or *para* position increases yield compared to an unsubstituted aromatic aldehyde, while a substituent at the *meta* position decreases yield. Moreover, adding a nitro group to the aromatic aldehyde led to a significant drop in yield, while 4-methoxybenzladehyde and 4-fluorobenzaldehyde had approximately equal yields. Substitution of halides at the *para* position resulted in interesting trends: 4-chlorobenzaldehyde led to a precipitous drop in yield, while 4-bromobenzaldehyde restored high yield but resulted in an allene side product (Scheme 15). The synthesis of PAs in the solid phase was also reported, starting with the immobilised 4-formylbenzoic acid by anchoring to Wang resin. The synthesis of five different *p*-HOOC- or *p*-MeOOC-substituted PAs was achieved in media to good isolated yields, from 10% to 65% (Scheme 15).

3.2. Silver and Gold Salts

Initial studies of the A^3 coupling reaction also investigated the efficacy of silver and gold salts as catalysts [32,33]. The first silver-catalysed A^3 coupling reaction was reported by Li in 2003 [32] and the optimised catalytic protocol incorporated water, as the solvent, at 100 °C with 1.5–3 mol% loading of AgI. The PAs were synthesised in moderate to high yields, with aliphatic aldehyde components being the highest-yielding substrate. In contrast, aromatic aldehydes required prolonged times and produced PAs in lower yields. Moreover, only trace amounts of product were obtained when acyclic amines were used (Scheme 16).

Early work by Li [33] demonstrated that Au(I) and Au(III) salts (AuCl, AuI, $AuBr_3$, and $AuCl_3$) could be used to catalyse the reaction with a variety of substrates. The optimised reaction used an $AuBr_3$ catalyst under an inert atmosphere in water. The reaction produced high yields even with 0.25% catalyst loading. Moreover, unlike the silver or copper salts

screened by Li, the gold catalyst worked well with aliphatic and aromatic aldehydes (Scheme 17).

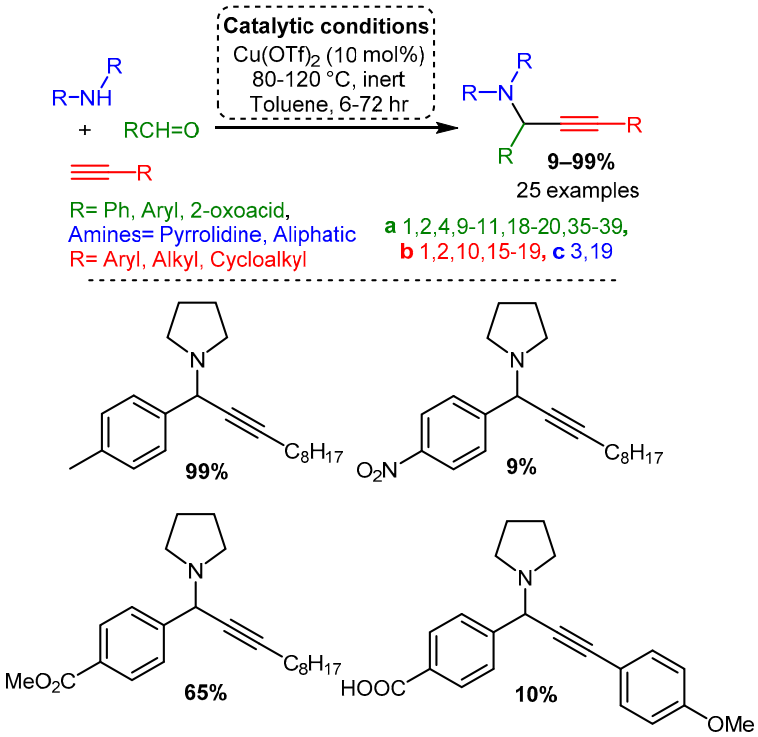

Scheme 15. Synthesis of PAs through an A^3 coupling in homogeneous and solid-phase conditions.

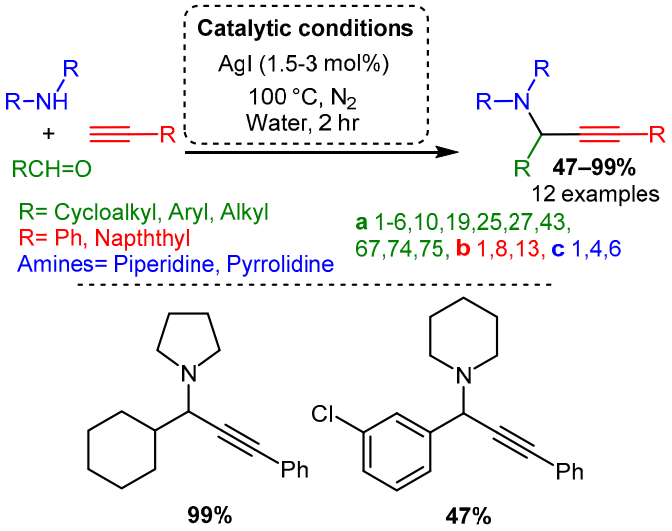

Scheme 16. Optimised conditions for Ag(I) salts.

According to our extensive classification, gold was the only group XI catalyst able to catalyse the A^3 coupling reaction when α-oxyaldehydes were used as substrate [88]. Using higher catalytic loadings (5 mol%), the reaction at room temperature under an inert atmosphere produced good yields with a moderate preference for one diastereomer. This diastereoselectivity most likely resulted from the coordination of the iminium intermediate, thereby biasing acetylide addition (Scheme 18). Interestingly, while Ag(I) catalysts were unable to catalyse the A^3 coupling reaction when an α-hydroxyaldehyde was used as a substrate, they were more effective than gold catalysts when α-alkylaldehydes were used. However, this variation was not extensively studied (results not shown).

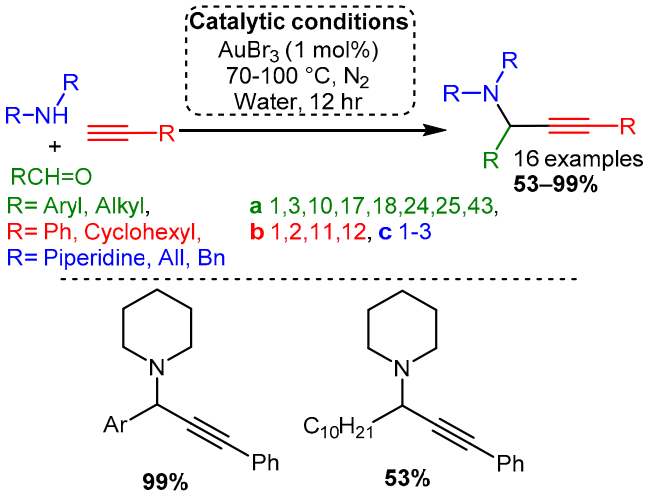

Scheme 17. Optimised conditions for Au(III) salts.

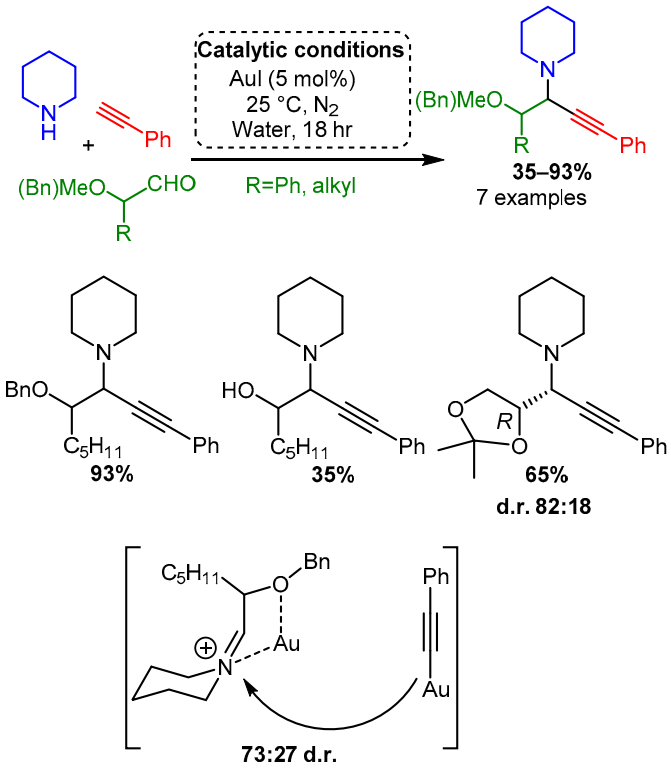

Scheme 18. Au(I) catalysed A^3 reaction of α-oxyaldehydes and the proposed bimetallic mechanism that explains the observed diastereoselectivity.

Complimenting the reported homogenous catalysts, a heterogeneous gold catalyst was developed by Corma in which the partially charged and electron-deficient gold atoms were stabilised on nanocrystalline ZrO_2 or CeO_2 [89]. As mentioned before, this review focuses on homogeneous metal-based methodologies; therefore, Corma's work is beyond the scope; however, it is interesting to note that these Au nanoparticles produced PAs in high yields, while also showing high diastereoselectivity when a chiral amine was used. In this study, a direct correlation was found between the formation of the Au(III) species, while no clear trend was observed for the Au(I) or Au(0) species. Notably, high yields were maintained even when an aliphatic alkyne or aldehyde were used together, although all amine substrates were secondary, and most were cyclic.

3.3. Other Metals

Of the metals outside group XI reported to catalyse the A^3 coupling reaction, zinc and iron have been the most extensively studied, although indium, cadmium, cobalt, and nickel have all demonstrated promising catalytic activity. The use of a diethylzinc catalyst to alkynylated a C-N π bond was reported by Vallee, where the more electrophilic nitrones were used in place of imines to access N-propargyl-hydroxylamines in high yields [43]. The reaction required high catalyst loadings (20 mol%) and was carried out at room temperature under a nitrogen atmosphere. The reaction proceeded slowly in dichloromethane but was considerably improved using toluene, with time to completion varying from 1.5 to 30 h (Scheme 19).

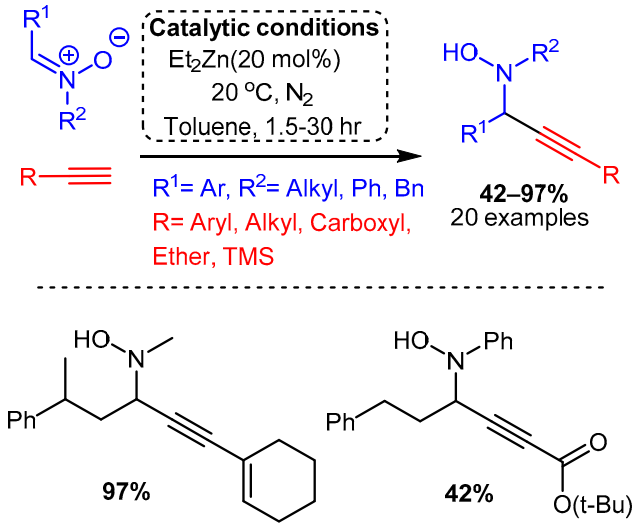

Scheme 19. Use of Et_2Zn catalyst to add a terminal alkyne to a nitrone, as reported by Vallee and co-workers.

A more traditional A^3 coupling reaction was reported by Bolm, who first used a dimethylzinc catalyst to alkynylate pre-formed and protected imines and then applied the catalyst to the three-component reaction [44]. High temperatures, reaction times of 24 h, and extremely high catalyst loadings (150 mol%) were necessary to alkynylate the protected electron-withdrawing imines (R^1CH=N-PG). The three-component reaction, which was conducted at room temperature, required 48–96 h and even higher catalyst loadings of 250–350 mol%. Moreover, the reported yields varied considerably, with an average of 67% yield for the protected imines and 64% for the one-pot reaction (Scheme 20).

More recent studies have focused on zinc salts in place of organic zinc derivatives. Chandak [46] explored the solvent-free A^3 coupling reaction catalysed by $Zn(OTf)_2$ in a study that lends itself to easy comparison to the above-discussed exploration of $Cu(OTf)_2$ as a catalyst [87] (Scheme 15). The $Zn(OTf)_2$ required lower catalytic loading (5 mol%) and catalysed the reaction in green, solvent-free conditions with high yields (Scheme 21). As with the $Cu(OTf)_2$ catalyst, the electronic effects on the aromatic aldehyde did not alter the yield significantly. However, the zinc catalyst appears less sensitive to steric constraints than the copper catalyst. Of note, the zinc catalyst produced high yields when an aromatic alkyne was used, while the copper catalysts had the highest yields with an aliphatic alkyne; it should be mentioned, however, that the scope of alkyne used in both cases was limited.

Catalytic studies by Wang [90] and Li [37] have shown that PAs can be accessed in high yields by using $FeCl_3$ in high loading (10 mol%). In both cases, the optimised reactions required high temperatures. However, the use of an inert atmosphere and toluene solvent by Wang and co-workers resulted in the corresponding PAs in average yields 10–20% higher than those achieved with solvent-free and open-air conditions in the later study of Li and co-workers (Schemes 22 and 23). These differences may be accounted for by

variation in substrates, although it is challenging to conclude the exact substrate effects without further evidence.

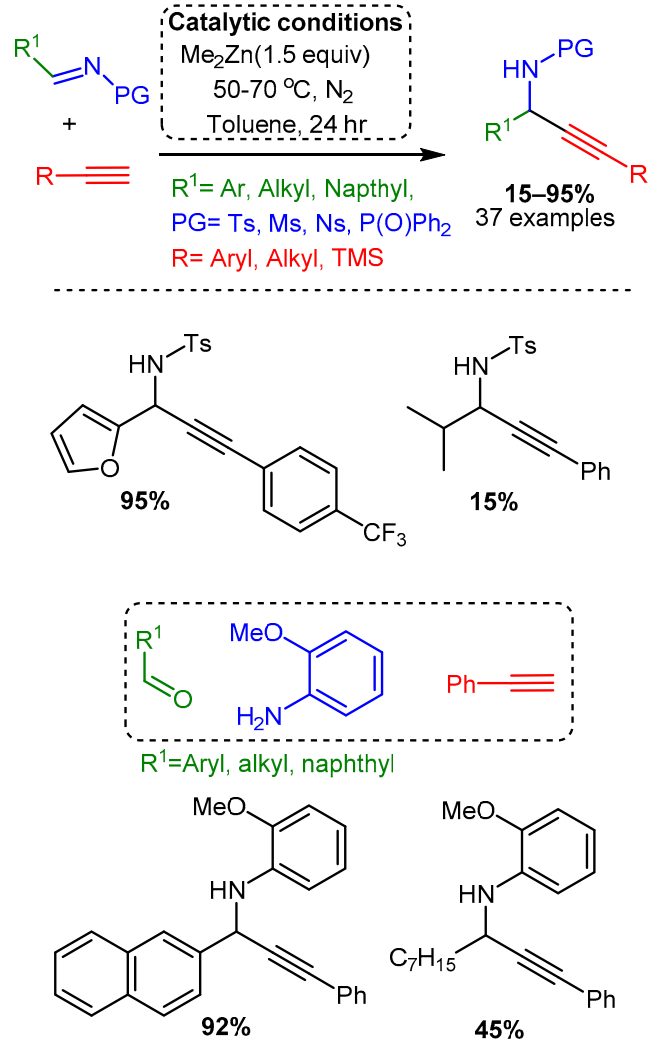

Scheme 20. Dimethylzinc-mediated alkynylation of imines for the synthesis protected propargylic amines.

3.4. Proposed In Situ Mechanisms

Significant advances have been made in understanding the catalytic mechanism using various organic ligands. Cu(I) and Cu(II) catalysts are most often employed in these studies due to their low cost, stability, and versatility. By understanding the catalytic mechanism, the hard–soft, HOMO–LUMO, and non-covalent interactions can be tailored to match specific combinations of catalyst, solvent, and substrates, thereby extending the applicability of the A^3 coupling reaction and other metal-catalysed C-H activated additions. The proposed in situ catalytic cycles follow a similar path to the one in Scheme 24. This path involves the following steps:

1. A monomeric metal species forms a π-complex with the terminal alkyne;
2. The C_{sp}-H bond is activated. Studies have indicated the activation of the C_{sp}-H bond via IR and NMR spectroscopy [30,31]. The coordinating metal labilises the terminal hydrogen, allowing a weak base such as the amine component and/or anion to deprotonate and form the active acetylide;
3. The newly formed acetylide attacks the imine (or the iminium intermediate);
4. Decomplexation releases the PA and regenerates the metal catalyst.

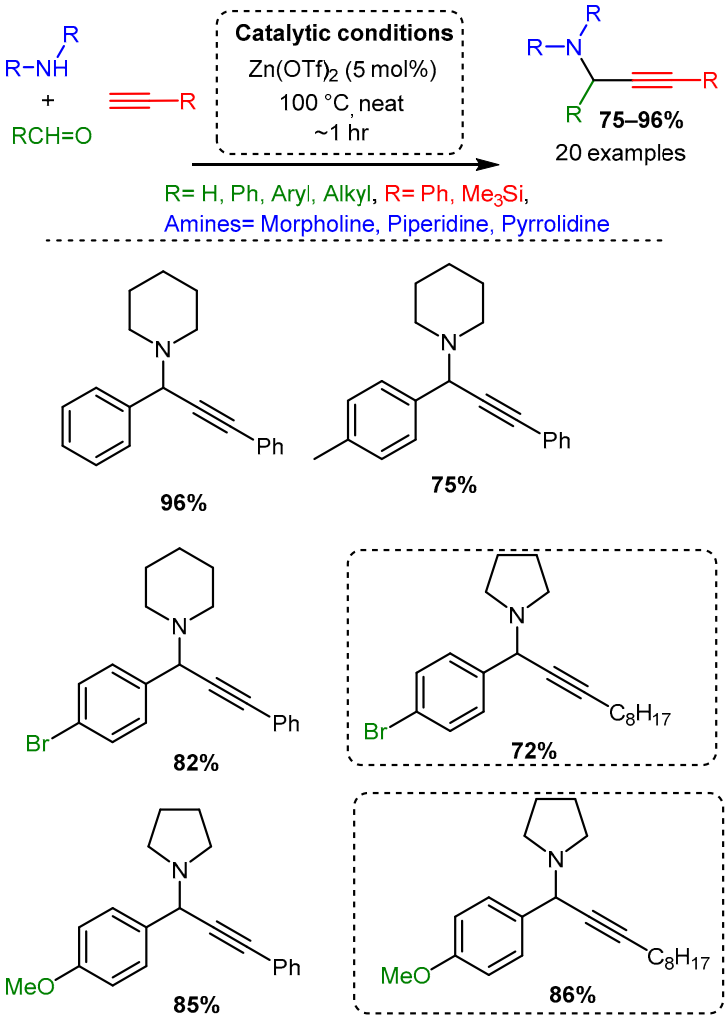

Scheme 21. $Zn(OTf)_2$ catalysis of the A^3 coupling reactions. Dashed line boxes denote comparable products from the $Cu(OTf)_2$ catalysed reaction [84].

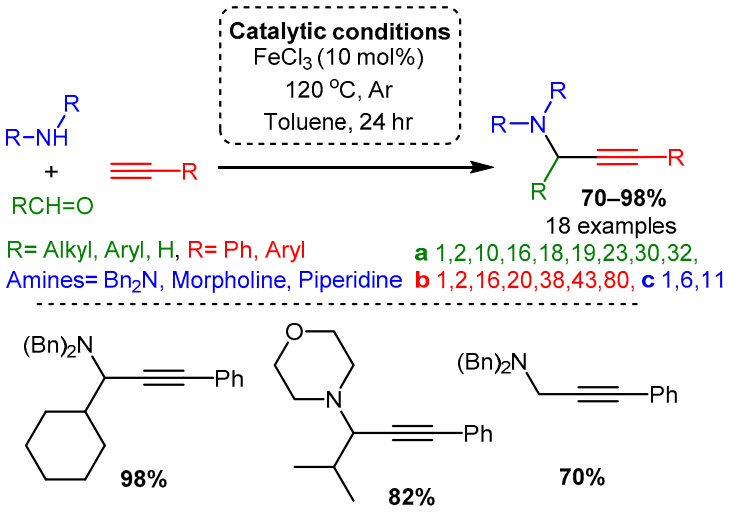

Scheme 22. Iron-catalysed A^3 coupling reaction under argon atmosphere and toluene solvent.

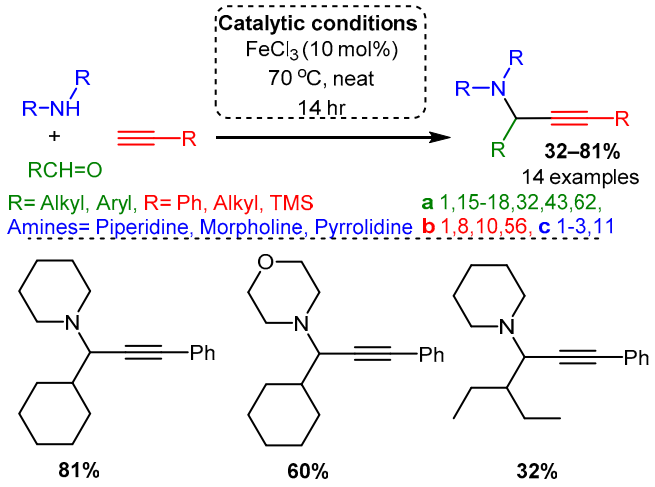

Scheme 23. Iron-catalysed A^3 coupling reaction in open air and absence of solvent.

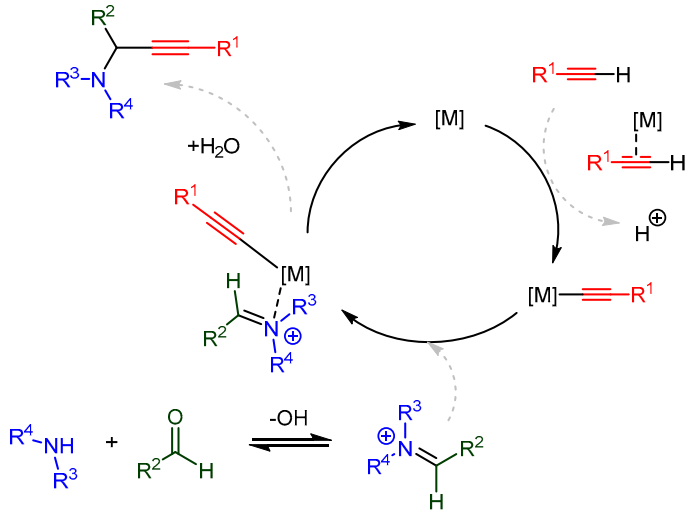

Scheme 24. The proposed in situ single metal catalysed mechanism for synthesizing PAs.

4. A^3 Coupling with In Situ Formed Catalysts

One of the most common ligands used to promote enantioselectivity in the A^3 coupling reaction is those containing one, two, or three heteroatoms. High yields and *ee* have been achieved with bi- and tridentate such as Binam [91–93], Box (bis(oxazoline)) [51], Pybox (bis(oxazolinyl)pyridines) [47,50,51,63,88,94–96], Phebim [97], Pybim [41,49,97], and their derivatives.

In 2002, Li reported the first highly enantioselective Cu(I)-catalysed direct alkyne-imine addition [47]. This pioneering work explored both Box and PyBox ligands and found that a PyBox ligand combined with Cu(OTf) provided the highest yields and enantioselectivities with a toluene solvent at a moderately elevated temperature of 40 °C (Scheme 25). Li's pioneering work demonstrated that such ligands could be used to achieve high yields and enantioselectivity, but left open questions regarding ligand design, reaction conditions, and substrate scope. Use of a ligand to catalyse the A^3 coupling reaction has two functions: activating the catalyst and promoting enantioselectivity. Advances in ligand design have increased yields and enantioselectivities, while simultaneously lowering reaction temperature and time, employing milder conditions and, in some cases, green solvents. Herein, we summarise the advances in ligand design, focusing on homoligands (i.e., ligands where all coordinating atoms are the same), heteroligands (i.e., ligands that involve two or more coordinating atoms), and attempting a comparison of the developed ligands.

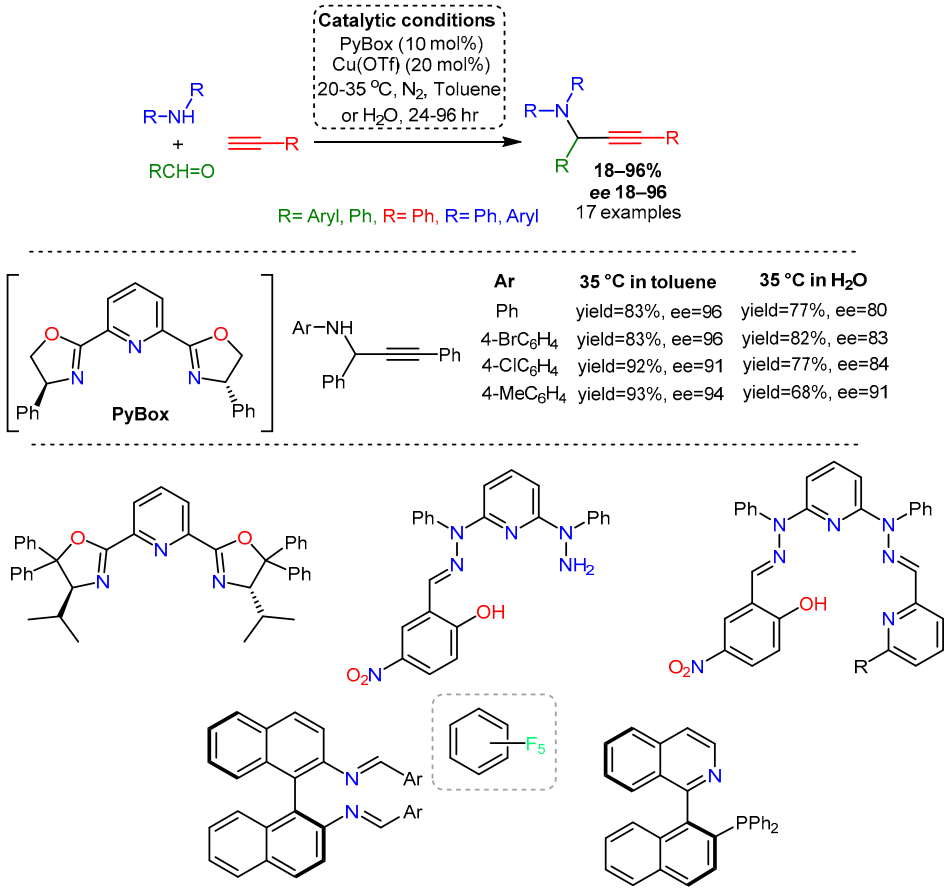

Scheme 25. (**upper**) The first in situ generated A^3 coupling example using a PyBox ligand [47]. (**lower**) Representative examples of prominent ligands used to facilitate the A^3 coupling in situ protocols.

4.1. Monodentate Ligands

P-Ligands

In addition to the commonly used N-Ligands, several groups have attempted to use P-homoligands to catalyse the A^3 coupling reaction. Wang combined triphenyphosphine, tricyclohexylphosphine, or 1,1′-Bis(diphenylphosphino)ferrocene (DPPF) with an $FeCl_3$ metal salt [90]. These P-Ligands were noted to accelerate the reaction and achieve moderately high yields (Scheme 26).

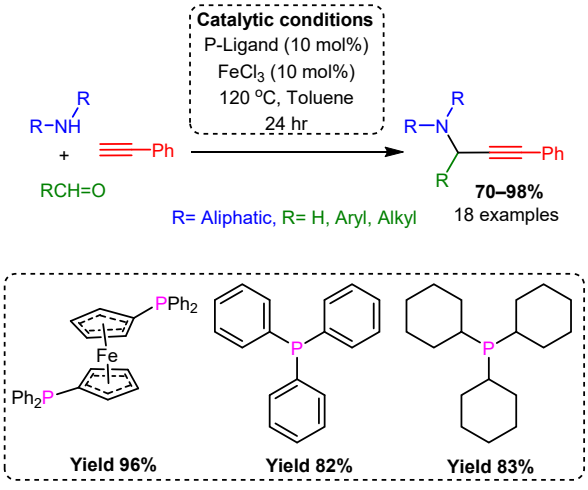

Scheme 26. Iron catalysed ligand-free A^3 coupling reaction in the presence of phosphines.

Similarly, Li employed the monodentate triphenylphosphine ligand with $CoCl_2$ to accelerate the reaction [36]. In this work, the two ligands coordinated to the cobalt salt, thereby acting as a bidentate ligand. While other P-mono and bidentate ligands, including Binap, were tested, none achieved yields as high as triphenylphosphine. Several alkyl and aryl-substituted propargyl amines were synthesised under the proposed catalytic conditions (Scheme 27).

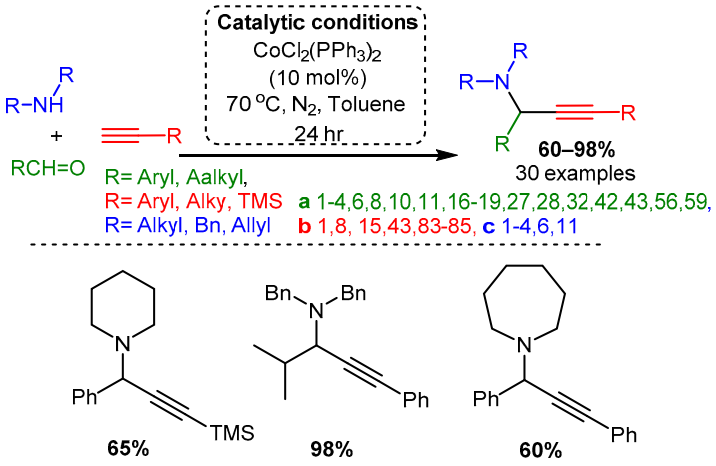

Scheme 27. Cobalt-catalysed transformation of alkynyl C–H bond into propargyl amine derivatives via an A^3 coupling reaction.

Arndtsen used several additional monodentate P-ligands combined with L-Boc-Proline to yield PAs with high *ee* values [98]. In this work, the flexibility afforded by the monodentate phosphine ligands and amino acid combination allowed for tuning the catalyst to accommodate more challenging substrates. This work synthesised several chiral aniline-substituted derivatives in good isolated yields and high *ee* (Scheme 28).

As described previously (see Scheme 11), more recently, Jang reported a unique application of the A^3 coupling reaction with phosphine ligands to synthesise both symmetrical and unsymmetrical 3-amino-1,4-diynes [84]. Their optimisation studies found that *N*- and carbene ligands were not as effective as the monodentate triphenylphosphine ligand alone. The proposed methodology leads to the corresponding symmetrical and unsymmetrical 3-amino-1,4-diyne derivatives depending on the starting alkyne.

4.2. Bidentate Ligands

The bidentate ligand Binam and its derivatives have been used with Cu and Ag catalysts to form PAs stereoselectively. The atropoisomeric Binam is structurally similar to Binol, an O-ligand discussed below.

4.2.1. Homobidentate Ligands N,N-Ligands/Binam

The Binol analogue 1,1′-bi-2-naphthylamine (Binam) has had an important role in asymmetric synthesis and constitutes one of the most well studied C2-symmetric ligands to induce enantioselectivity. Use of Binam to catalyse the A^3 coupling reaction was first reported by Dell'Anna in 2004 [92]. In this preliminary work, several Binam catalysts containing aromatic rings attached to the coordinating amine were tested, with the highly electron-withdrawing pentafluorobenzene moiety achieving the highest yields and *ee*. Notably, the inclusion of pyridine moieties as part of the ligand scaffold could not catalyse the reaction; the authors hypothesised that introducing two additional coordinating N-atoms rendered the Cu catalyst inactive. Celentano later applied the same ligand to explore the substrate scope of the reaction (Scheme 29) [91].

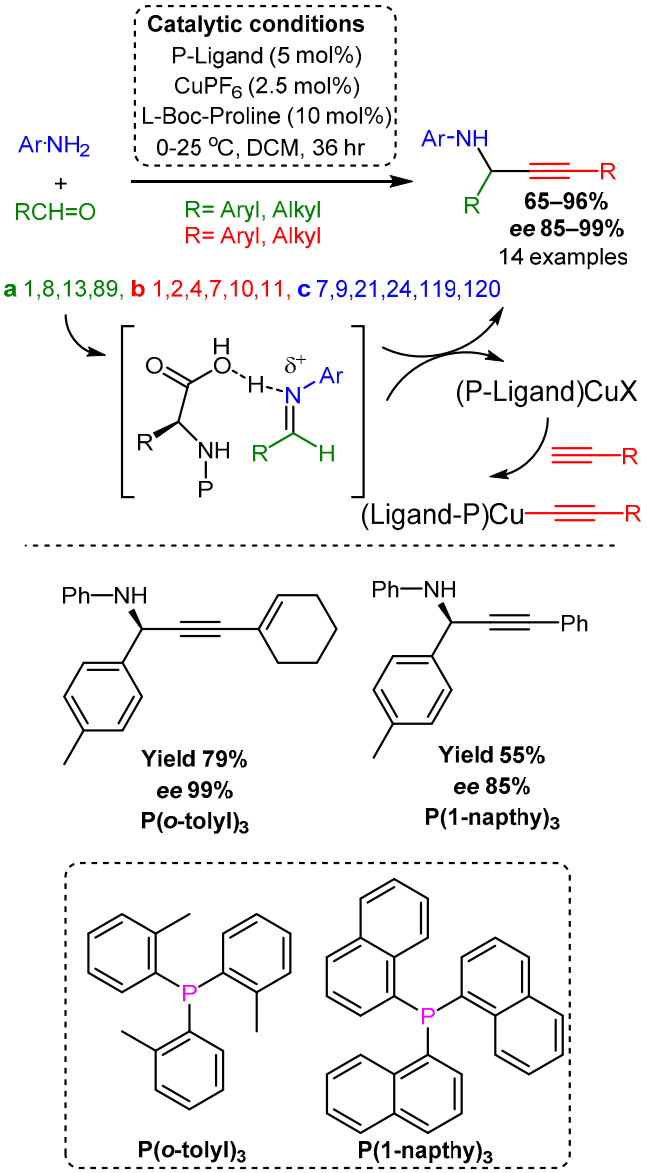

Scheme 28. *L*-Boc-proline catalysed enantiomerical synthesis of propargyl amines catalysed by Cu | PF in the presence of P-ligands.

In a later study, Ishihara used several bidentate Binam ligands to catalyse the A^3 coupling reaction but ultimately identified that aminoaryloxy ligands derived from the commercially available Binol yielded higher *ee*. Unlike the Binol derivatives discussed later, which coordinate to the metal catalyst using an oxygen atom and require moieties at the 3,3′ position, this catalyst induces chirality by employing an aminoaryloxy moiety [93]. A proposed transition state model hypothesised that the nitrogen atoms coordinate with Cu in a bidentate fashion while the oxygen serves as a hinge (Scheme 30).

4.2.2. Homobidentate Ligands O,O-Homoligands/Binol

O,O-homoligands, notably Binol, have been used to catalyse the A^3 coupling reaction. Pedro employed a Zn catalyst with Binol derivatives to synthesise PAs with high yield, *ee*, and substrate scope [42]. In this work, Pedro noted that successful reactions involved a Binol derivative with moieties at the 3,3′ positions; high yields and *ee* were obtained when either bromide or 3,5-trifluormethylphenyl substituents were used. Ultimately, the group decided to use the aromatic moiety, noting that the more sterically hindered ligand achieved higher enantioselectivities (Scheme 31).

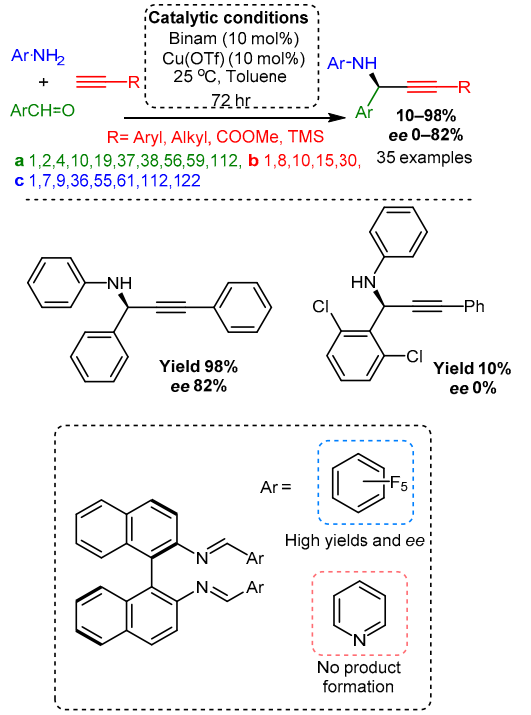

Scheme 29. Enantioselective synthesis of PAs catalysed by copper(I)−Bisimine complexes.

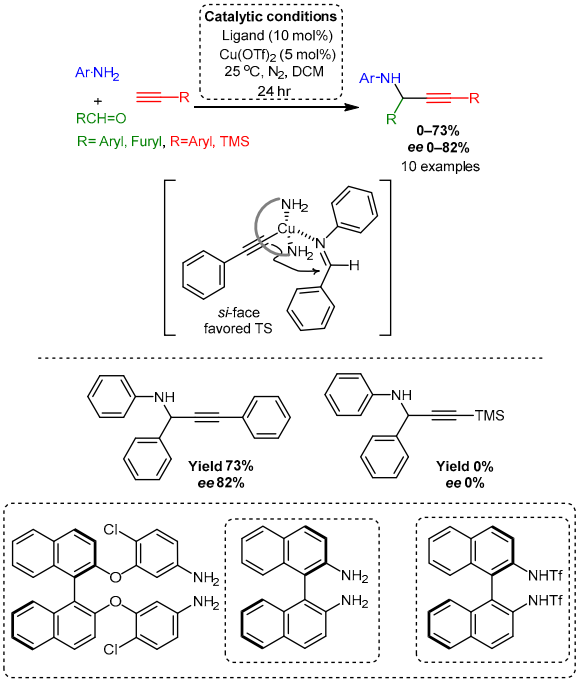

Scheme 30. Enantioselective alkynylation to aldimines catalyzed by chiral 2,2′-di(2-aminoaryloxy)-1,1′-binaphthyl-Copper(I) complexes.

Pu employed Binol derivatives with a combination of zinc and titanium to achieve high yields and enantioselectivities [45]. Herein, Binol derivatives were designed to incorporate a dimorpholinylmethyl moiety at the 3,3′ positions, facilitating chiral induction by restricting substrate entry and allowing additional coordination between the heteroatoms and the metal salt. The importance of the 3,3′ position for chiral induction was emphasised, and ligands without both moieties could not achieve significant *ee* (Scheme 32).

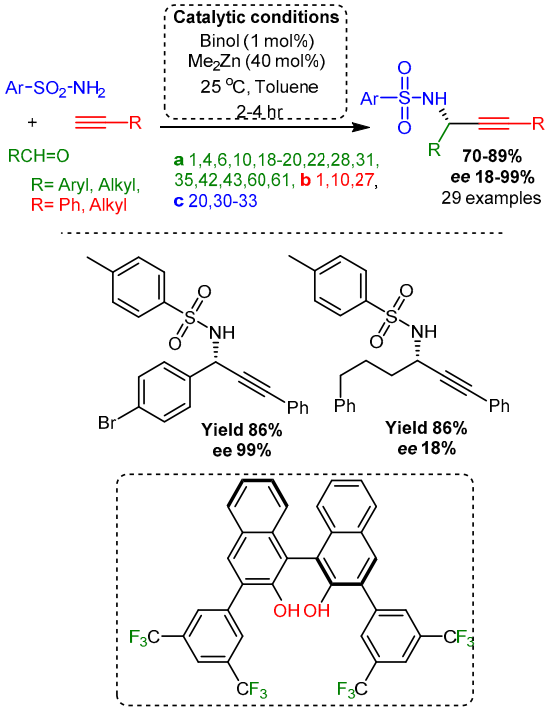

Scheme 31. Highly enantioselective zinc/Binol-catalysed alkynylation of *N*-sulfonyl aldimines.

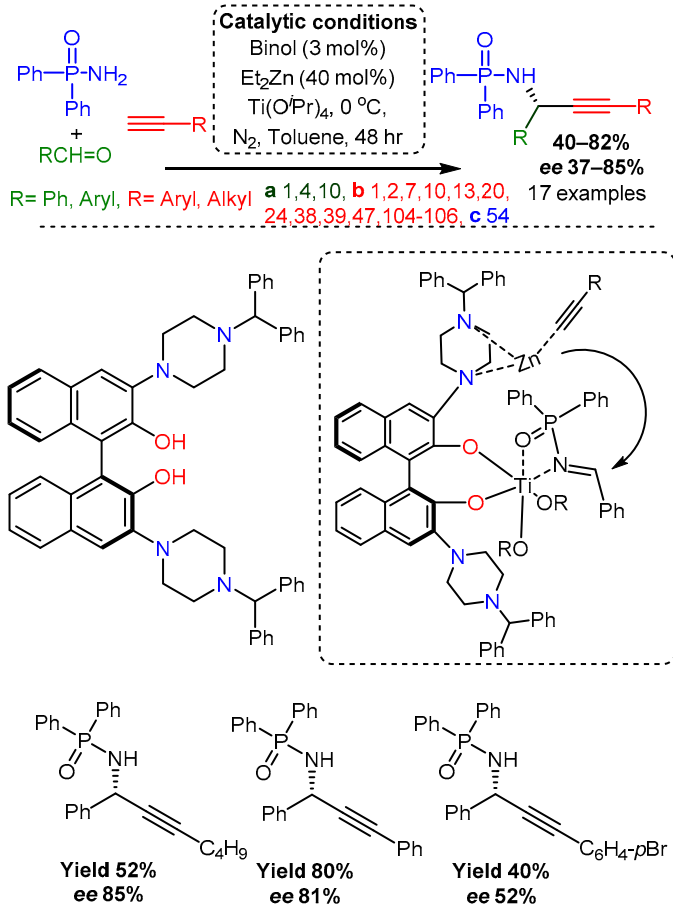

Scheme 32. Zn-Binol-catalysed asymmetric addition of alkyl and aryl Alkynes to *N*-(Diphenylphosphinoyl)imines.

4.2.3. Heterobidentate P,N-Ligands

4.2.3.1. Quinap

In 2002, Knochel reported the first copper-catalysed asymmetric alkyne addition to enamines, an early variant of the modern A^3 reaction. The P,N-ligand Quinap was used to achieve enantioselectivity in this work [52]. Since this pioneering work, P,N-ligands have been explored by several groups and optimisation of ligand design to increase yield and *ee* at low temperatures with low catalyst loading is an ongoing area of investigation. Our meta-analysis reveals that P,N-ligands are the third most frequently employed. The efficacy of these ligands can be explained in part by incorporating hard and soft coordinating atoms, nitrogen and phosphorous, respectively.

Unlike the more modern A^3 coupling, Knochel's first report of the Quinap-catalyzed enantioselective A^3 coupling reaction used pre-formed enamine substrates and several alkynes (Scheme 33, left). Following this proof-of-principle study, Knochel expanded the scope of the asymmetric A^3 coupling reaction using Quinap in two studies [20,99]. First, several combinations of amine, alkyne, and aldehyde were used with a copper catalyst and Quinap (Scheme 33, right). Subsequently, trimethylsilylacetylene and dibenzylamine were used to explore the aldehydes amenable to this methodology. Knochel demonstrated that the Quinap catalyst could be recycled and reused up to three times.

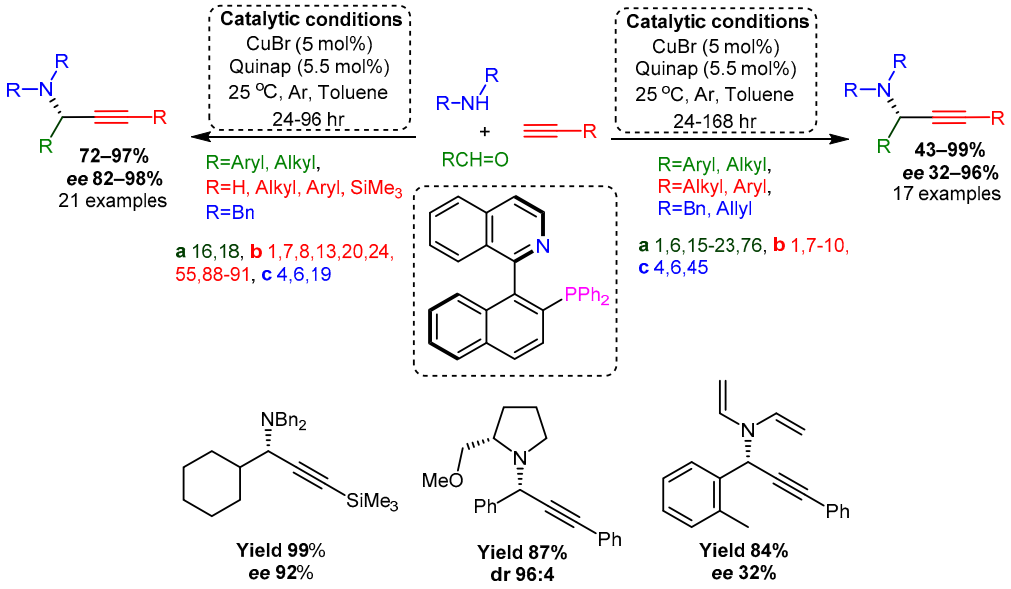

Scheme 33. Two different methods for PA synthesis with the use of Quinap.

4.2.3.2. Pinap

The use of Quinap in asymmetric A^3 coupling reactions was further explored by Carreira, who introduced the Quinap analogue Pinap [100]. This analogue is more amenable to chemical modifications that could enhance ligand efficacy and has the advantage of being more easily synthesised and resolved (Scheme 34). In these reactions, the stereogenic centre in the phenethyl group is proposed to induce the observed product configuration via subtle remote effects.

Carreira and co-workers later expanded the scope of Pinap and addressed two critical disadvantages of previous methodologies: long reaction times (>48 h) and versatility of the amine [101]. Specifically, while N,N'-dibenzylamine facilitated high yields and enantioselectivities, removal of these protecting groups proved costly or technically demanding. These challenges were overcome by incorporating 4-piperidone hydrochloride hydrate as the amine component and using DCM as the solvent. The use of 4-piperidone allowed facile conversion of the tertiary PA to a primary product via ammonium chloride and amino-methylated polystyrene resin in ethanol at 100 °C (Scheme 35).

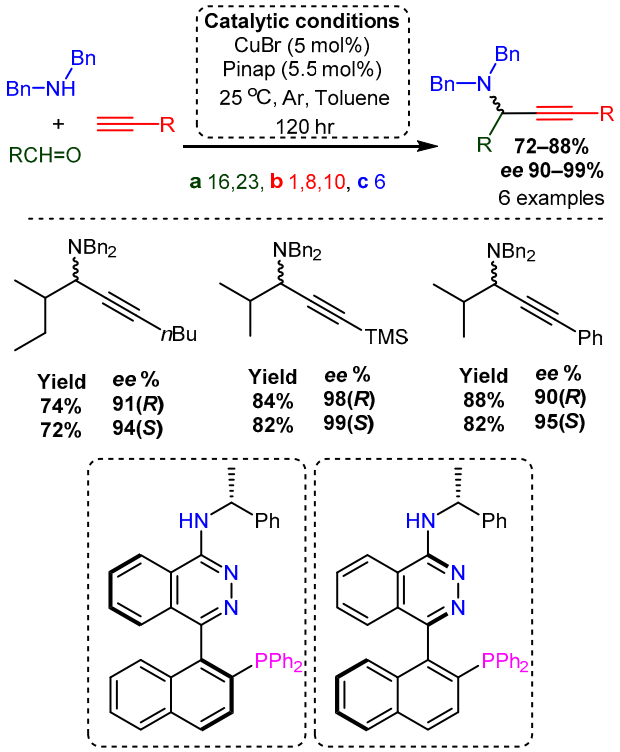

Scheme 34. Biaryl P,N ligands for asymmetric catalysis of propargyl amine derivatives synthesis using CuBr.

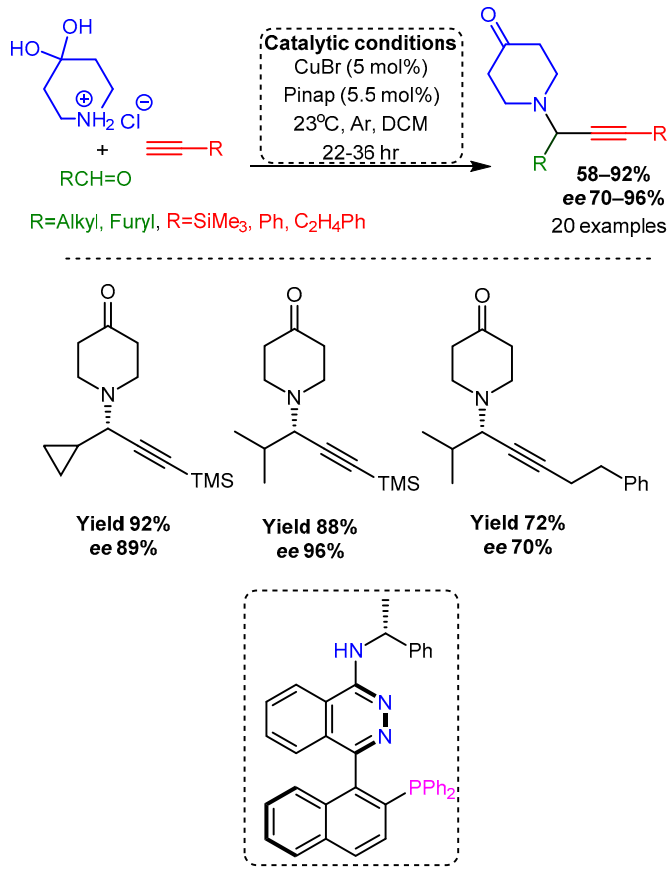

Scheme 35. Enantioselective synthesis of primary PAs using 4-piperidinone as a convenient protecting group.

4.2.3.3. StackPhos and StackPhim

A significant innovation in P,N-ligand design was introduced by Aponick in 2013 [69]. In this seminal work, Aponick describes a new paradigm of biaryl atropisomer design: in place of incorporating large substituents to destabilise the rotational transition state, the barrier to biaryl rotation could be increased by stabilising the chiral ground state conformation. This principle led to the design of StackPhos, a ligand with an imidazole system containing one nitrogen atom able to coordinate to the metal salt and the other attached to a perfluorinated phenyl ring moiety that is structurally located by π-stack with the naphthalene component. This chiral conformation was confirmed via x-ray crystallography. The use of StackPhos in the A^3 coupling reaction achieved high yields and enantioselectivities at low temperatures and short reaction times (24 h) with aliphatic and aromatic aldehydes (Scheme 36).

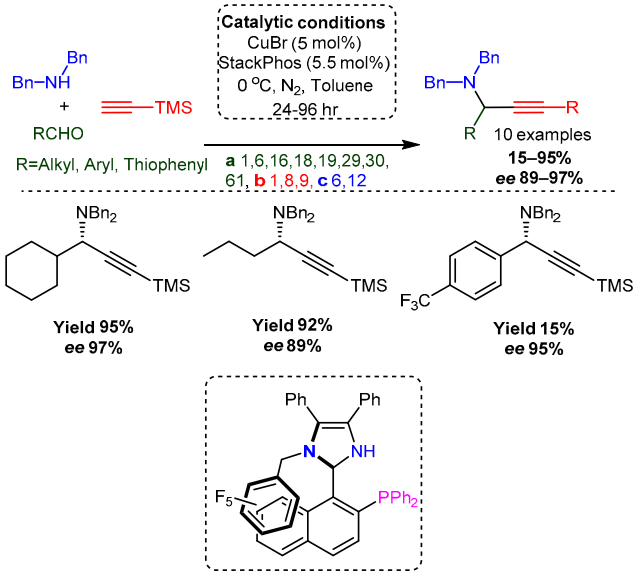

Scheme 36. Enantioselective A^3-coupling employing a chiral imidazole-based biaryl P,N-ligand (StackPhos).

Aponick also used StackPhos to synthesise unsymmetric skipped diynes [102]. The enantioselective synthesis of 1,4-diynes containing divergent groups, i.e., those with different electronic or steric effects, remains challenging due to the unwanted formation of side products. A robust methodology to access these compounds is highly desirable since this motif is commonly seen in natural products, for example, in the chlorinated lipid family taveuniamides. While previous reports have used the A^3 coupling to synthesise skipped diynes [84] (Schemes 11 and 29), this work by Aponick describes the first enantioselective preparation of amino skipped diynes with broad substrate scope and similar substituents and several applications in natural product synthesis (Scheme 37).

Later on, the StackPhos catalyst was also used to synthesise alkynediols which could subsequently undergo gold-catalysed cyclisation. In this work, StackPhos could not generate 1,4-aminoalcohols in adequate enantioselectivities, which prompted the design of StackPhim: StackPhim replaces the five-membered aromatic heterocycle in StackPhos with two new chiral centres [68]. In comparing StackPhos with StackPhim, StackPhos resulted in higher yields, but StackPhim resulted in higher enantioselectivities. These results indicate that chiral induction is affected by ligand axial chirality and backbone chirality; in this case, StackPhos has axial but not backbone chirality and is, therefore, a more promiscuous catalyst. The scope and utility of StackPhim were demonstrated on several A^3 reactions synthesising 1,4-aminoalcohols and their subsequent gold-catalysed cyclisation (Scheme 38).

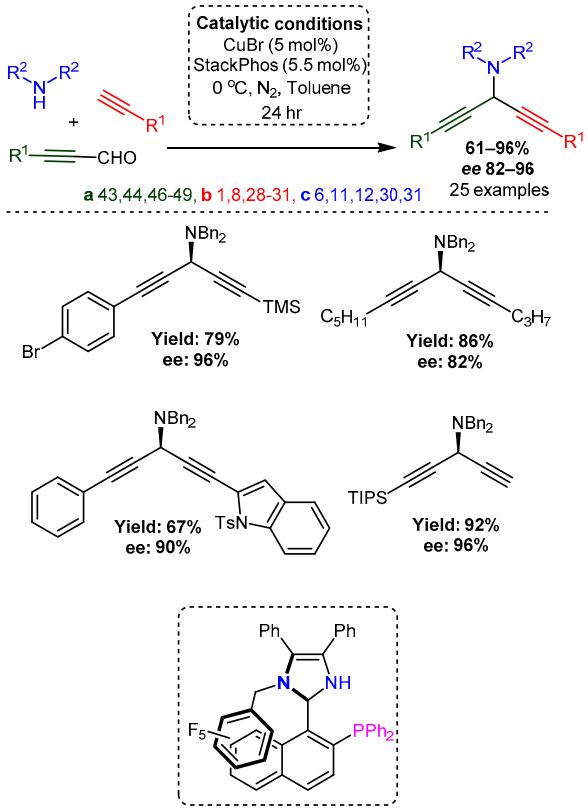

Scheme 37. Cu/StackPhos-catalysed enantioselective synthesis of amino skipped diynes.

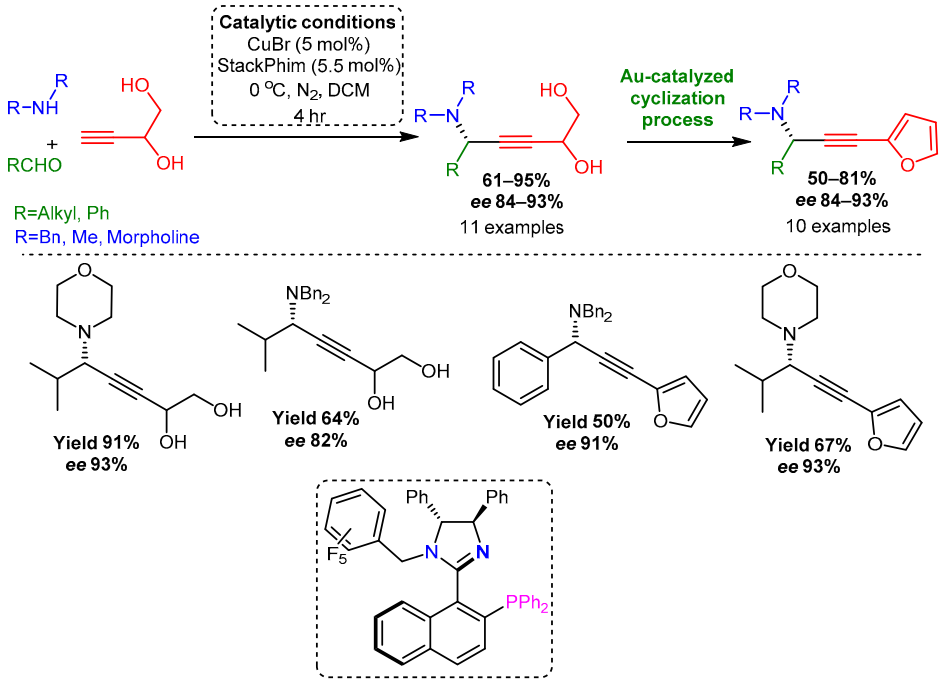

Scheme 38. Cu/StackPhim-catalysed enantioselective synthesis of amino alkynyl diols.

Guiry and co-workers further reported the synthesis and application of StackPhim (Scheme 39, upper) [71]. Noting that ligands such as StackPhos and Quinap required a resolution step involving palladium to isolate the enantiomerically pure ligands, incorporating the chiral imidazoline in StackPhim can act as an inbuilt resolution unit. Of note, StackPhim, as used by Guiry's team, required less catalyst and ligand loading than

Aponick's work, although the reaction times were longer. The scope of StackPhim as a chiral ligand was further expanded by Guiry in later work [103]. This study used the more challenging propargylic alcohol with a wide range of aldehydes and amines (Scheme 39, lower), yielding the corresponding PAs in moderate to excellent yields and *ee*.

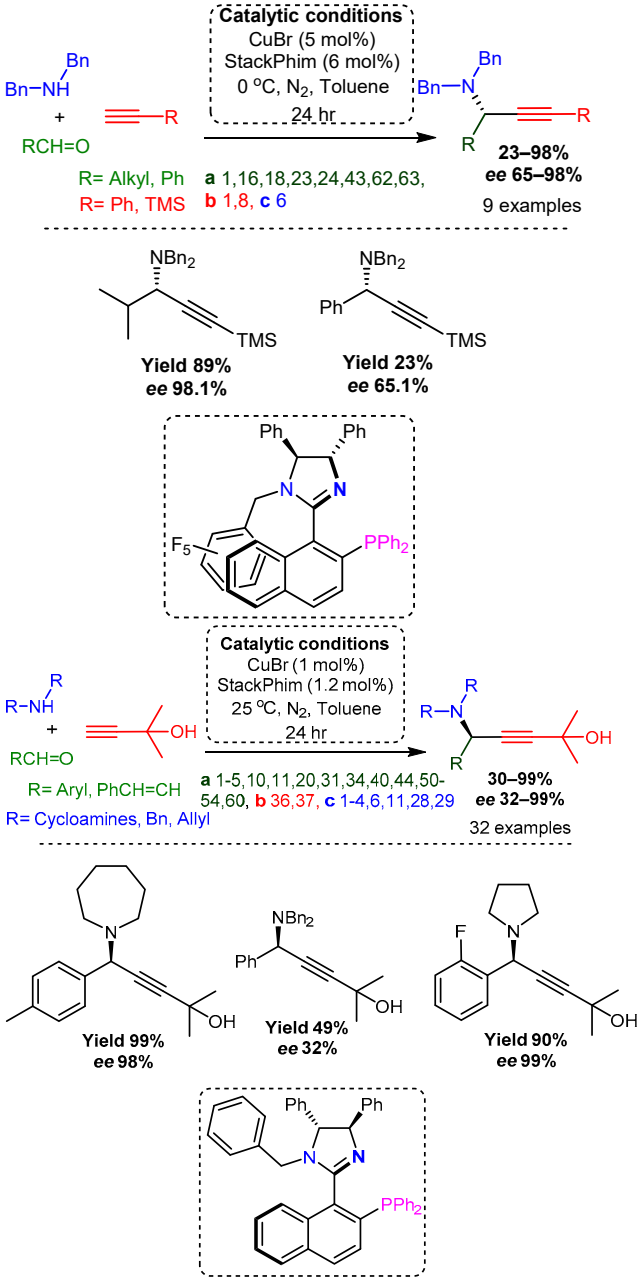

Scheme 39. Diastereofacial approach for the synthesis of axially chiral P,N-ligand towards A^3 coupling process (**upper**). Catalytic enantioselective A^3 coupling between aromatic, alkenylic, and alkynylic aldehydes with propargylalcohol and cycloamines (**lower**).

4.2.3.4. Pyrinap

The most recent novel P,N-ligand used in the A^3 coupling reaction was reported by Ma [104]. Building on the Binap scaffold, while desiring a more flexible ligand that could accept a range of substrates, Ma produced the Pyrinap, which incorporates both the axial chirality seen in Quinap and the backbone chirality seen in Pinap. Notably, while Pyrinap deviates from the biaryl motif seen in Quinap and Pinap to promote axial chirality, the barrier of rotation for Pyrinap was higher than the similar ligands Pinap, StackPhim, and

StackPhos. The novel Pyrinap catalyst was used on a wide range of substrates and applied to several unique natural product scaffolds (Scheme 40). Additionally, this methodology was applied to the synthesis of (*S*)-(-)-*N*-acetylcolchinol, a tubulin polymerisation inhibitor (Scheme 40, lower).

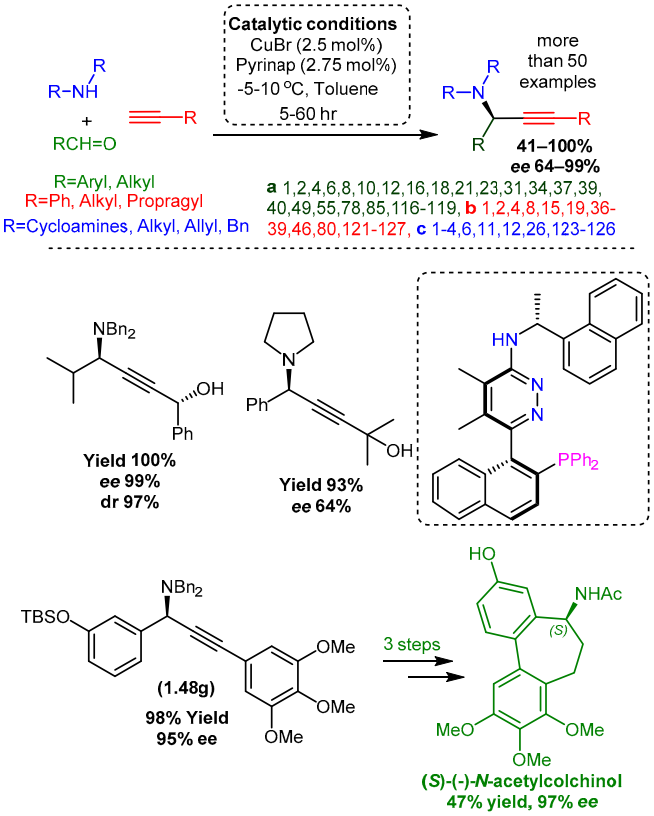

Scheme 40. Pyrinap ligands for enantioselective syntheses of amines.

4.2.4. Heterobidentate N,O-Ligands

In 2003, Hoveyda and Snapper reported a protocol for chiral PAs' enantioselective synthesis with up to 90% *ee* [41]. This method involved the Zr-catalyzed ($Zr(O$*i*$-Pr)_4 \cdot HO$*i*$-Pr$) addition of mixed alkynylzinc reagents to arylimines in the presence of chiral amino acid-based ligands (Scheme 41). The subsequent oxidative removal of the *o*-anisidyl group afforded the free amine, which could be acylated to yield the corresponding product in 90% *ee*, thus providing an efficient way to obtain optically enriched secondary alkynylamines.

In 2006, five Au(III) salen-based complexes were incorporated into the A^3 coupling reaction [105]. Authors used or modified already known protocols to synthesise these complexes and characterised them with ^{1}H-NMR, IR, and FAB-MS. The protocol is environmentally friendly; only 1% catalyst loading is required, in aqueous solutions, at 40 °C and inert atmosphere (Scheme 42). The reaction completes in 24 h, and with chiral prolinol derivatives as the amine component, excellent diastereoselectivities (up to 99:1) are obtained. Notably, the protocol was extended to synthesising PA-modified artemisinin derivatives with intact delicate endoperoxide moieties. Subsequent cytotoxicity studies of these artemisinin derivatives exhibited IC50 values up to 1.1 µM against a human hepatocellular carcinoma cell line (HepG2).

The following year, Li, Chan et al. [106] synthesised a family of chiral tridentate *N*-tosylated aminoimine ligands incorporated along with $Cu(OTf)_2$ and Me_2Zn in toluene for the room temperature enantioselective addition of phenylacetylene to *N*-aryl arylimines. This protocol was applied to a limited number of PAs and yielded the corresponding products in moderate to good yields (42–89%) and good *ee* (73–92%) (Scheme 43).

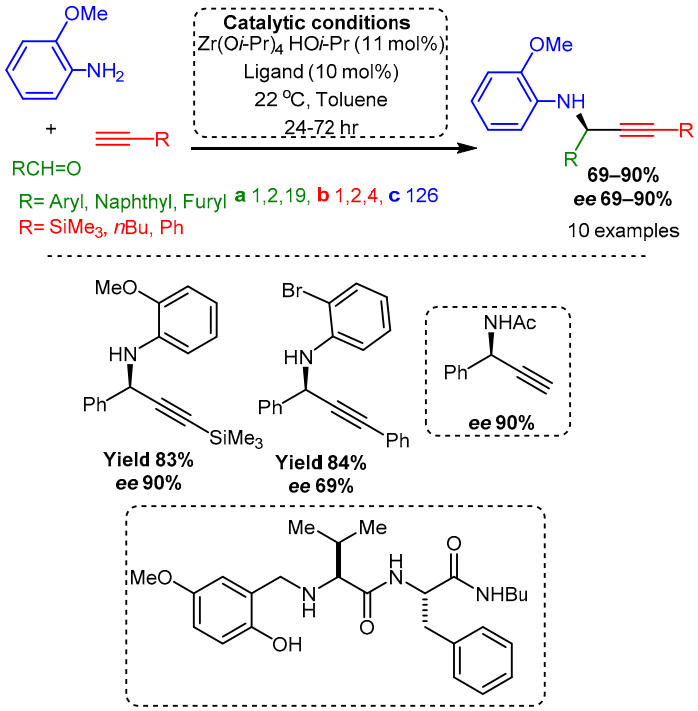

Scheme 41. Zr catalysed the enantioselective synthesis of propargyl amines starting with alkynylzinc and arylimines.

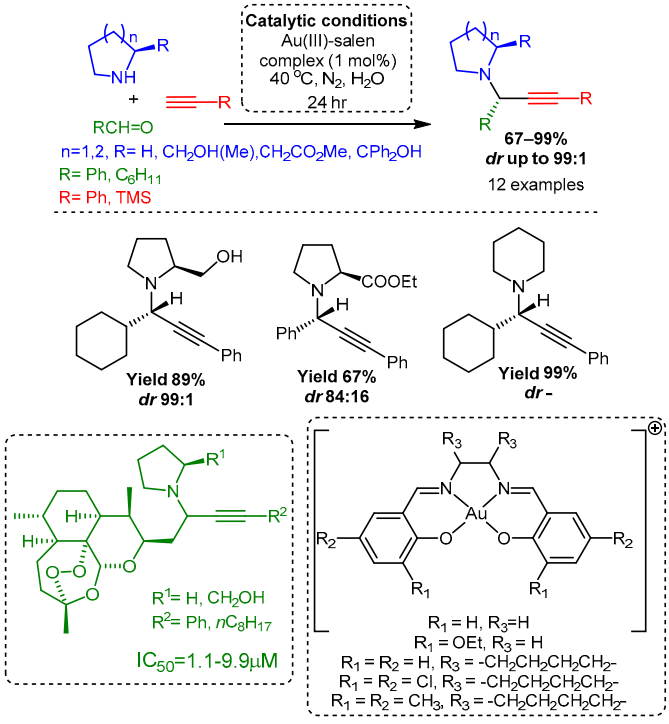

Scheme 42. Gold(III) salen complex-catalysed synthesis of PAs via a A^3 coupling reaction.

Seidel reported a protocol involving copper iodide and an easily accessible hybrid ligand possessing both a carboxylic acid and a thiourea moiety a few years later [72]. PAs are obtained with up to 96% *ee*, and catalyst loadings can be as low as 1 mol% (Scheme 44). In the absence of directing groups, pyrrolidine-derived PAs can be transformed to the corresponding allenes without loss of enantiopurity, which is a significant improvement compared to the previous effort demonstrated in 2013 [81].

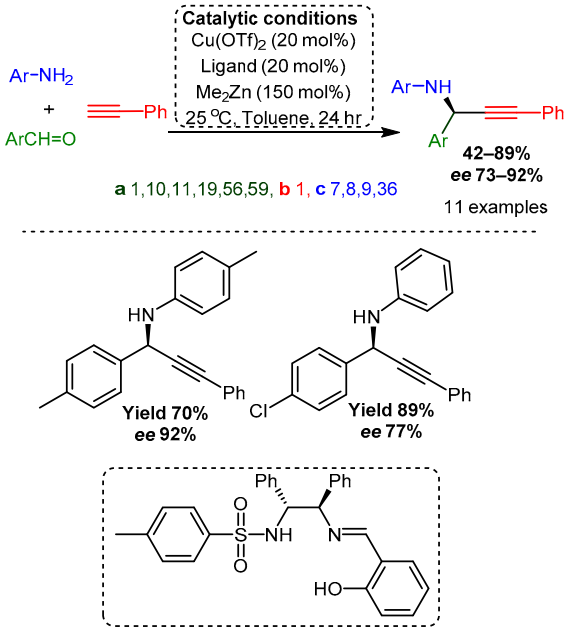

Scheme 43. Chiral tridentate *N*-tosylated aminoimine ligands Cu(II) complex-catalysed enantioselective addition of phenylacetylene to *N*-aryl arylimines.

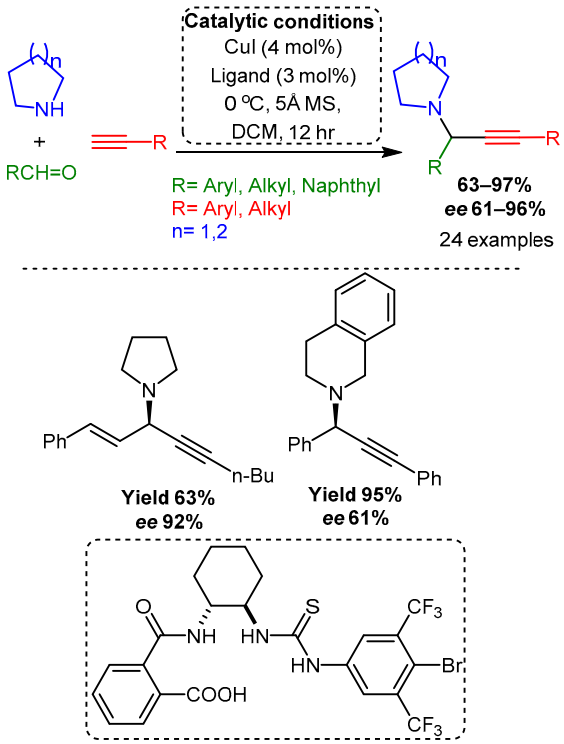

Scheme 44. Enantioselective A^3 Reactions of Secondary Amines with a Cu(I)/Acid−Thiourea Catalyst Combination.

Recently, Khare reported an efficient three component coupling protocol of aromatic aldehyde, deoxy sugar-based alkyne (α-2-deoxy propargyl glycoside), and heterocyclic amine that yielded chiral PAs with good to excellent in a stereoselective manner [107]. The method uses CuI as the catalyst and bifunctional ligand l-proline and is applicable in many substrates (Scheme 45).

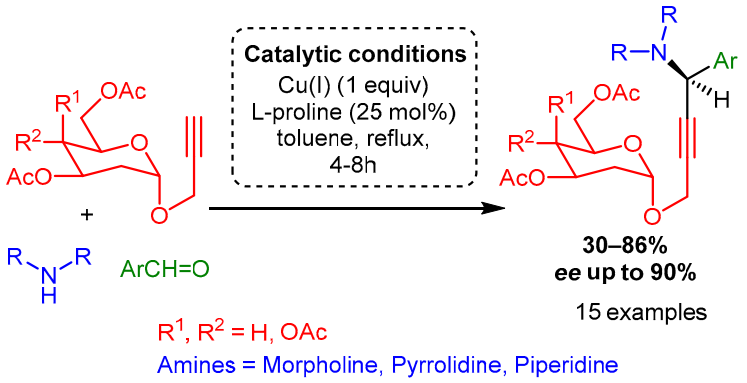

Scheme 45. Copper-mediated A^3-coupling reaction for the preparation of enantioselective deoxy sugar-based chiral PAs using bifunctional ligand L-proline.

4.2.5. Heterobidentate N,S-Ligands

Naeimi reported the only paradigm in this category in 2014 [108]. In this work, a novel thiosalen ligand based on a thioether has been prepared and readily coordinated with copper(I) salts (CuCl, CuBr, CuI, and CuCN). The new organometallic catalyst was used for the direct and enantioselective alkynylations of imines in an A^3-coupling reaction. In this reaction, the corresponding PAs were obtained as single products in excellent yields and with good enantioselectivities, as shown in Scheme 46.

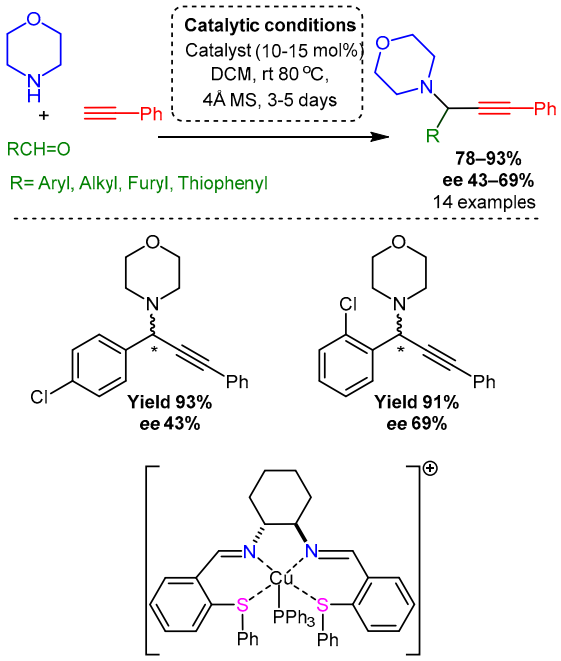

Scheme 46. An asymmetric A^3-coupling reaction catalysed by thioether-based copper(I) Schiff base complex.

4.3. Tridentate Ligands

Tridentate ligands such as PyBim and PyBox incorporate an aromatic pyridine ring with an additional ligand to activate the metal. The flanking oxazoline moieties restrict substrate access and confer product stereoselectivity.

4.3.1. Pybox

Since Li's initial report in 2002, PyBox ligands have been extensively explored. Chan attempted to increase the yield of Li's original ligand by using a surfactant [94]. Furthermore, Chan introduced a ligand wherein the isopropyl moieties in Li's initial ligand

were replaced with an indene-analogue and used a $CuPF_6$ catalyst [50]. Similarly, Boysen replaced these moieties with D-Glucosamine, increasing the ligand size and introducing secondary coordination effects (Scheme 47) [96]. Despite these efforts, the increased ligand complexity did not increase reaction yield or scope.

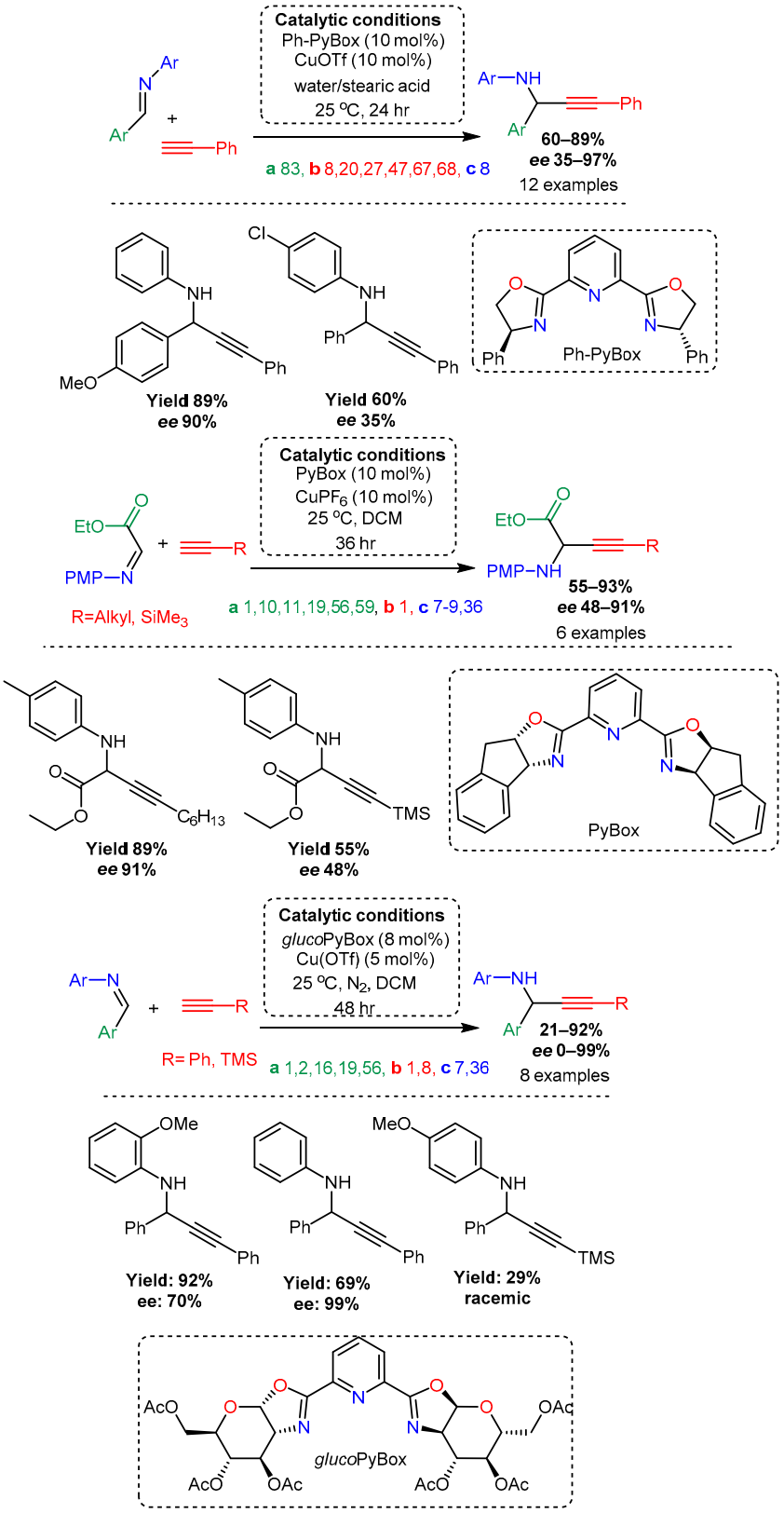

Scheme 47. Cu/PyBox catalytic system for the enantioselective addition of alkynes to imines.

Singh further expanded the scope and downstream versatility of the enantioselective A^3 coupling reaction using PyBox ligands [95]. PAs were generated in high yields and enantioselectivities using a PyBox catalyst, room temperature, and a Cu(I) salts. Later experiments explored alkynylation/lactamisation cascades to easily synthesise enantiomerically enriched isoindolinones on the gram scale or synthesise (indol-2-yl)methanamines in two additional steps [14,51]. Notably, attempts to employ Box-type ligands either failed to catalyse the reaction or led to the corresponding products in low yields (Scheme 48).

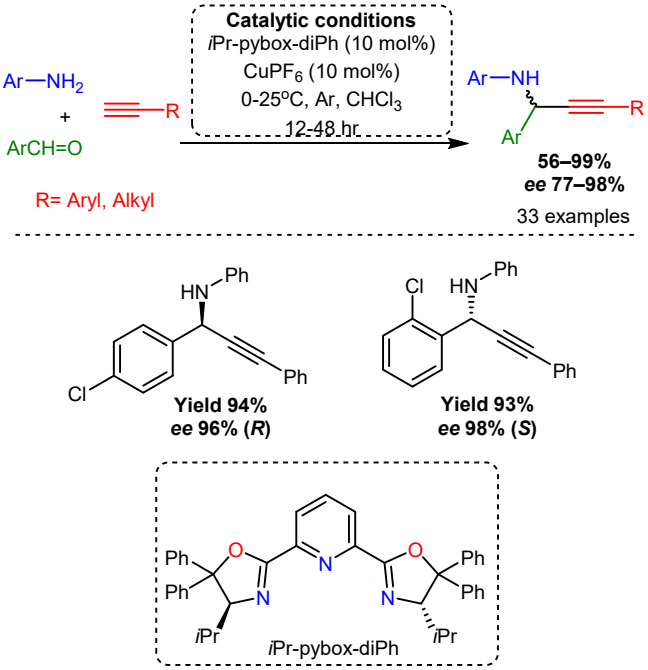

Scheme 48. Enantioselective one-pot three-component synthesis of Pas with *i*Pr-pybox-diPh ligand.

4.3.2. Pybim

Pybim ligands incorporate the main structural motif of PyBox ligands, but introduce additional complexity by replacing the oxazoline oxygen with a nitrogen atom and thereby introducing a dual functionality. This functionality can create a secondary coordination effect and potentially increase yield and *ee*.

Toru used several PyBim ligands to catalyse the A^3 component reaction, ultimately selecting a ligand with a benzoate secondary coordination sphere [97]. Notably, the use of the tridentate PheBim, a PyBim analogue that replaces the pyridine nitrogen with a carbon atom, did not lead to high yields and *ee*. PheBim ligands form a σ-bond with the metal centre, thus improving the thermostability of the complex (Scheme 49).

PyBim ligands were further explored by Nakamura, who used a surfactant to increase yield and *ee* [49]. In this methodology, the addition of a *tert*-Butyl substituent to the nitrogen atom of the imidazoline ligand combined with sodium dodecyl sulfate increases yield by promoting hydrophobic-hydrophobic interactions and allowing the reaction to proceed in the water. Using a hydrophobic ligand and a surfactant allowed the reaction to occur on tap or seawater with retention of high yield and *ee* (Scheme 50).

4.3.3. Acid-Thiourea

As described above, Seidel reported in 2015 an enantioselective A^3 coupling protocol that involved secondary amines, Cu(I) salts, and a hybrid acid–thiourea co-catalyst [72]. The efficacy of a series of co-catalysts was examined, and the best outcome was derived from the co-catalyst shown in Scheme 44. This work noted that the carboxylate could conceivably interact with copper to form a cuprate complex or serve as the counterion to an intermediate iminium species. These roles could be fulfilled by iodide, which appeared

to be involved in the enantiodetermining step. Notably, pyrrolidine-based PAs lacking directing groups can be transformed into allenes without enantiopurity loss.

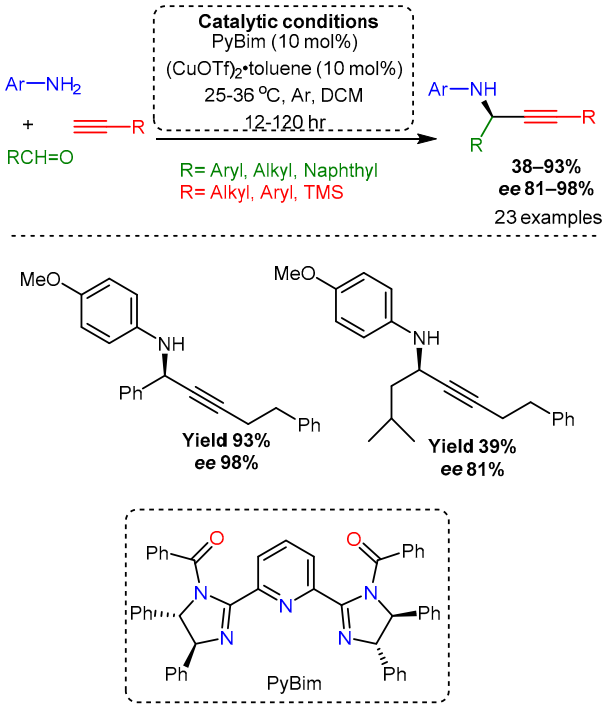

Scheme 49. Cu-PyBim catalysed A^3 coupling between aldehydes, arylamines, and alkynes for the enantioselective synthesis of PA derivatives.

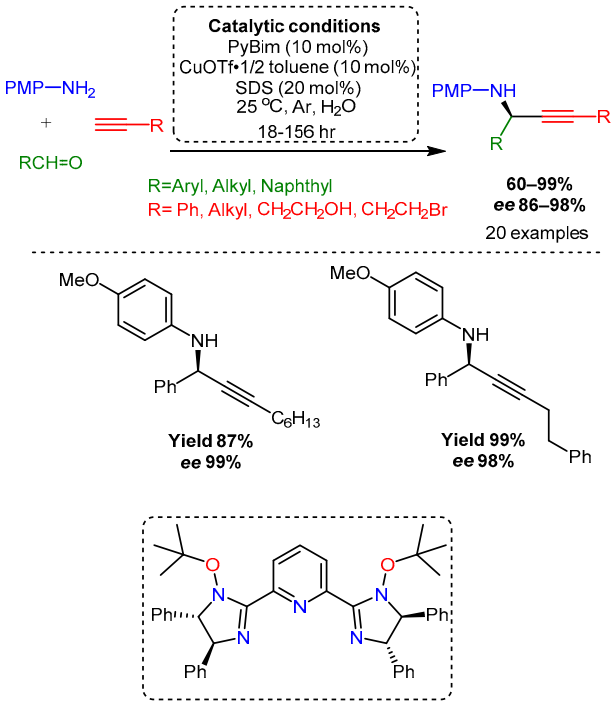

Scheme 50. Direct enantioselective three-component synthesis of optically active Pas in water.

4.4. NHC (Carbenes)

While N-Heterocyclic carbenes (NHCs) have been widely used as ligands in transition metal catalysis, NHCs have been used almost exclusively with Ag catalysts in the A^3 coupling reaction. Unlike more transient carbene species, NHCs contain a singlet ground-

state electronic configuration, which allows σ-donor ability via the sp^2-hybridized lone pair on the carbon into the metal [109].

The first use of an NHC with a Ag(I) catalyst was reported by Wang in 2008 [110]. In this work, successful ligands employed bulky moieties on the imidazolium salt (i.e., Bn > Me), and the greatest yields were achieved when the catalyst was placed on a polystyrene polymer support. Notably, the polystyrene-supported catalyst could be easily recovered and reused without significant loss of yield or catalyst leaching even after multiple cycles (Scheme 51).

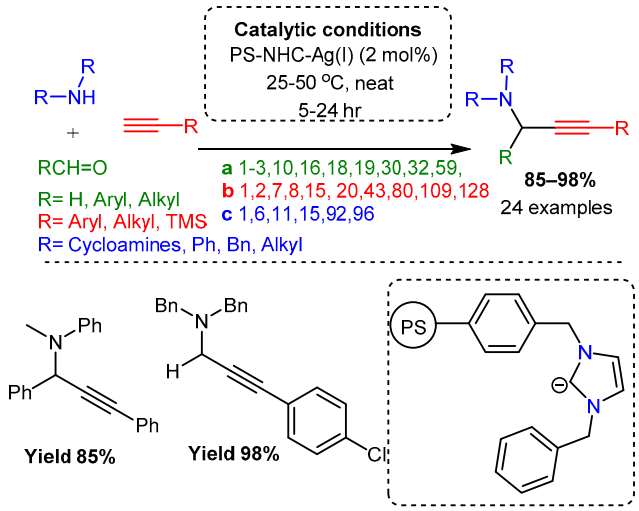

Scheme 51. A^3 coupling reactions catalysed by a reusable PS-supported NHC–Ag(I) under solvent-free reaction conditions.

In a later study, Navarro and co-workers used well-known and commercially available NHC ligands to catalyse the A^3 coupling reaction at room temperature, air, and less than three hours [111]. With amenable substrates, reaction times could be reduced to 20 min with yields up to 96% at catalyst loadings of 1 mol% (Scheme 52).

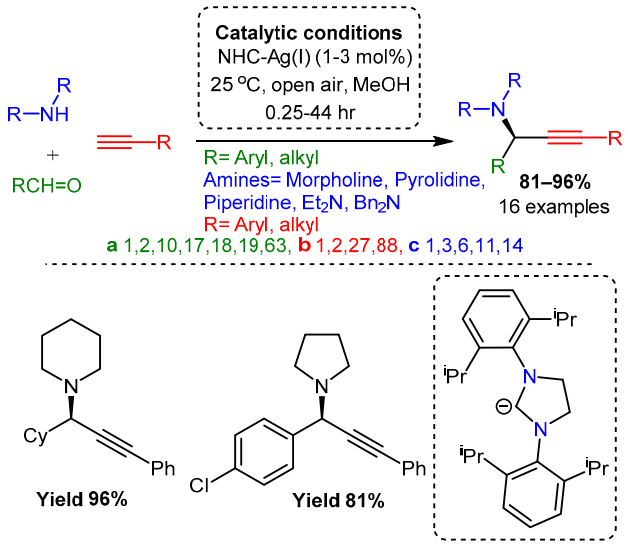

Scheme 52. *N*-heterocyclic carbene-Ag(I) complexes as catalysts for A^3 reactions.

Longo recently synthesised and applied NHC-Ag and Au complexes to the A^3 coupling reaction [112]. These complexes achieved high yields on the model system employed, and the Au-based complexes achieved higher yields than the previously reported Ag catalysts. DFT analysis attributed the higher reactivity to the Cl substituent on the NHC

complex, suggesting that the electron-withdrawing Cl substituents create an electropositive metal centre. In turn, the nucleophilic alkyne can more readily coordinate with the catalyst at the start of the catalytic cycle (Scheme 53).

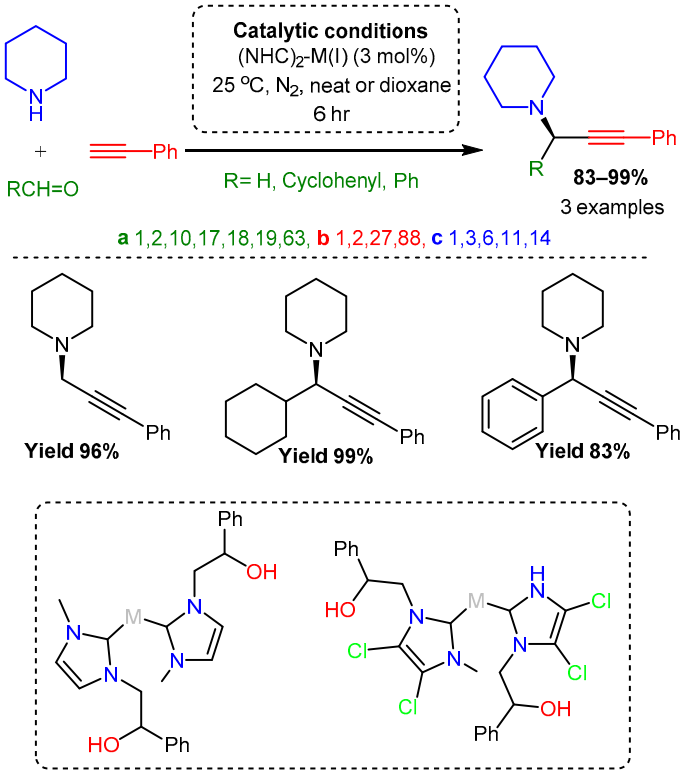

Scheme 53. NHC-silver and gold complexes active in A^3 coupling reaction.

5. A^3 Coupling with Well-Characterised Compounds

Well-characterised compounds that facilitate the synthesis of PAs will be presented in this chapter in chronological order. Knochel's pioneer work from 2002 [52] reported the enantioselective synthesis of PAs by copper-catalysed addition of alkynes to enamines. This protocol yields enantiomerically enriched, functionalised, and protected PAs under mild conditions. As discussed previously in this review, the catalytic system combines copper(I) sources and Quinap ligand (see Section 4.2.3.1). Notably, the authors first examined the efficacy of CuBr in synthesising PAs and subsequently introduced the chiral Quinap ligand into the catalytic protocol to enantiomerically access PAs. All catalytic reactions were conducted with in situ mixing of the reactants and the catalytic system; this example should be placed in the in situ sections of this review (see Section 4); however, the authors determined a crystal structure of a dimeric compound $[Cu(I)_2(\mu_2\text{-}Br)_2(quinap)_2]$ (**1**, Scheme 54).

The first example of a well-characterised silver compound for the A^3 coupling was reported in 2011 by Zou et al. [113] Authors isolated and fully characterised a family of N-heterocyclic carbene (1-cyclohexyl-3-arylmethylimidazolylidene) silver halides, and subsequently tested their catalytic efficacy in the A^3 coupling reaction. These well-defined species were found to promote the reaction of 3-phenylpropionaldehyde, phenylacetylene, and piperidine in only 2 h, 3% loading, and at 100 °C. From these studies, it is evident that the halide variation (Cl vs. Br) has a slight effect on performance, while the scope of the reaction was limited to only a few examples. The dimeric compound [AgCl(CyNaph-NHC)] (**2**, Scheme 55) was found to be the best pre-catalyst. Lastly, the authors proposed a slightly different mechanism considering the halide's presence without performing any experiment for mechanistic understanding.

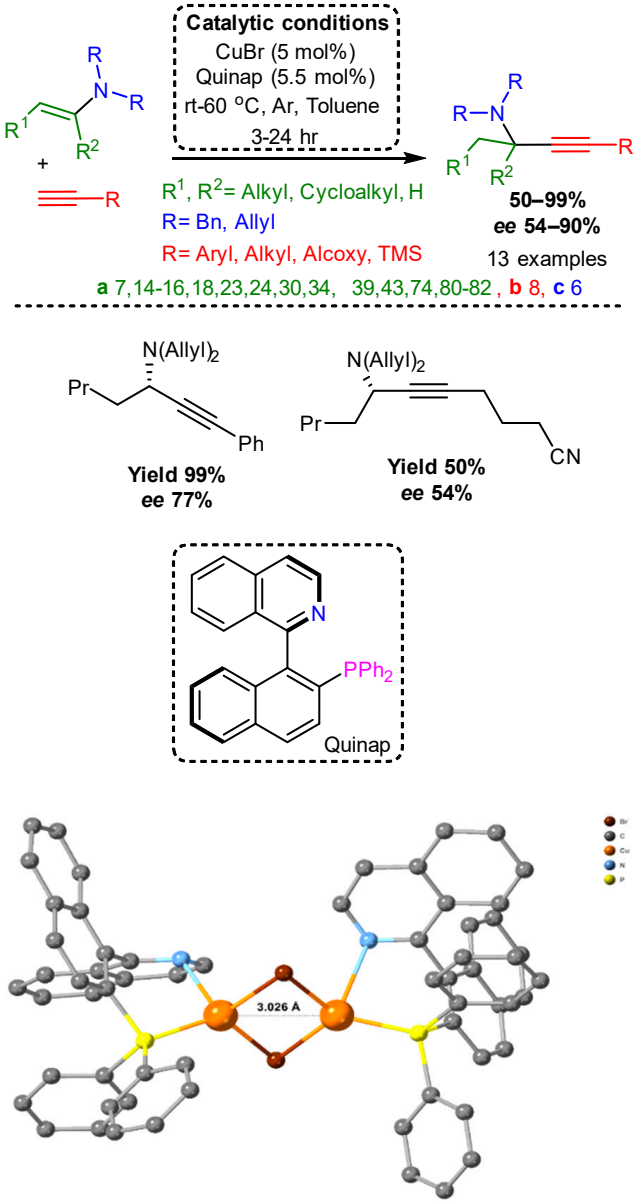

Scheme 54. (**upper**) Copper/Quinap-catalyzed the enantioselective synthesis of PAs by adding alkynes to enamines. (**lower**) The crystallographically characterised pre-catalyst.

A year later, Sun et al. [114] reported the synthesis and characterisation of a one-dimensional zig zag coordination polymer built from 1,4-bis(4,5-dihydro-2-oxazolyl)benzene (bdob) and Ag(I) nitrate and formulated [$Ag(NO_3)$(bdob)] (**3**, Scheme 56). Compound **3** was found to promote the A^3 coupling reaction in the open air at 1.9% catalyst loading and room temperature in the absence of additives. The authors identified the scope and limitations of their approach. The method applies to a good range of alkynes, aldehydes and amines; however, reactions with primary amines and aromatic aldehydes did not yield the desired product. Mechanistic understanding studies, compound stability, catalyst or reaction monitoring, and catalyst recovery efforts are not reported; therefore, the formation of molecular catalytically active species may not be excluded.

In 2015, Chen and Lao reported a dicopper(I) complex, $[Cu(I)_2(pip)_2]$ (**4**, Scheme 57), where pip is the (2-picolyliminomethyl)pyrrole anion, which was found to promote the A^3 coupling with a very low loading (0.4%) [115]. The reaction is completed within 2 h at 110 °C in toluene solvent and applies to a wide range of PAs (31 examples). Notably, the scope of the protocol does not include/omits primary aromatic amines and propargylic alcohols.

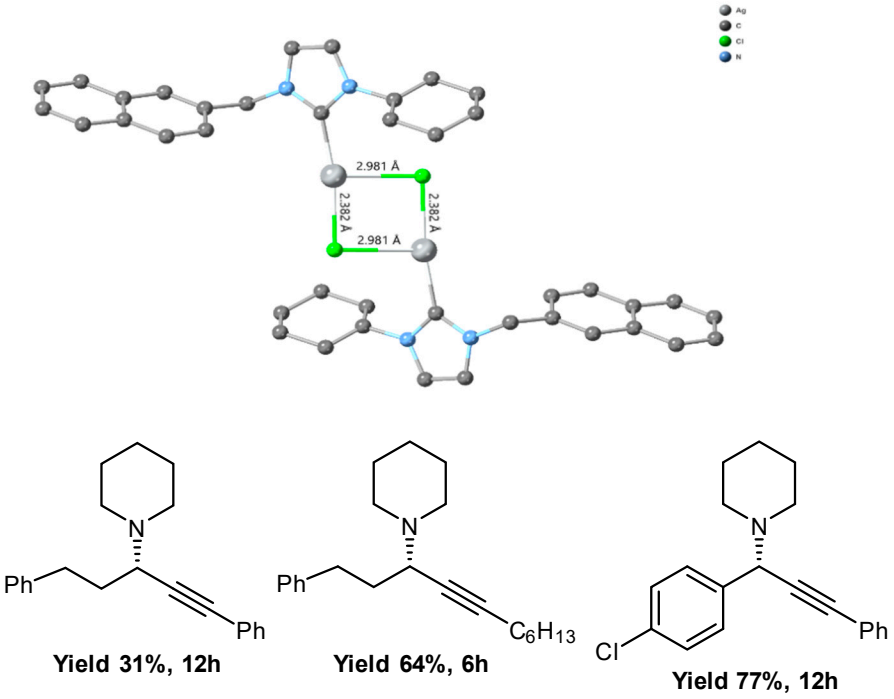

Scheme 55. (**upper**) The crystallographically characterised N-heterocyclic carbene-Ag(I) halides of 1-cyclohexyl-3-arylmethylimidazolylidenes pre-catalyst. (**lower**) Selected PA examples.

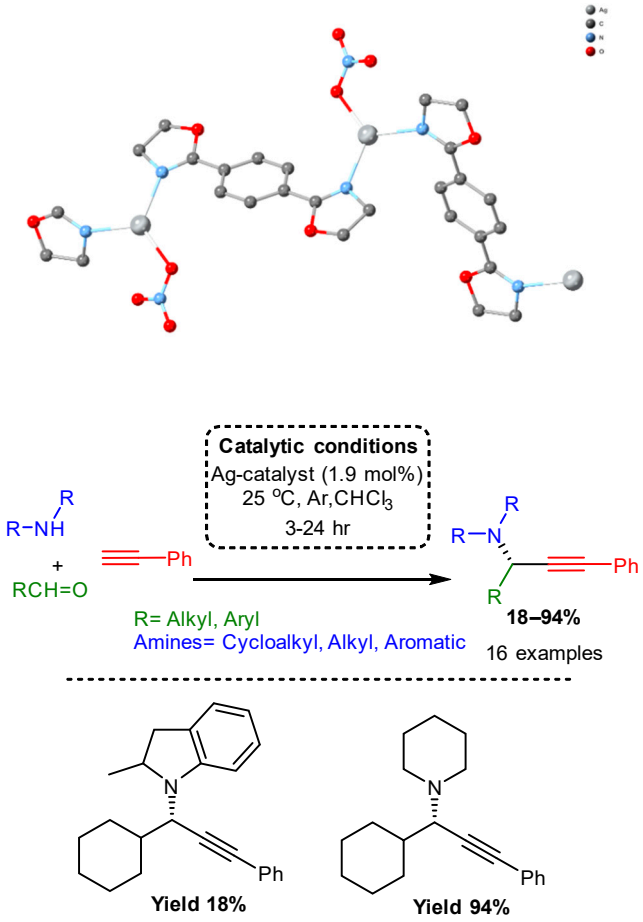

Scheme 56. (**left**) The crystallographically characterised Ag-precatalyst (**right**) scope and limitations of the method.

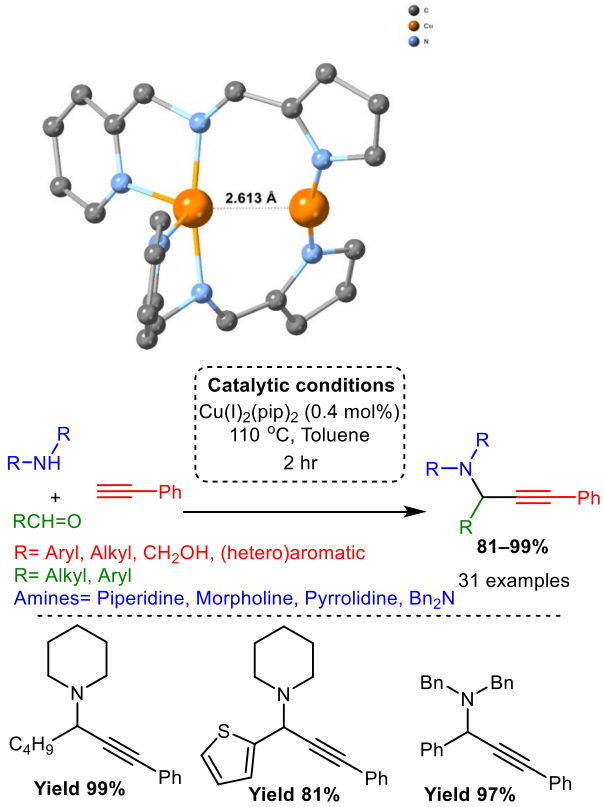

Scheme 57. (**left**) The crystallographically characterised pre-catalyst (**right**) the scope and limitations of the method catalysed by the dimeric complex.

In 2017, the first use of a tetrametallic Cu(I) complex to promote the A^3 coupling was reported by Garcia and Ocando-Mavárez [116]. The authors synthesised and characterised a copper(I) complex with *tert*-butyldiallylphosphine ligands. Single X-ray diffraction studies identified a cubane-like structure of the copper complex of formula $[CuCl\{\kappa^1(P)\text{-}^tBu\text{-}P(CH_2CH=CH_2)_2\}]_4$ (**5**). However, variable temperature NMR studies indicated a dynamic behaviour in solution generated by the cubane chair isomerisation due to the low stability of the cube-like structure caused by the strong strain of the Cu_4Cl_4 core for steric reasons. Compound **5** catalyses efficiently (17 examples) the A^3-coupling reaction of aromatic and aliphatic aldehydes with cyclic amines and phenylacetylene, yielding the corresponding Pas under mild reaction conditions and the absence of solvent (Figure 1 upper). Later this year, the same team reported the use of a known mononuclear compound [Cu{1-phenyl-2,5-bis(2-thienyl)phosphole}$_2$Cl] (**6**) [117] as a pre-catalyst in the A^3 coupling [118]. Compound **6** promotes single and double A^3-coupling reactions to synthesise mono- and bis-Pas, respectively (Figure 1, lower). The protocol has a broad scope, including aromatic and aliphatic aldehydes with cyclic amines and phenylacetylene, low pre-catalyst loading, high stability, and no need to use either purified reagents or a glovebox.

In 2017, our groups communicated their first effort to develop Cu(II) compounds as pre-catalysts for the A^3 coupling reaction [55]. Among a family of air-stable benzotriazole-based coordination compounds, we identified that compound $[Cu^{II}(L)_2(CF_3SO_3)_2]$ (**7**) was the most efficient pre-catalyst (Figure 2 upper). The protocol uses relatively mild conditions and provides results for a good range of substrates, mainly when aliphatic aldehydes and secondary amines are employed. Furthermore, it eliminates the need for expensive metal salts, inert atmosphere, and high loadings and uses 2-propanol, an environmentally friendly solvent [119]. We have also attempted to elucidate the reaction mechanism from an inorganic perspective; through a thorough synthesis and study of targeted coordination compounds, we evaluated how factors such as coordination geometry, anion, and ligand tuning affect the catalytic activity.

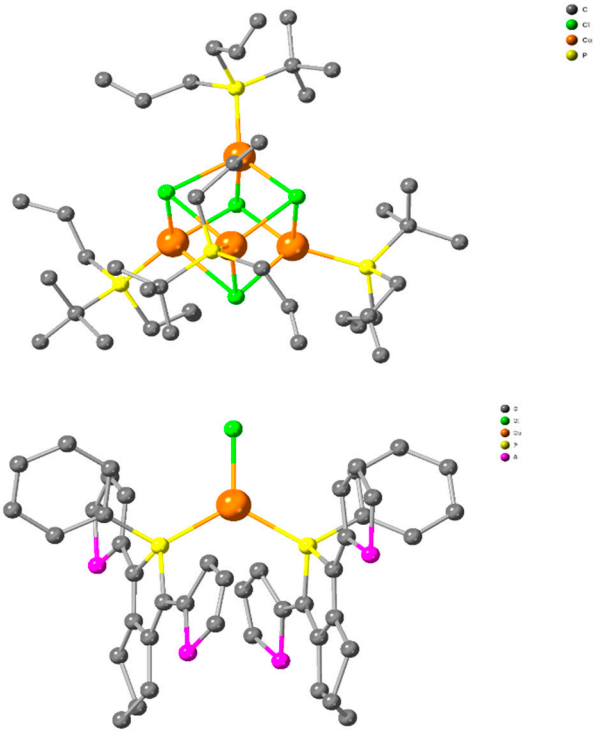

Figure 1. Novel tetramer copper(I) complexes containing diallylphosphine ligands. Compound **5** (**upper**) Compound **6** (**lower**).

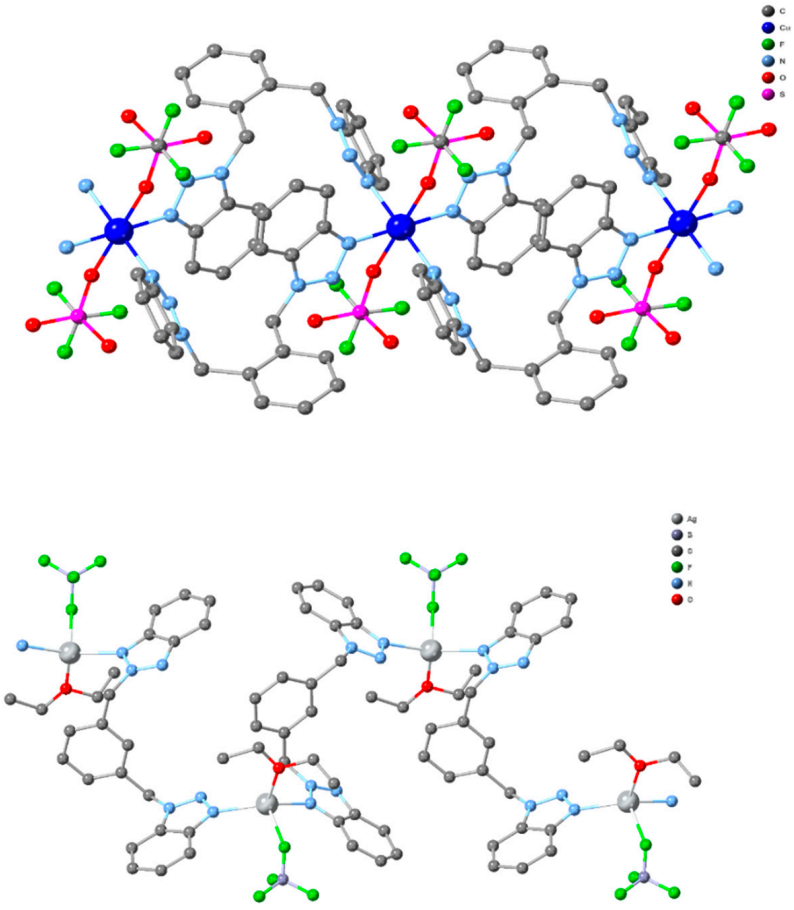

Figure 2. Compound **7** (**upper**) and compound **8** (**lower**).

One year later, inspired by the successful Ag-based paradigms described above, we elucidated the efficacy of Ag-benzotriazole compounds in promoting the A^3 coupling [120]. From our studies, we identified compound [Ag(L)(BF_4)(Et_2O)] (**8**) as the optimum pre-catalyst, affording several PAs in very good to excellent yields that are comparable or superior to other reported Ag^I-based methods (Figure 2 lower). The protocol involves easy synthetic conditions and avoids the use of an inert atmosphere or environmentally harsh solvents. Notably, compound **8** surpasses compound **7** in catalytic efficacy since only 0.5 mol% pre-catalyst loadings is required. However, in both cases, the A^3 coupling reaction is completed at elevated temperatures, a drawback that prohibits us from monitoring the reaction or identifying the active catalyst; therefore, we decided to explore and identify other systems that would permit reaction completion at room temperature.

In 2020, Peewasan and Powell reported a dimeric Cu(II) complex formulated as [$Cu_2(H_5L)(NO_3)_2$]NO_3·solv (**9**) [121], which was found to catalyse the A^3 coupling reaction. The protocol proceeds at room temperature for 24 h in *i*-PrOH and 1% catalyst loading with a good scope; however, no products were obtained when the aromatic and/or aliphatic primary amines were used. In addition, the stability of **9** was monitored using ESI-TOF mass spectrometry (Figure 3). These solution studies confirmed that the dimer retains its structure and that one coordinated nitrate is removed from one Cu centre, thus resulting in a free reactive site on copper. This allows a possible mechanism for the A^3 coupling reaction of this system to be proposed.

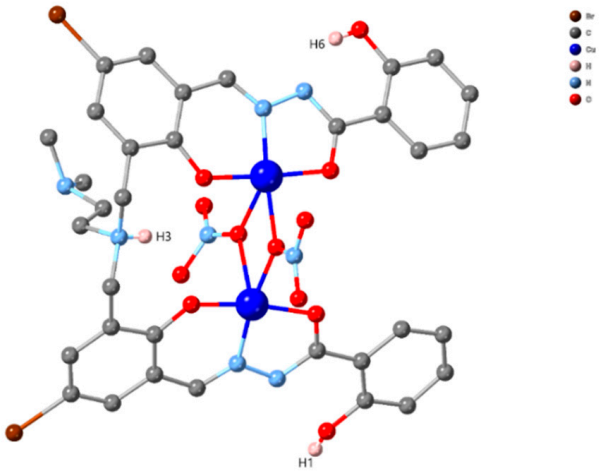

Figure 3. The crystallographically characterised pre-catalyst compound **9**.

In 2020, our group presented a Cu(II) based protocol that efficiently catalyses the A^3 coupling reaction in the open air and at room temperature using a salen-type compound {Cu(II)L} (**10**) (Scheme 58 upper) [122]. Notably, similar systems were reported before our work, but these protocols required elevated temperatures [123]. Our protocol has a good scope, unsuitable for primary amines or aromatic aldehydes, though the reaction is completed within 72 h, while the catalyst is recoverable and retains its structure. Vital to the success of this protocol is the use of the phenoxido salen-based ligand, which orchestrates topological control permitting alkyne binding with concomitant activation of the C–H bond and simultaneously acting as a template temporarily accommodating the abstracted acetylenic proton, and continuously generating, via in situ formed radical and a Single Electron Transfer (SET) mechanism, a transient Cu(I) active site to facilitate this transformation, as shown in Scheme 58. The proposed mechanism results from control experiments that included cyclic voltammetry, single-crystal X-ray diffraction, and theoretical studies.

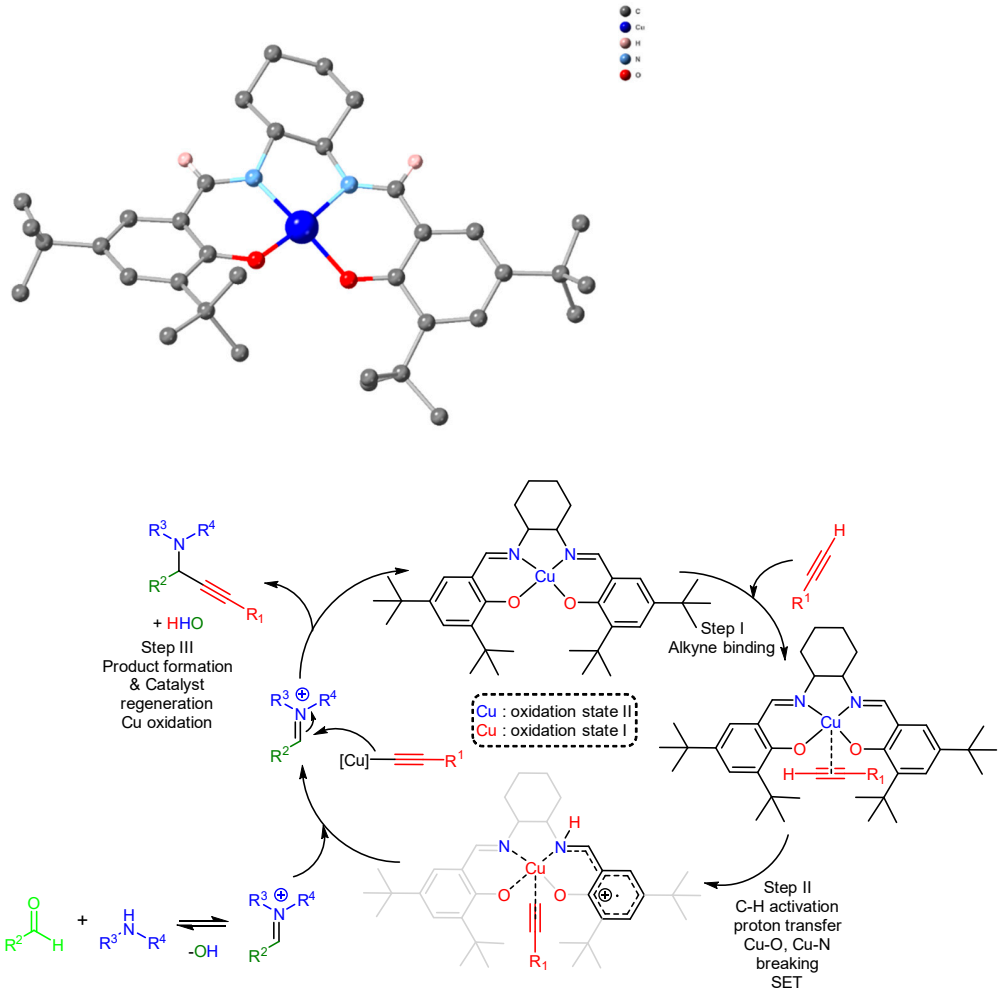

Scheme 58. The crystallographically characterised complex **10** and the possible reaction mechanism for A^3 coupling. Reproduced from ref. [124] with permission from the Royal Society of Chemistry.

In the same year, Singh reported a family of Cu(II) complexes that efficiently catalysed the A^3 coupling reaction at elevated temperatures, in toluene solvent, with very low catalyst loading and an extended scope [124]. Among this family of complexes, compound [Cu(II)(HL)(ClO_4)] (**11**), shown in Figure 4, achieved the highest yields, leading the authors to suggest a possible mechanism that involved a Cu(I)-acetylide intermediate.

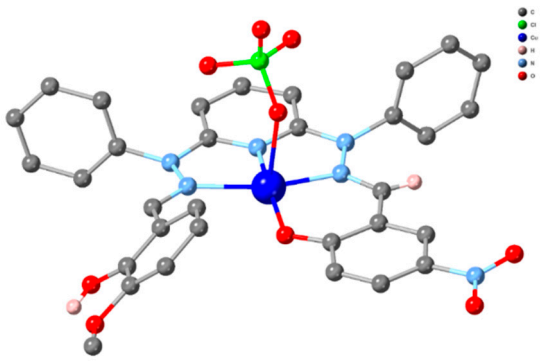

Figure 4. The crystallographically characterised pre-catalyst compound **11**.

In our last effort to identify efficient Cu(II) based A^3 protocols, we incorporated the bidentate 1-(2-pyridyl)benzotriazole (pyb) ligand to synthesise compound [$Cu^{II}(OTf)_2(pyb)_2$] ·2 CH_3CN (**12**) (Scheme 59 upper) [125]. Compound **12** enables the synthesis of a wide

range of PAs by the A^3 coupling reaction at room temperature in the absence of additives. The $N_{bridging}$ atom of this hybrid ligand imposes exclusive *trans* coordination at Cu and allows ligand rotation, while the overall structure of the ligand, in particular, the presence of the $N_{pyridine}$ atom, modulates charge distribution and flux, thus orchestrating structural and electronic pre-catalyst control permitting alkyne binding with simultaneous activation of the C−H bond through an in situ catalytically active [Cu^{I}(OTf)(pyb)] species. This notion is not feasible in the *cis*-[$Cu^{II}(OTf)_2(bpy)_2$], indicating that the stereochemistry of the pre-catalyst and the nature of the *N*,*N*′-bidentate ligand are parameters to be taken into account when designing such catalysts. We performed various experiments, including cyclic voltammetry, theoretical calculations, and reactions in the open air and under Ar or N_2 atmosphere, to understand the reaction mechanism; the proposed mechanism that involves two different pathways is shown in Scheme 59 lower.

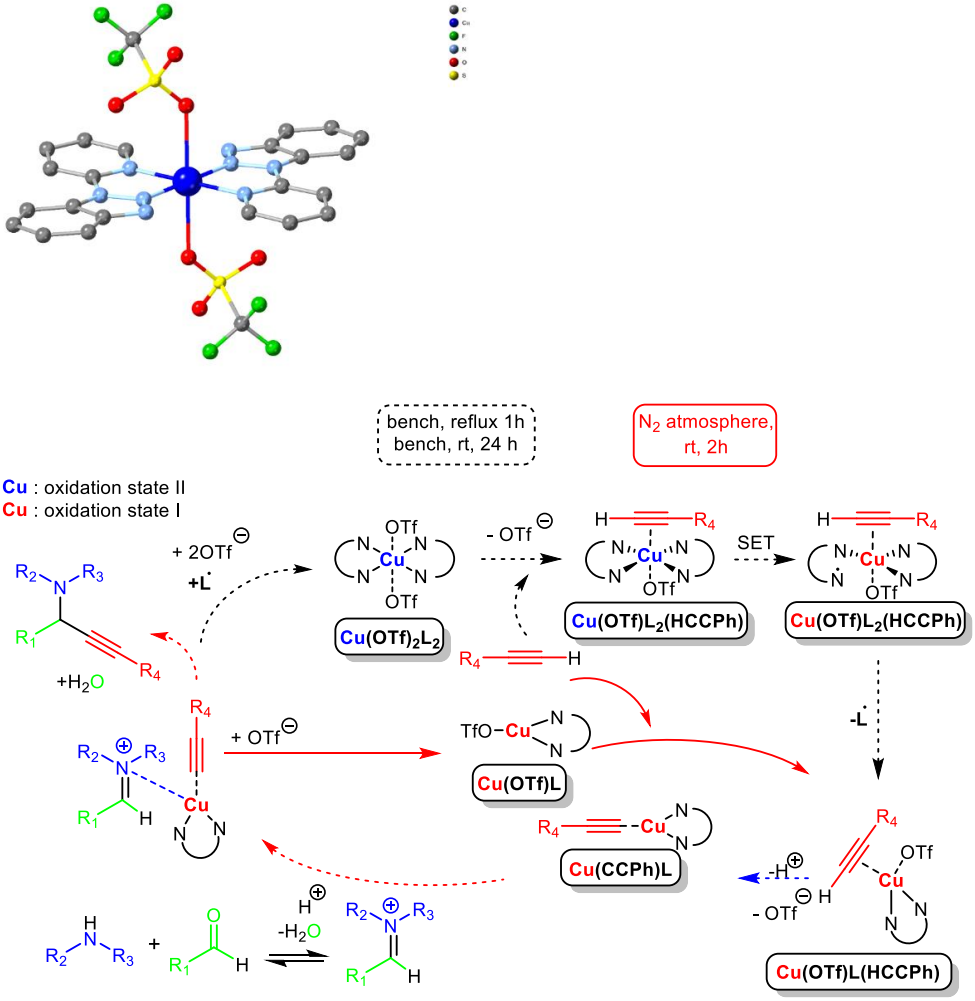

Scheme 59. The crystal structure of compound **12** (**upper**) and the proposed mechanism for the A^3 coupling (**lower**), reproduced with permission from ref. [126] Chemistry—A European Journal; published by John Wiley and Sons, 2021.

6. Visualisation and Comparisons

The extended classification allows us to identify popular general aspects of the synthetic protocols suggesting that the protocols involving in situ generated catalytic species are the dominant synthetic method (74–26%) (Figure 5A), Cu is the most prevalent metal centre used for this transformation (68%) (Figure 5B), bidentate ligands are the most common ligands used followed by tridentate analogues (Figure 5C), whereas ligands containing N or P heteroatoms are the most common (Figure 5D), 42% of the experiments have been

carried out in the open air (Figure 5E), non-coordinating solvents such as toluene and dichloromethane are the most popular choice (Figure 5F). Finally, almost half of the experiments have been conducted at room temperature (Figure 5 lower), whereas lower temperatures have been used to improve the enantioselectivity.

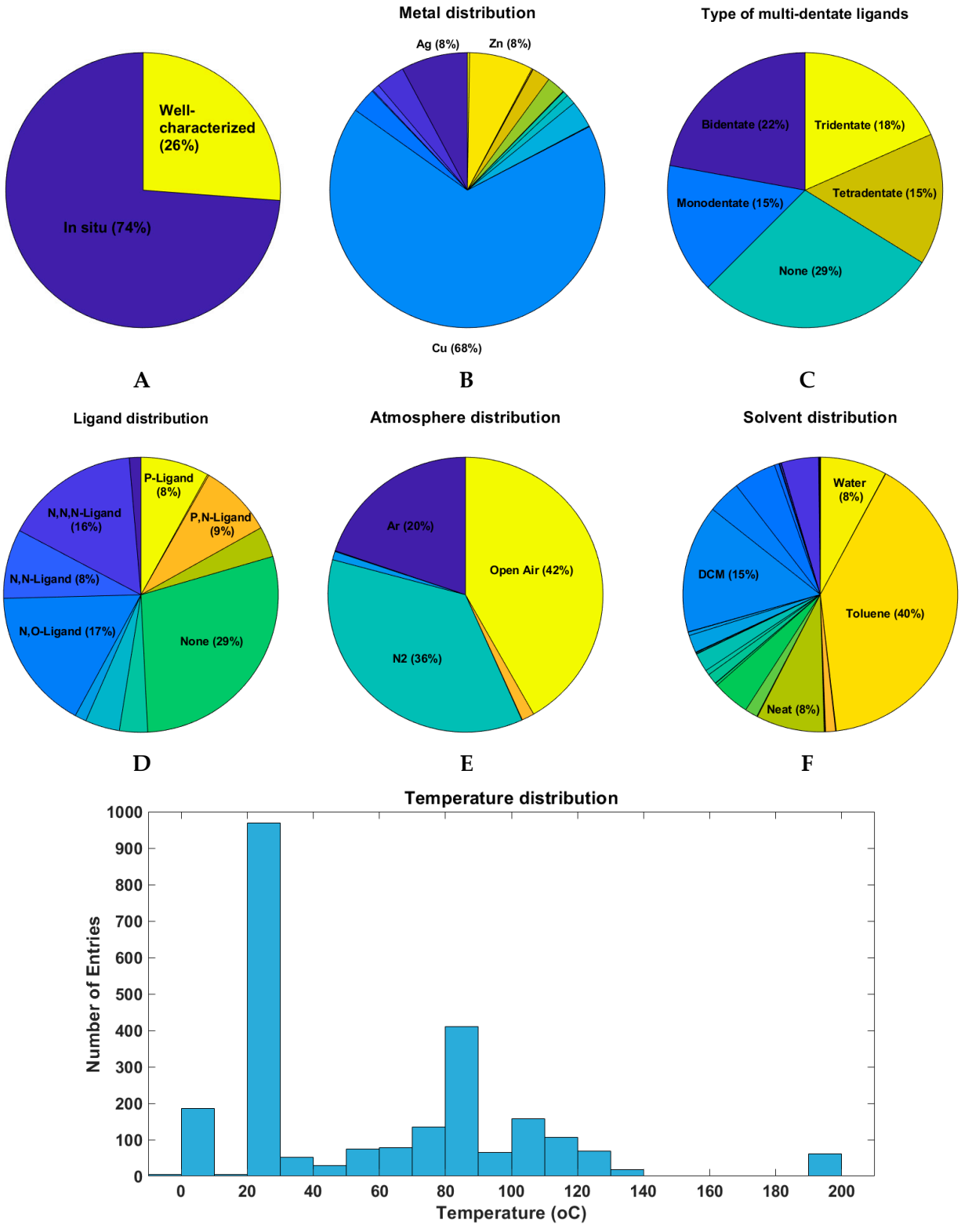

Figure 5. (**upper**) Distribution for in situ and well-characterised entries (**A**), metal distribution (**B**), type of ligand distribution (**C**), (**middle**) ligand distribution (**D**), atmosphere distribution (**E**), solvent distribution (**F**), (**lower**) temperature distribution.

6.1. Solvent

We attempt to visualise the impact of the solvent on the yield and the chirality of the final product (Figure 6). From these data, it is evident that non-coordinating solvents improve yield and *ee*; therefore, it is wise to envisage solvents such as chloroform, dichloromethane, and toluene as the best to use for the A^3 coupling reaction.

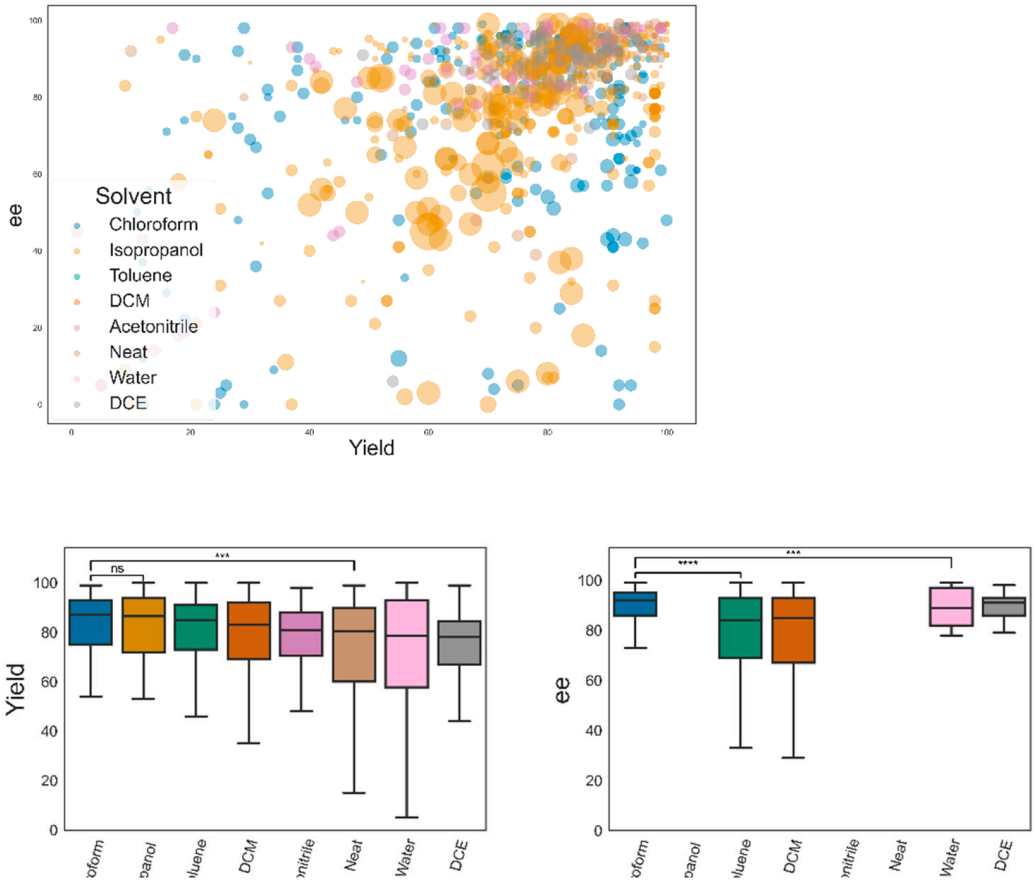

Figure 6. (**upper**) Solvent effects on yield and *ee*. Catalysts with more than 5 entries, solvents with more than 50 entries, and yields greater than 0 shown (**lower**) yield (**left**) and *ee*s (**right**) of solvents. Statistical analysis performed using Student's *t*-test ($p = 0.97$, 0.0006) ($p = 3.92 \times 10^{-7}$, 0.003). Symbol Meaning: ns $p > 0.05$, *** $p \leq 0.001$, **** $p \leq 0.0001$ (For the last two choices only).

6.2. Metals

As previously mentioned, a variety of metal salts have been used to catalyse the A^3 coupling reaction. Of these, the most frequently used are Cu (1634 entries), Ag (189 entries), Zn (182 entries), Au (82 entries), and Fe (77 entries). Across these conditions, Au showed a significantly higher yield than Cu ($p = 0.0067$) and all other metals but has been in limited use, possibly due to its high cost (Figure 7, left). Moreover, only Cu and Zn have catalysed the enantioselective A^3 coupling reaction, with Cu performing significantly better than zinc ($p = 0.013$, Figure 7, right).

To provide an insight into the effects of different metal salts and ligands on A^3 yield and enantioselectivity, salts with more than 50 instances were selected for and analysed (Figure 8). Comparison of metal salt yields revealed that $CuPF_6$ had the highest yield (median = 90%), $ZnEt_2$ had the lowest yield (median = 65.5%), and CuBr was the most widely used (276 entries, 20 references). Out of the 15 salts with over 50 entries, only 7 had been used to catalyse the enantioselective A^3 coupling reaction, highlighting the many unexplored salts used in asymmetric A^3 reactions. In addition, CuBr had the highest *ee* (median = 92%) and $ZnEt_2$ had the lowest *ee* (median = 73%) of the salts used in enantioselective reactions. Bulk analysis of reactions obfuscates tuning of catalysts and ligands,

and so we further selected metal salts with more than 50 instances and yields greater than 50%. These results did not significantly alter the median or standard deviations for each salt, suggesting that different combinations of metal salt, ligand, and substrate can lead to different yields and *ee*.

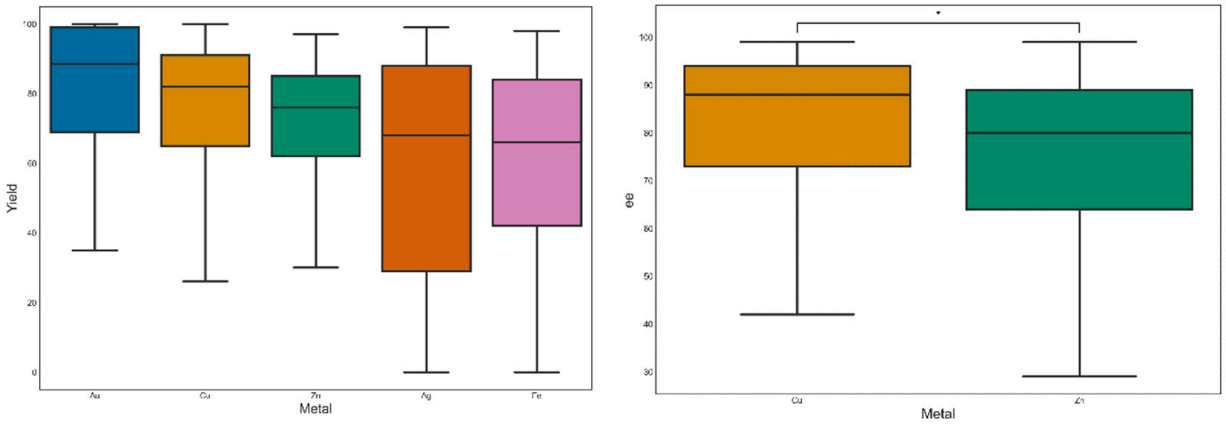

Figure 7. (**left**) Yields of different metals with more than 50 entries (**right**) *ee* of enantioselective A^3 reactions (*ee* > 0). Statistical analysis performed using Student's *t*-test ($p = 0.013$). Symbol Meaning: * $p \leq 0.05$ (For the last two choices only).

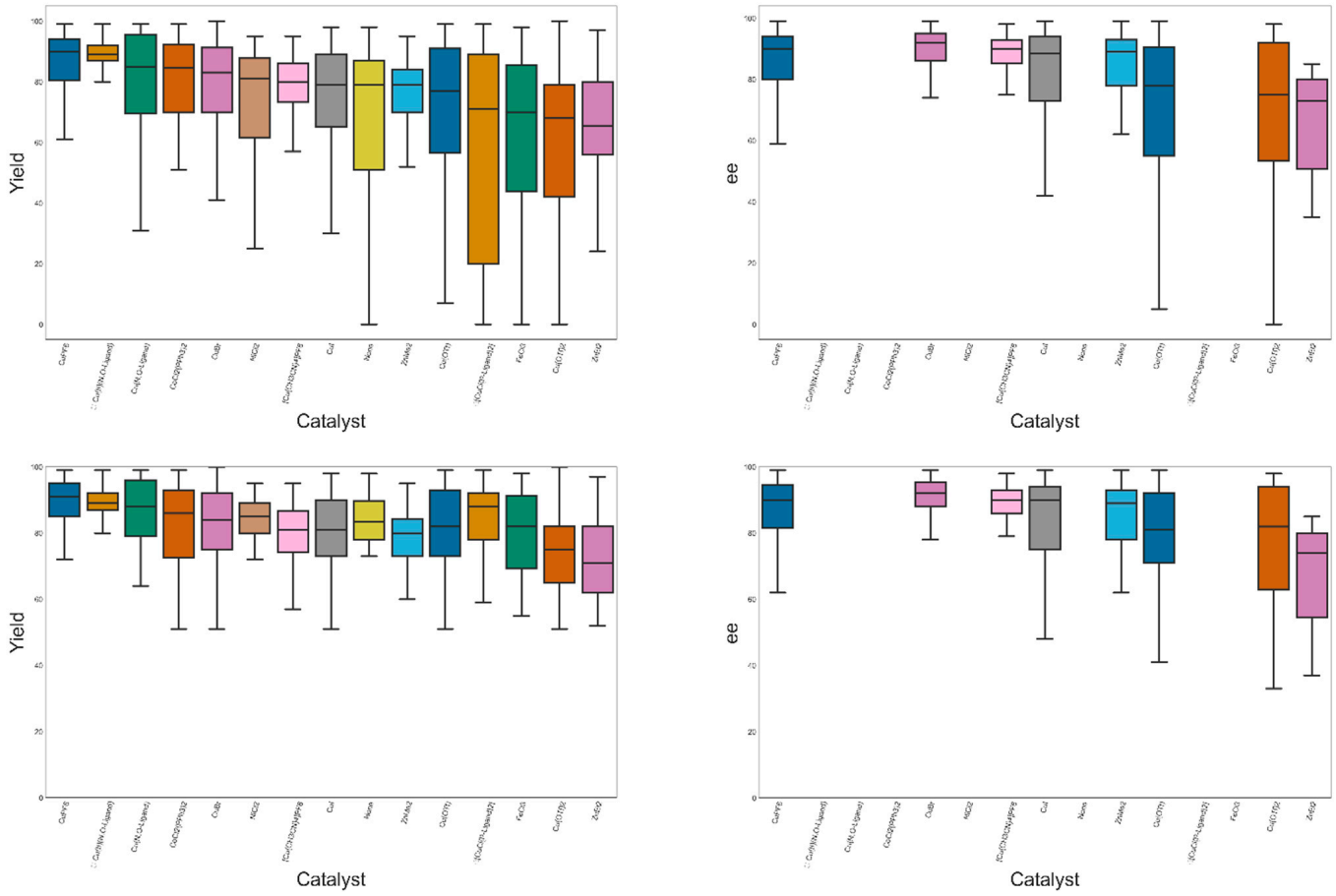

Figure 8. (**upper**) Yields (**left**) and *ee* (**right**) of different metal salts with more than 50 entries. (**lower**) Yields (**left**) and *ee* (**right**) of different metal salts with more than 50 entries and yield greater than 50%.

6.3. Ligands

Ligand effects on yield and *ee* were analysed by comparing the ligands with greater than 25 entries (Figure 9). Unlike the metal salts, the highest yielding ligands did not correlate with high *ee*. For example, the highest yielding ligand, (2-picolyliminomethyl)pyrrole (median yield = 96.5%), showed no enantioselectivity, while the ligand StackPhos showed 94% median *ee* with only 79% median yield. These results reinforce the idea that catalyst and ligand selection can be tuned according to the substrate to produce the desired product.

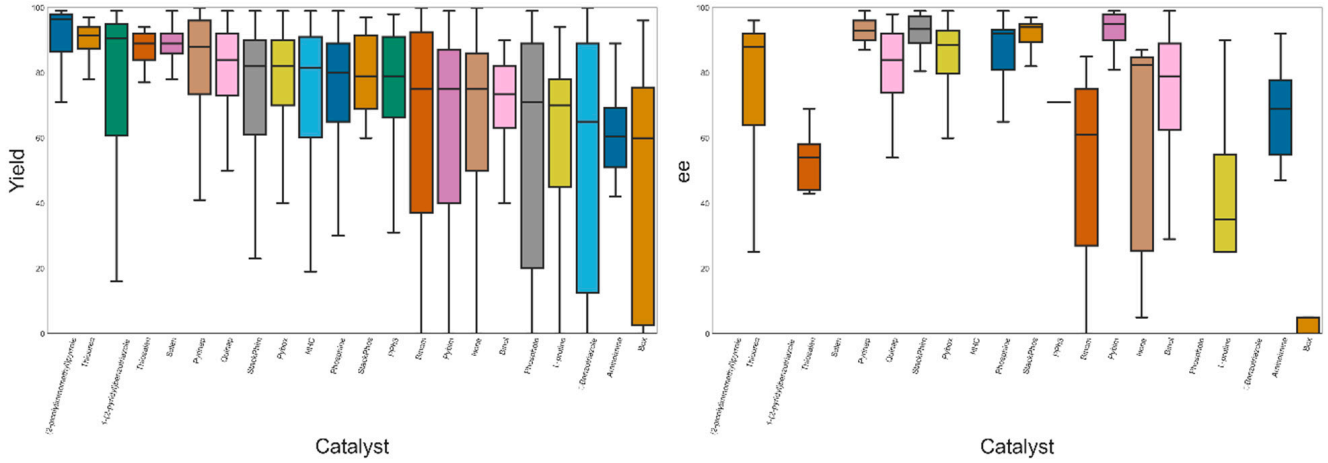

Figure 9. (**left**) Yields of ligands with more than 25 entries. (**right**) *ee* of ligands with more than 25 entries.

Ligands were categorised according to their coordinating atom and analysed to examine the effects of different coordinating atoms on PA yield and *ee* (Figure 10). Overall, the employed ligands had similar median yields of 82.4 ± 5.6% but divergent enantioselectivities (median of 79.6 ± 14.4%).

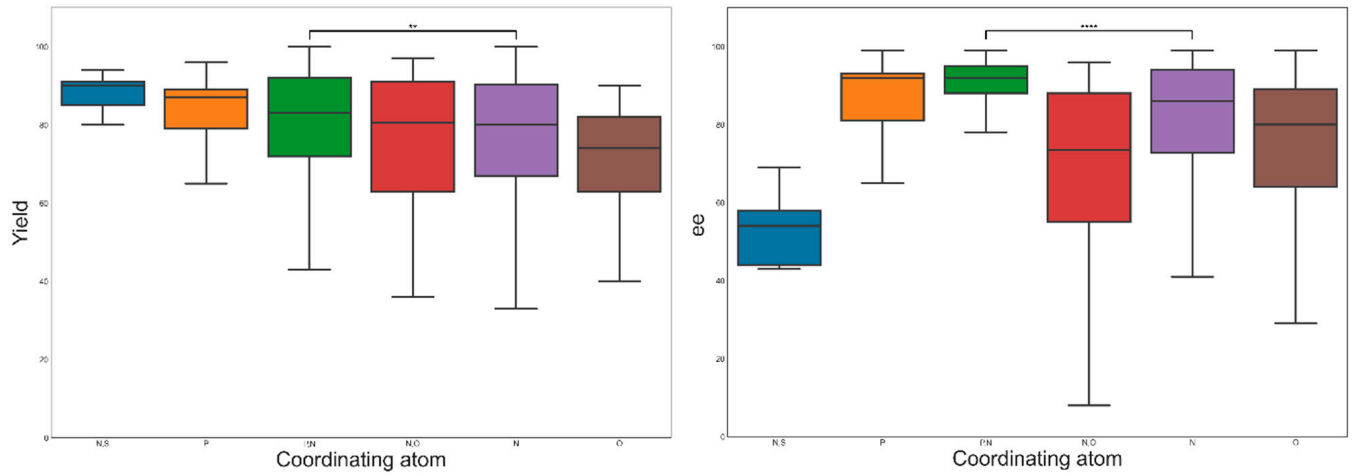

Figure 10. (**left**) Yield of enantioselective A^3 reactions (*ee* > 0). Statistical analysis performed using Student's *t*-test ($p = 0.0098$) (**right**) *ee* of enantioselective A^3 reactions (*ee* > 0). Statistical analysis performed using Student's *t*-test ($p = 1.56 \times 10^{-10}$). Symbol Meaning: ** $p \leq 0.01$, **** $p \leq 0.0001$ (For the last two choices only).

Since the ligand classes with the highest *ee* employed a phosphorous or nitrogen coordinating atom, we further explored the effect of multiple coordination spheres (i.e., monodentate, bidentate, tridentate) on yields and enantioselectivities (Figure 11). Our analysis revealed that bidentate N-ligands (e.g., Pybim) had significantly lower yields and enantioselectivities than tridentate counterparts (e.g., Pybox). Moreover, introducing a secondary coordination sphere (e.g., Binam) resulted in a reduction in yields and *ee*.

The P,N-ligands employed to catalyse the asymmetric A^3 reaction have been exclusively bidentate ligands without a secondary coordination sphere (Figure 12). We extended our analysis to these ligands since several new P,N-ligands have been synthesised in recent years (e.g., Pyrinap). Intriguingly, we found no significant increase in yield when comparing the most recently employed ligand, Pyrinap, and the first-employed ligand, Quinap. While Pyrinap did show a significant increase in *ee* compared to Quinap, in comparison with similar advanced P,N-ligands StackPhim/StackPhos showed no significant increase in enantioselectivity.

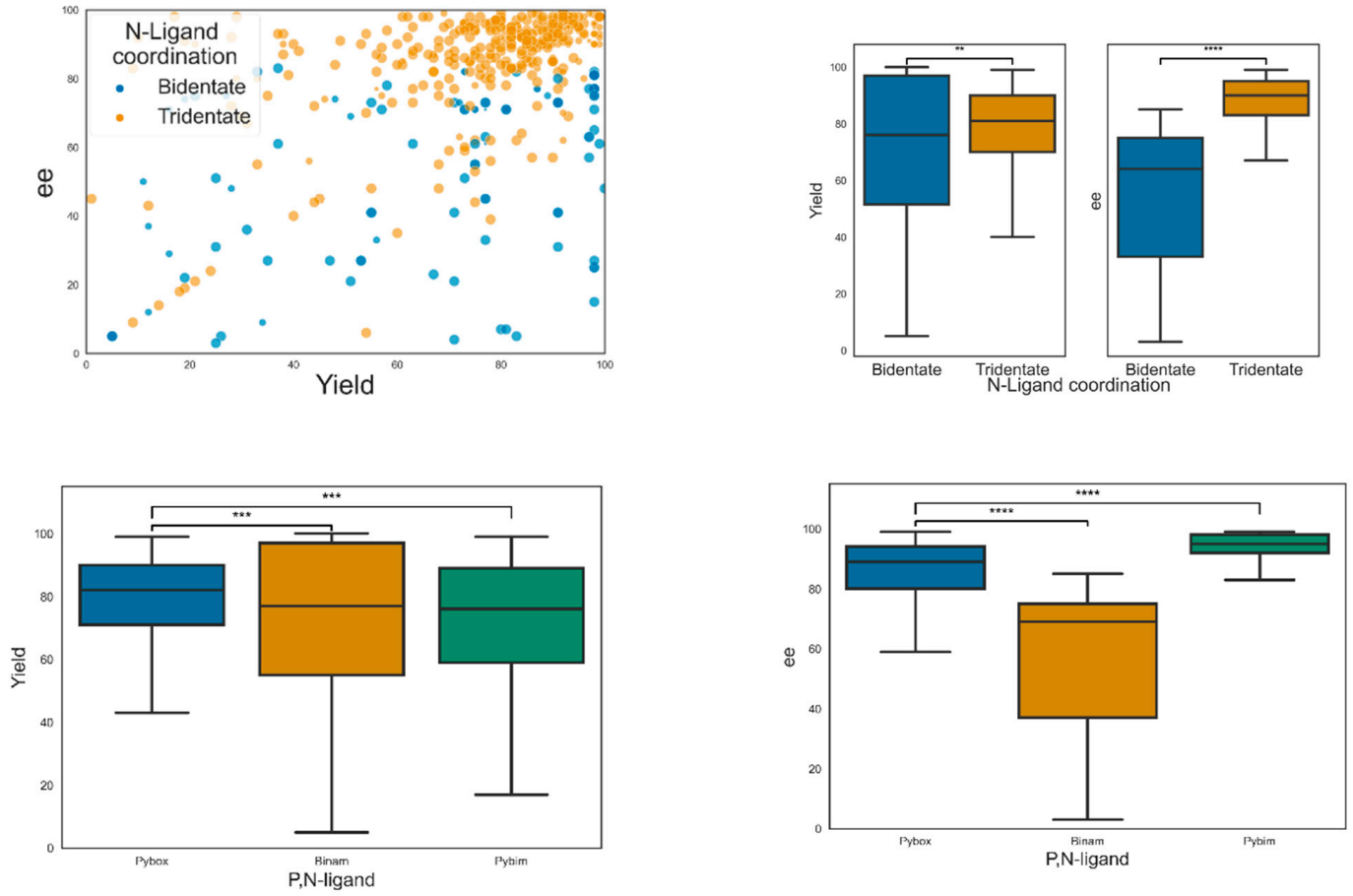

Figure 11. (**upper**) Distribution of N-homoligands by coordination. (**left**) Comparison of yield and *ee* for N-homoligands. Significance calculated using Student's *t*-test (p = 0.004, 1.74×10^{-39}) (**right**). (**Lower**) Comparison of yield N-homoligands with secondary coordination sphere, the significance was calculated using Student's *t*-test (p = 0.0074, 0.0011) (**left**) Comparison of *ee* N-homoligands with secondary coordination sphere. Significance calculated using Student's *t*-test ($p = 1.55 \times 10^{-27}$, 0.00015) (**right**). Symbol Meaning: ** $p \leq 0.01$, *** $p \leq 0.001$, **** $p \leq 0.0001$ (For the last two choices only).

6.4. Substrates

The yield, enantioselectivity, and speed of the A^3 coupling reaction are influenced by both the metal catalyst and the substrate selection. In this review, we have classified substrates according to their functionality: aromatic (e.g., aniline), cyclic (e.g., morpholine), aliphatic (e.g., pivalaldehyde), and hybrid (e.g., 2-phenylpropanal).

6.4.1. Amines

Our database reveals that 140 cyclic, 15 aliphatic, 588 aromatic, and 110 hybrid amines have been used as substrates in the A^3 coupling reaction. Of these, 592 have been primary, and 261 have been secondary. Comparison of these amines (Figure 13) reveals a wide variation in the yields and enantioselectivities, likely due to the catalyst, solvent, and temperature effects. Despite the heavy use of aromatic amines, our database reveals a significant increase in PA yield when using cyclic amines (Figure 13B, p = 0.00019) although this trend is not observed when looking at enantioselective reactions. As has been previously observed, secondary amines have a significantly higher yield and *ee* than primary amines (Figure 13D), likely due to the differences in reactivities of the imine and iminium intermediates.

6.4.2. Aldehydes

Our database reveals that 19 cyclic, 673 aromatic, 114 aliphatic, and 47 hybrid aldehydes have been used as substrates in the A^3 coupling reaction. The broad distribution of aromatic aldehydes (Figure 14) highlights the importance of reaction conditions in dictating both yield and enantioselectivity. Comparison of median yields and *ee* (Figure 14 lower) reveals that the cyclic aldehydes, despite being sparsely used, have a significantly higher yield and *ee* than the widely used aromatic class.

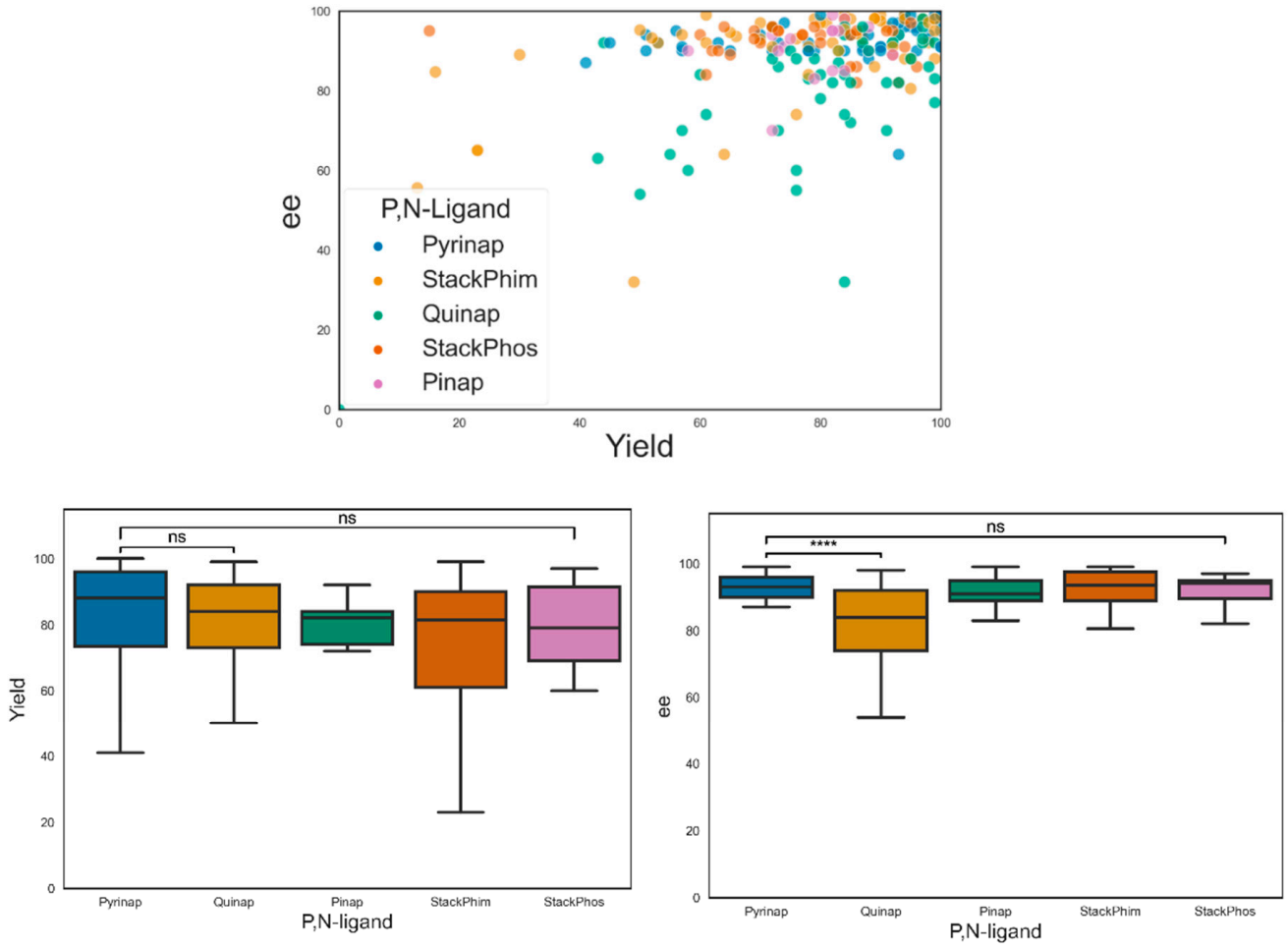

Figure 12. *ee* vs. yields of P,N-ligands. Statistical analysis performed using Student's *t*-test (p = 0.085, 0.27; $p = 2.81 \times 10^{-6}$, 0.37). Symbol Meaning: ns $p > 0.05$, **** $p \leq 0.0001$ (For the last two choices only).

6.4.3. Alkynes

Similarly, our database revealed 5 cyclic, 612 aromatic, 228 aliphatic, and 8 α-2-deoxy sugar aldehydes used as substrates. As observed with the aldehyde and amine components, the aromatic alkynes have a broad distribution of yields and *ee*. The cyclic alkynes (e.g., 1-ethynylcyclohex-1-ene) had lower yields and *ee* than aromatic and aliphatic alkynes; notably, there was a significant difference observed in the yields of aliphatic and aromatic alkynes but not in the *ee* (Figure 15 lower). These suggest that the effect a substrate has on yield does not affect the enantioselectivity of the reaction.

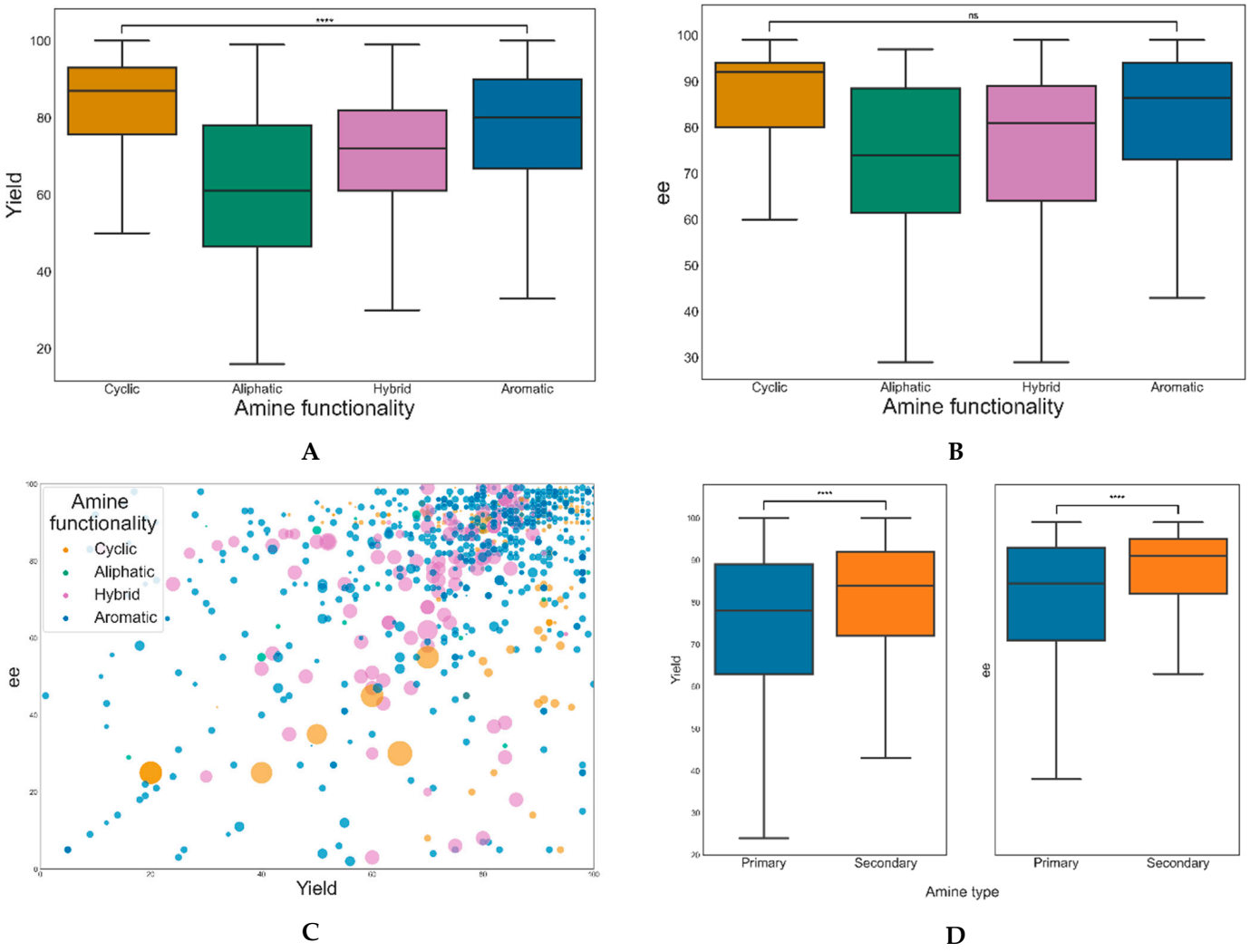

Figure 13. (**A**) Yield of amines with different functionalities; statistical analysis performed using Student's *t*-test ($p = 0.0002$). (**B**) *ee* of amines with different functionalities; statistical analysis performed using Student's *t*-test ($p = 0.19$). (**C**) Distribution of amines with enantioselectivites greater than 0, (**D**) comparison of primary vs. secondary amines on yield and *ee*. Statistical analysis for C and D wasperformed using Student's *t*-test ($p = 1.42 \times 10^{-5}$, 3.54×10^{-5}) (**right**). Symbol Meaning: ns $p > 0.05$, **** $p \leq 0.0001$ (For the last two choices only).

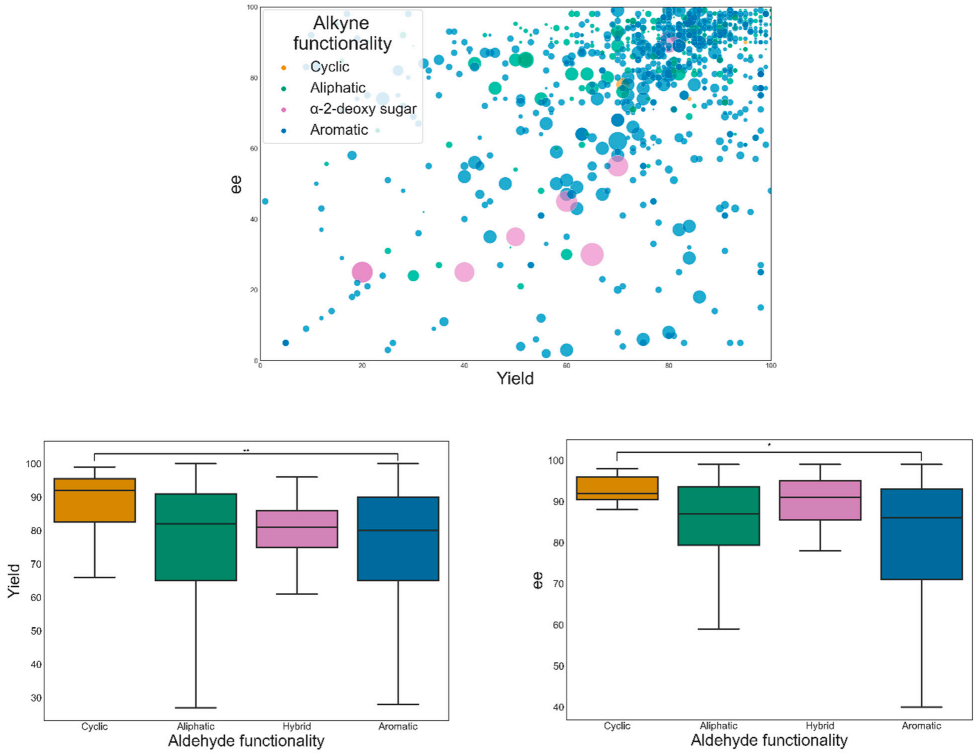

Figure 14. (**upper**) Distribution of aldehydes with enantioselectivites greater than 0. (**lower**, **left**) Yield of aldehydes with different functionalities. Statistical analysis performed using Student's *t*-test ($p = 0.0045$); (**lower**, **right**) *ee* of aldehydes with different functionalities. Statistical analysis performed using Student's *t*-test ($p = 0.015$). Symbol Meaning: * $p \leq 0.05$, ** $p \leq 0.01$ (For the last two choices only).

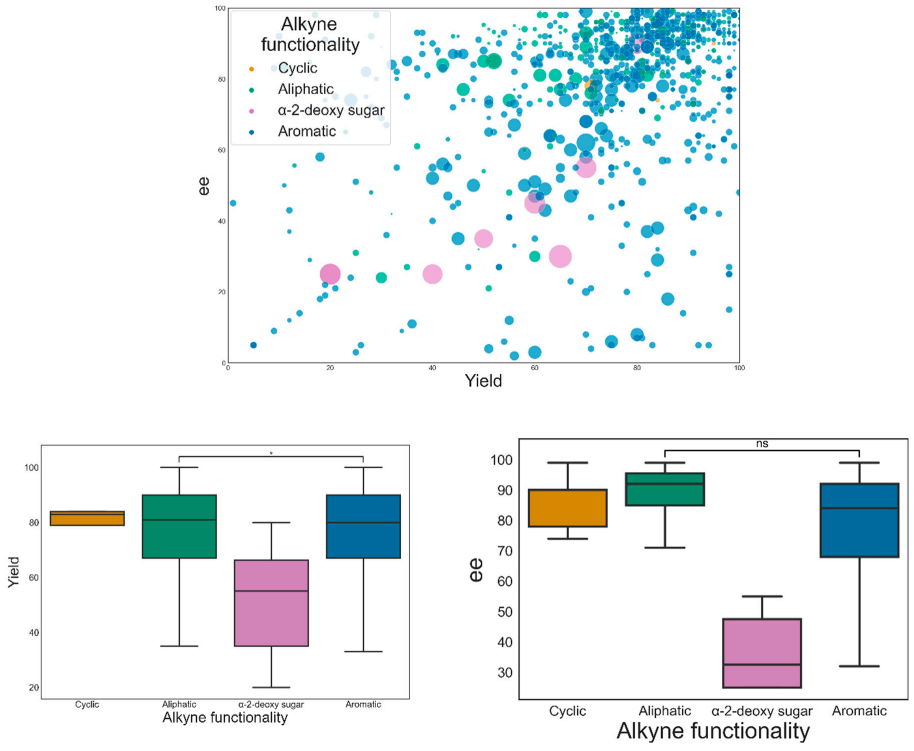

Figure 15. (**upper**) Distribution of alkynes with enantioselectivites greater than 0. (**lower**) Yield of alkynes with different functionalities. Statistical analysis was performed using Student's *t*-test ($p = 0.023$) *ee* of aldehydes with different functionalities. Statistical analysis was performed using Student's *t*-test ($p = 0.015$). Symbol Meaning: ns $p > 0.05$, * $p \leq 0.05$ (For the last two choices only).

6.5. Well-Characterised vs. In Situ

The interest in PAs originates from their chiral nature; however, only in 40% of the database has the enantioselectivity of the final product been determined. Achieving high *ee* values may result from several parameters, i.e., catalyst, substrate, solvent, temperature etc.; however, the graph of the yield and enantioselectivity as a function of the catalyst loading and solvent used supports the use of non-coordinating solvents promotes high yields and *ee*. By comparing in situ (blue) and well-characterised (brown) protocols, we determine the most popular and efficient aldehydes, amines and alkynes, projected according to their efficiency. The graph contains entries that appear more than 20 times in the knowledgeable database (Figures 16 and 17). The direct comparison of the two methods (in situ vs. well-characterised) is vague since more entries for the well-characterised protocols are required to extract a safe conclusion.

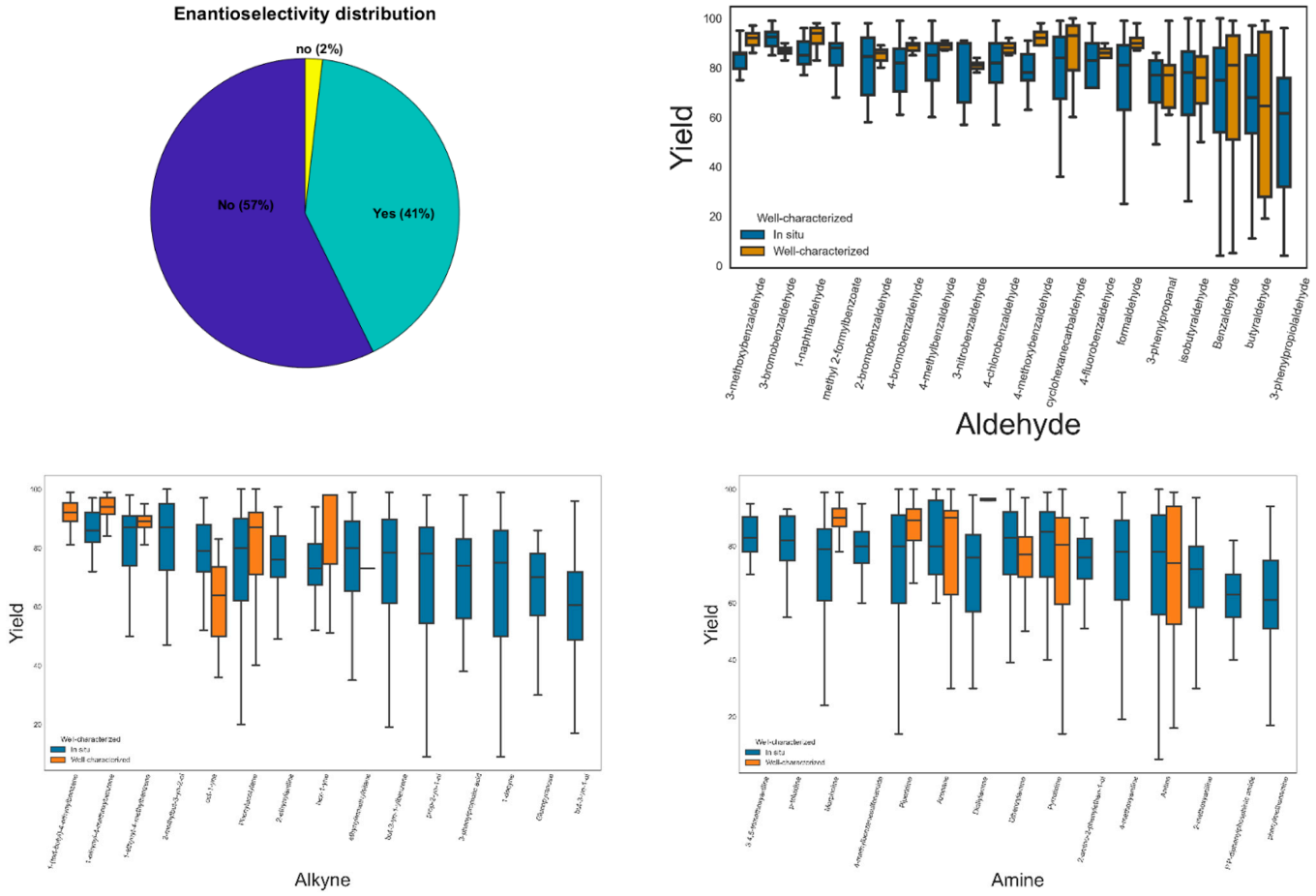

Figure 16. (**upper left**) Enantioselectivity distribution in 2376 entries. (**upper right**) Yield comparison of aldehydes between well-characterised—in situ. (**lower**) Yield comparison of alkynes between well-characterised—in situ (**left**); Yield comparison of amines between well-characterised—in situ (**right**).

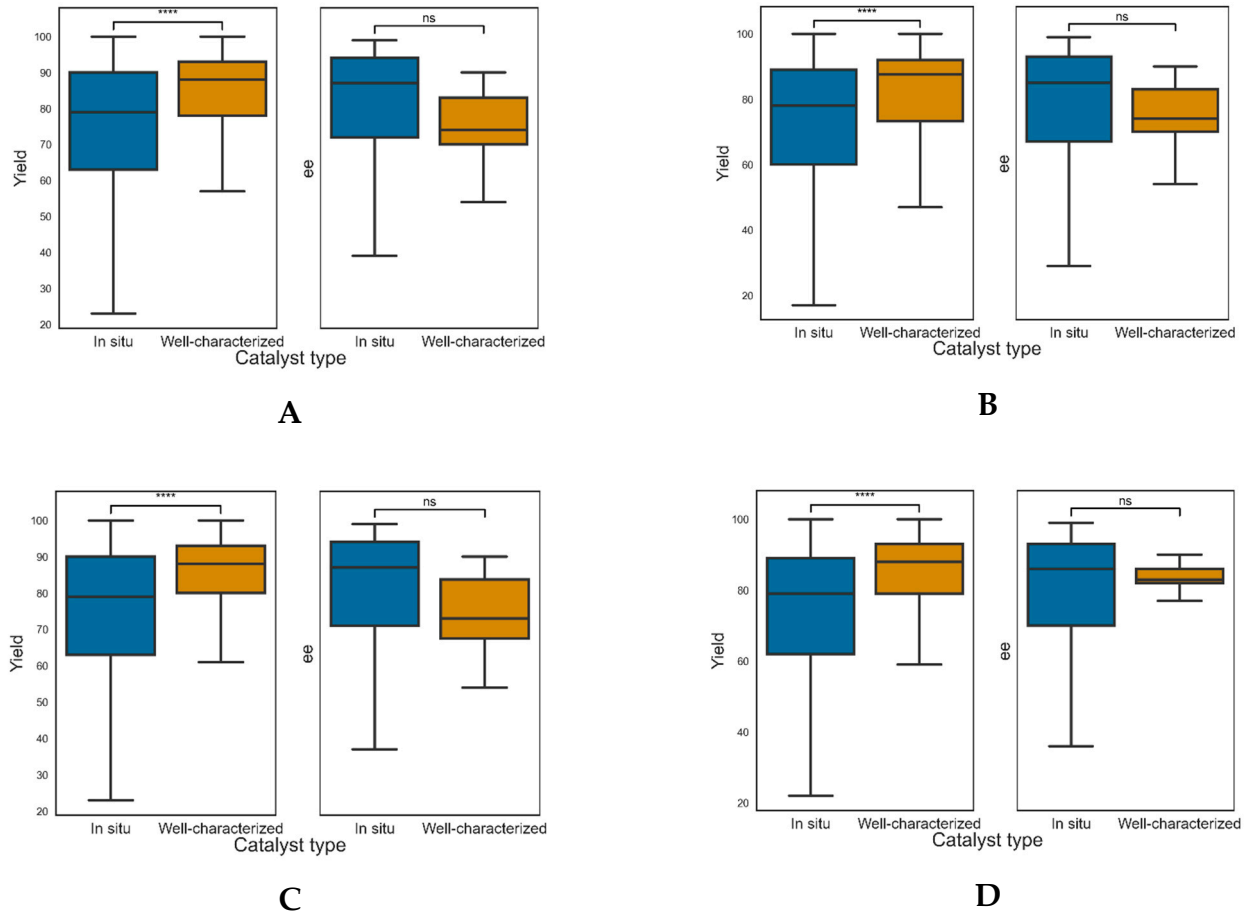

Figure 17. General comparison of yield and *ee* for well-characterised and in situ protocols. Yields and *ee* of well-characterised vs. in situ catalysts. Statistical analysis was performed using Student's *t*-test ($p = 1.47 \times 10^{-11}$, 0.58). (**A**) Aldehydes yields and *ee* of well-characterised vs. in situ catalysts. Statistical analysis was performed using Student's *t*-test ($p = 1.84 \times 10^{-7}$, 0.83). (**B**) Alkynes Yields and *ee* of well-characterised vs. in situ catalysts. Statistical analysis was performed using Student's *t*-test ($p = 8.91 \times 10^{-14}$, 0.52). (**C**) Amines Yields and *ee* of well-characterised vs. in situ catalysts. Statistical analysis performed using Student's *t*-test ($p = 1.77 \times 10^{-13}$, 0.56) (**D**). Symbol Meaning: ns $p > 0.05$, **** $p \leq 0.0001$ (For the last two choices only).

However, from a first glance, when each substrate is grouped (Figure 17B–D), it seems that yield improves significantly with the use of the well-characterised species, while in situ protocols provide higher enantioselectivities. This discrepancy may vary if more well-characterised examples are reported.

7. Summary and Concluding Remarks

The A^3 coupling reaction has become a popular organic transformation in the last two decades; interest is driven by the value of the organic scaffold and the simplicity of the catalytic protocol. For the in situ methods, by fine-tuning the number and nature of the coordinating heteroatoms in the ligand, it is now possible to obtain PAs in a highly enantioselective manner. On the other hand, for the well-characterised protocols, due to the simplicity of the method (i.e., available and inexpensive starting materials, the limited number of by-products that aid in identifying PA formation), the A^3 coupling reaction has become a model reaction on which to test the catalytic efficacy of new complexes. This review summarises all homogenous metal-based catalysed protocols that promote the A^3 coupling reaction reported until the first week of January 2021. Our meta-analysis avoids the traditional summarising method and allows immediate visualisation and under-

standing of this complex molecular transformation. We created a database that contains several variables, and its use provides some useful trends regarding the type of the catalyst, best yields, and *ee*; however, more data and systematic, especially mechanistic, studies are required to extract safe conclusions. For example, our consistent efforts in developing methods with Cu(II) well-characterised species recently provided an extraordinary protocol with low catalyst loading, and efficiency at room temperature and short time, in contrast to other reports [126]. This evidence confirms the complexity of this research problem and simultaneously indicates that several parameters, not only limited to the design/selection of the ligand (e.g., N,N, or P,N), should be considered when new catalytic systems are developed. We envisage that this paradigm will assist synthetic groups, contribute to the development of new catalyst–ligand combinations for the A^3 reaction, and pave the way for future synthetic developments and applications in other organic transformations. Moving forward, we envisage that the proper use and expansion of this classification will provide the inorganic, organic, catalytic, and synthetic communities with new knowledge to transition into a machine learning process.

Supplementary Materials: The database with the classification (excel form) can be downloaded at: https://www.mdpi.com/article/10.3390/catal12060660/s1.

Author Contributions: J.F. contacted with the literature selection and first draft of the manuscript. I.N.L. contribute with the manuscript written and corrections. G.E.K. conducted and supervised the idea and wrote the manuscript with the final corrections. All authors have read and agreed to the published version of the manuscript.

Funding: This research received no external funding.

Data Availability Statement: All data supporting this study is provided as Supplementary Information accompanying this paper.

Acknowledgments: J.F. and G.E.K. thank the University of Sussex for the International Junior Research Associate programme (IJRA, Summer 2020).

Conflicts of Interest: The authors declare no conflict of interest.

References

1. Dömling, A.; Wang, W.; Wang, K. Chemistry and Biology of Multicomponent Reactions. *Chem. Rev.* **2012**, *112*, 3083–3135. [CrossRef]
2. Elsevier, C.J.; Reedijk, J.; Walton, P.H.; Ward, M.D. Ligand Design in Coordination Chemistry: Approaches to New Catalysts, New Materials, and a More Sustainable Environment. *Dalton Trans.* **2003**, *10*, 1869–1880. [CrossRef]
3. Stradiotto, M.; Lundgren, R.J.; Buchwald, S.L.; Milstein, D. *Ligand Design in Metal Chemistry: Reactivity and Catalysis*; John Wiley & Sons: Hoboken, NJ, USA, 2016; ISBN 9781118839621.
4. Elsevier, C.J. Catalytic and Stoichiometric C-C Bond Formation Employing Palladium Compounds with Nitrogen Ligands. *Coord. Chem. Rev.* **1999**, *185–186*, 809–822. [CrossRef]
5. Sampani, S.I.; McGown, A.; Vargas, A.; Abdul-Sada, A.; Tizzard, G.J.; Coles, S.J.; Spencer, J.; Kostakis, G.E. Solvent-Free Synthesis and Key Intermediate Isolation in Ni_2Dy_2 Catalyst Development in the Domino Ring-Opening Electrocyclization Reaction of Furfural and Amines. *J. Org. Chem.* **2019**, *84*, 6858–6867. [CrossRef] [PubMed]
6. Andreou, D.; Kallitsakis, M.G.; Loukopoulos, E.; Gabriel, C.; Kostakis, G.E.; Lykakis, I.N. Copper-Promoted Regioselective Synthesis of Polysubstituted Pyrroles from Aldehydes, Amines, and Nitroalkenes via 1,2-Phenyl/Alkyl Migration. *J. Org. Chem.* **2018**, *83*, 2104–2113. [CrossRef] [PubMed]
7. Kallitsakis, M.; Loukopoulos, E.; Abdul-Sada, A.; Tizzard, G.J.; Coles, S.J.; Kostakis, G.E.; Lykakis, I.N. A Copper-Benzotriazole-Based Coordination Polymer Catalyzes the Efficient One-Pot Synthesis of (*N*′-Substituted)-Hydrazo-4-Aryl-1,4-Dihydropyridines from Azines. *Adv. Synth. Catal.* **2017**, *359*, 138–145. [CrossRef]
8. Kumar, P.; Griffiths, K.; Lymperopoulou, S.; Kostakis, G.E. Tetranuclear Zn_2 Ln_2 Coordination Clusters as Catalysts in the Petasis Borono-Mannich Multicomponent Reaction. *RSC Adv.* **2016**, *6*, 79180–79184. [CrossRef]
9. Rösler, S.; Ertl, M.; Irrgang, T.; Kempe, R. Cobalt-Catalyzed Alkylation of Aromatic Amines by Alcohols. *Angew. Chem. Int. Ed.* **2015**, *54*, 15046–15050. [CrossRef]
10. Daw, P.; Chakraborty, S.; Garg, J.A.; Ben-David, Y.; Milstein, D. Direct Synthesis of Pyrroles by Dehydrogenative Coupling of Diols and Amines Catalyzed by Cobalt Pincer Complexes. *Angew. Chem. Int. Ed.* **2016**, *55*, 14373–14377. [CrossRef]
11. Deibl, N.; Ament, K.; Kempe, R. A Sustainable Multicomponent Pyrimidine Synthesis. *J. Am. Chem. Soc.* **2015**, *137*, 12804–12807. [CrossRef]

12. Maji, M.; Kundu, S. Cooperative Ruthenium Complex Catalyzed Multicomponent Synthesis of Pyrimidines. *Dalt. Trans.* **2019**, *48*, 17479–17487. [CrossRef]
13. Zhang, M.; Fang, X.; Neumann, H.; Beller, M. General and Regioselective Synthesis of Pyrroles via Ruthenium-Catalyzed Multicomponent Reactions. *J. Am. Chem. Soc.* **2013**, *135*, 11384–11388. [CrossRef]
14. Bisai, V.; Suneja, A.; Singh, V.K. Asymmetric Alkynylation/Lactamization Cascade: An Expeditious Entry to Enantiomerically Enriched Isoindolinones. *Angew. Chem. Int. Ed.* **2014**, *53*, 10737–10741. [CrossRef]
15. Zhang, Y.; Huang, L.; Li, X.; Wang, L.; Feng, H. Chemo- and Diastereoselective Synthesis of N-Propargyl Oxazolidines through a Copper-Catalyzed Domino A^3 Reaction. *J. Org. Chem.* **2019**, *84*, 5046–5055. [CrossRef]
16. Liu, C.; Wang, G.; Wang, Y.; Pereshivko, O.P.; Peshkov, V.A. Copper-Catalyzed Reaction of Secondary Propargylamines with Ethyl Buta-2,3-Dienoate for the Synthesis of 1,6-Dihydropyridines. *European J. Org. Chem.* **2019**, *2019*, 1981–1985. [CrossRef]
17. Singh, P.; Adolfsson, D.E.; Ådén, J.; Cairns, A.G.; Bartens, C.; Brännström, K.; Olofsson, A.; Almqvist, F. Pyridine-Fused 2-Pyridones via Povarov and A^3 Reactions: Rapid Generation of Highly Functionalized Tricyclic Heterocycles Capable of Amyloid Fibril Binding. *J. Org. Chem.* **2019**, *84*, 3887–3903. [CrossRef]
18. Carmona, R.C.; Wendler, E.P.; Sakae, G.H.; Comassetoa, J.V.; Santos, A.A. Dos A^3-Coupling Reaction as a Strategy towards the Synthesis of Alkaloids. *J. Braz. Chem. Soc.* **2015**, *26*, 117–123.
19. Zhou, S.; Tong, R. Three-Step Catalytic Asymmetric Total Syntheses of 13-Methyltetrahydroprotoberberine Alkaloids. *Org. Lett.* **2017**, *19*, 1594–1597. [CrossRef]
20. Gommermann, N.; Knochel, P. Practical Highly Enantioselective Synthesis of Terminal Propargylamines. An Expeditious Synthesis of (S)-(+)-Coniine. *Chem. Commun.* **2004**, *20*, 2324–2325. [CrossRef]
21. Díez-González, S. Copper(I)–Acetylides: Access, Structure, and Relevance in Catalysis. In *Advances in Organometallic Chemistry*; Academic Press Inc.: Cambridge, MA, USA, 2016; Volume 66, pp. 93–141.
22. Yamamoto, Y.; Gridnev, I.D.; Patil, N.T.; Jin, T. Alkyne Activation with Brønsted Acids, Iodine, or Gold Complexes, and Its Fate Leading to Synthetic Application. *Chem. Commun.* **2009**, 5075–5087. [CrossRef]
23. Crabtree, R.H.; Lei, A. Introduction: CH Activation. *Chem. Rev.* **2017**, *117*, 8481–8482. [CrossRef]
24. Afewerki, S.; Córdova, A. Enamine/Transition Metal Combined Catalysis: Catalytic Transformations Involving Organometallic Electrophilic Intermediates. *Top. Curr. Chem.* **2019**, *377*, 38. [CrossRef]
25. Mukherjee, S.; Yang, J.W.; Hoffmann, S.; List, B. Asymmetric Enamine Catalysis. *Chem. Rev.* **2007**, *107*, 5471–5569. [CrossRef]
26. Erkkilä, A.; Majander, I.; Pihko, P.M. Iminium Catalysis. *Chem. Rev.* **2007**, *107*, 5416–5470. [CrossRef]
27. Zou, Y.Q.; Hörmann, F.M.; Bach, T. Iminium and Enamine Catalysis in Enantioselective Photochemical Reactions. *Chem. Soc. Rev.* **2018**, *47*, 278–290. [CrossRef]
28. Innocenti, R.; Lenci, E.; Trabocchi, A. Recent Advances in Copper-Catalyzed Imine-Based Multicomponent Reactions. *Tetrahedron Lett.* **2020**, *61*, 152083. [CrossRef]
29. Jie, X.; Shang, Y.; Chen, Z.N.; Zhang, X.; Zhuang, W.; Su, W. Differentiation between Enamines and Tautomerizable Imines in the Oxidation Reaction with TEMPO. *Nat. Commun.* **2018**, *9*, 5002. [CrossRef]
30. Létinois-Halbes, U.; Pale, P.; Berger, S. Ag NMR as a Tool for Mechanistic Studies of Ag-Catalyzed Reactions: Evidence for in Situ Formation of Alkyn-1-Yl Silver from Alkynes and Silver Salts. *J. Org. Chem.* **2005**, *70*, 9185–9190. [CrossRef]
31. Fässler, R.; Tomooka, C.S.; Frantz, D.E.; Carreira, E.M. Infrared Spectroscopic Investigations on the Metallation of Terminal Alkynes by $Zn(OTf)_2$. *Proc. Natl. Acad. Sci. USA* **2004**, *101*, 5843–5845. [CrossRef]
32. Wei, C.; Li, Z.; Li, C.J. The First Silver-Catalyzed Three-Component Coupling of Aldehyde, Alkyne, and Amine. *Org. Lett.* **2003**, *5*, 4473–4475. [CrossRef]
33. Wei, C.; Li, C.-J. A Highly Efficient Three-Component Coupling of Aldehyde, Alkyne, and Amines via C-H Activation Catalyzed by Gold in Water. *J. Am. Chem. Soc.* **2003**, *125*, 9584–9585. [CrossRef] [PubMed]
34. Li, C.J.; Wei, C. Highly Efficient Grignard-Type Imine Additions via C-H Activation in Water and under Solvent-Free Conditions. *Chem. Commun.* **2002**, *2*, 268–269. [CrossRef] [PubMed]
35. Raghuvanshi, D.S.; Singh, K.N. Highly Efficient Cadmium-Catalyzed Three-Component Coupling of an Aldehyde, Alkyne, and Amine via C-H Activation under Microwave Conditions. *Synlett* **2011**, *3*, 373–377. [CrossRef]
36. Chen, W.-W.; Bi, H.-P.; Li, C.-J. The First Cobalt-Catalyzed Transformation of Alkynyl C-H Bond: Aldehyde-Alkyne-Amine (A^3) Coupling. *Synlett* **2010**, *3*, 475–479. [CrossRef]
37. Chen, W.W.; Nguyen, R.V.; Li, C.J. Iron-Catalyzed Three-Component Coupling of Aldehyde, Alkyne, and Amine under Neat Conditions in Air. *Tetrahedron Lett.* **2009**, *50*, 2895–2898. [CrossRef]
38. Li, P.H.; Wang, L. Mercurous Chloride Catalyzed Mannich Condensation of Terminal Alkynes with Secondary Amines and Aldehydes. *Chin. J. Chem.* **2005**, *23*, 1076–1080. [CrossRef]
39. Irfana Jesin, C.P.; Nandi, G.C. Catalyst-Controlled Dual Reactivity of Sulfonimidamides: Synthesis of Propargylamines and N-Propargyl Sulfonimidamides. *Chem. Eur. J.* **2019**, *25*, 743–749. [CrossRef]
40. Samai, S.; Nandi, G.C.; Singh, M.S. An Efficient and Facile One-Pot Synthesis of Propargylamines by Three-Component Coupling of Aldehydes, Amines, and Alkynes via C-H Activation Catalyzed by $NiCl_2$. *Tetrahedron Lett.* **2010**, *51*, 5555–5558. [CrossRef]
41. Traverse, J.F.; Hoveyda, A.H.; Snapper, M.L. Enantioselective Synthesis of Propargylamines through Zr-Catalyzed Addition of Mixed Alkynylzinc Reagents to Arylimines. *Org. Lett.* **2003**, *5*, 3273–3275. [CrossRef]

42. Blay, G.; Cardona, L.; Climent, E.; Pedro, J.R. Highly Enantioselective Zinc/Binol-Catalyzed Alkynylation of N-Sulfonyl Aldimines. *Angew. Chem. Int. Ed.* **2008**, *47*, 5593–5596. [CrossRef]
43. Pinet, S.; Pandya, S.U.; Chavant, P.Y.; Ayling, A.; Vallee, Y. Dialkylzinc-Assisted Alkynylation of Nitrones. *Org. Lett.* **2002**, *4*, 1463–1466. [CrossRef]
44. Zani, L.; Alesi, S.; Cozzi, P.G.; Bolm, C. Dimethylzinc-Mediated Alkynylation of Imines. *J. Org. Chem.* **2006**, *71*, 1558–1562. [CrossRef]
45. Ying, J.; Wu, X.D.; Wang, D.; Pu, L. Catalytic Asymmetric Addition of Alkyl and Aryl Alkynes to N-(Diphenylphosphinoyl)Imines. *J. Org. Chem.* **2016**, *81*, 8900–8905. [CrossRef] [PubMed]
46. Sarode, P.B.; Bahekar, S.P.; Chandak, H.S. $Zn(OTf)_2$-Mediated Expeditious and Solvent-Free Synthesis of Propargylamines via C-H Activation of Phenylacetylene. *Synlett* **2016**, *27*, 2209–2212. [CrossRef]
47. Wei, C.; Li, C.J. Enantioselective Direct-Addition of Terminal Alkynes to Imines Catalyzed by Copper(I)Pybox Complex in Water and in Toluene. *J. Am. Chem. Soc.* **2002**, *124*, 5638–5639. [CrossRef]
48. Bariwal, J.B.; Ermolat'Ev, D.S.; Van Der Eycken, E.V. Efficient Microwave-Assisted Synthesis of Secondary Alkylproparglamines by Using A^3-Coupling with Primary Aliphatic Amines. *Chem. Eur. J.* **2010**, *16*, 3281–3284. [CrossRef]
49. Ohara, M.; Hara, Y.; Ohnuki, T.; Nakamura, S. Direct Enantioselective Three-Component Synthesis of Optically Active Propargylamines in Water. *Chem. Eur. J.* **2014**, *20*, 8848–8851. [CrossRef]
50. Ji, J.X.; Wu, J.; Chan, A.S.C. Catalytic Asymmetric Alkynylation of α-Imino Ester: A Versatile Approach to Optically Active Unnatural α-Amino Acid Derivatives. *Proc. Natl. Acad. Sci. USA* **2005**, *102*, 11196–11200. [CrossRef]
51. Dhanasekaran, S.; Kannaujiya, V.K.; Biswas, R.G.; Singh, V.K. Enantioselective A^3-Coupling Reaction Employing Chiral CuI-i PrpyboxdiPh/ N-Boc-(l)-Proline Complex under Cooperative Catalysis: Application in the Synthesis of (Indol-2-Yl)Methanamines. *J. Org. Chem.* **2019**, *84*, 3275–3292. [CrossRef]
52. Koradin, C.; Polborn, K.; Knochel, P. Enantioselective Synthesis of Propargylamines by Copper-Catalyzed Addition of Alkynes to Enamines. *Angew. Chem. Int. Ed.* **2002**, *41*, 2535–2538. [CrossRef]
53. Sreenath, K.; Yuan, Z.; Macias-Contreras, M.; Ramachandran, V.; Clark, R.J.; Zhu, L. Dual Role of Acetate in Copper(II) Acetate Catalyzed Dehydrogenation of Chelating Aromatic Secondary Amines: A Kinetic Case Study of Copper-Catalyzed Oxidation Reactions. *Eur. J. Inorg. Chem.* **2016**, *2016*, 3728–3743. [CrossRef]
54. Park, K.; Heo, Y.; Lee, S. Metal-Free Decarboxylative Three-Component Coupling Reaction for the Synthesis of Propargylamines. *Org. Lett.* **2013**, *15*, 3322–3325. [CrossRef] [PubMed]
55. Loukopoulos, E.; Kallitsakis, M.; Tsoureas, N.; Abdul-Sada, A.; Chilton, N.F.; Lykakis, I.N.; Kostakis, G.E. Cu(II) Coordination Polymers as Vehicles in the A^3 Coupling. *Inorg. Chem.* **2017**, *56*, 4898–4910. [CrossRef] [PubMed]
56. Yu, C.X.; Hu, F.L.; Liu, M.Y.; Zhang, C.W.; Lv, Y.H.; Mao, S.K.; Liu, L.L. Construction of Four Copper Coordination Polymers Derived from a Tetra-Pyridyl-Functionalized Calix[4]Arene: Synthesis, Structural Diversity, and Catalytic Applications in the A^3 (Aldehyde, Alkyne, and Amine) Coupling Reaction. *Cryst. Growth Des.* **2017**, *17*, 5441–5448. [CrossRef]
57. Li, P.; Liu, Y.; Wang, L.; Xiao, J.; Tao, M. Copper(II)-Schiff Base Complex-Functionalized Polyacrylonitrile Fiber as a Green Efficient Heterogeneous Catalyst for One-Pot Multicomponent Syntheses of 1,2,3-Triazoles and Propargylamines. *Adv. Synth. Catal.* **2018**, *360*, 1673–1684. [CrossRef]
58. Naeimi, H.; Moradian, M. Copper(I)-N_2S_2-Salen Type Complex Covalently Anchored onto MCM-41 Silica: An Efficient and Reusable Catalyst for the A^3-Coupling Reaction toward Propargylamines. *Appl. Organomet. Chem.* **2013**, *27*, 300–306. [CrossRef]
59. McDonagh, C.; O'Conghaile, P.; Klein Gebbink, R.J.M.; O'Leary, P. Electrostatic Immobilisation of Copper(I) and Copper(II) Bis(Oxazolinyl)Pyridine Catalysts on Silica: Application to the Synthesis of Propargylamines via Direct Addition of Terminal Alkynes to Imines. *Tetrahedron Lett.* **2007**, *48*, 4387–4390. [CrossRef]
60. Chen, G.J.; Chen, C.Q.; Li, X.T.; Ma, H.C.; Dong, Y. Bin Cu_3L_2 Metal-Organic Cages for A^3-Coupling Reactions: Reversible Coordination Interaction Triggered Homogeneous Catalysis and Heterogeneous Recovery. *Chem. Commun.* **2018**, *54*, 11550–11553. [CrossRef]
61. Sun, W.J.; Gao, E.Q. MIL-101 Supported Highly Active Single-Site Metal Catalysts for Tricomponent Coupling. *Appl. Catal. A Gen.* **2019**, *569*, 110–116. [CrossRef]
62. Sun, W.J.; Xi, F.G.; Pan, W.L.; Gao, E.Q. MIL-101(Cr)-SO_3Ag: An Efficient Catalyst for Solvent-Free A^3 Coupling Reactions. *J. Mol. Catal. A Chem.* **2016**, *430*, 36–42. [CrossRef]
63. Li, Z.; Jiang, Z.; Su, W. Fast, Solvent-Free, Highly Enantioselective Three-Component Coupling of Aldehydes, Alkynes, and Amines Catalysed by the Copper(II)Pybox Complex under High-Vibration Ball-Milling. *Green Chem.* **2015**, *17*, 2330–2334. [CrossRef]
64. Sagadevan, A.; Pampana, V.K.K.; Hwang, K.C. Copper Photoredox Catalyzed $A^{3'}$ Coupling of Arylamines, Terminal Alkynes, and Alcohols through a Hydrogen Atom Transfer Process. *Angew. Chem. Int. Ed.* **2019**, *58*, 3838–3842. [CrossRef]
65. Karthikeyan, P.; Arunrao, A.S.; Narayan, M.P.; Kumar, S.; Kumar, S.S.; Bhagat, P.R. Novel 1-Glycyl-3-Methyl Imidazolium Chloride-Iron(III) Complex for Synthesis of Propargylamines. *Asian J. Chem.* **2012**, *24*, 4285–4289.
66. Esfandiary, N.; Pazoki, F.; Nakisa, A.; Azizi, K.; Radfar, I.; Heydari, A. Silver Chloride Supported on Vitamin B_1 -Organometallic Magnetic Catalyst: Synthesis, Density Functional Theory Study and Application in A^3-Coupling Reactions. *Appl. Organomet. Chem.* **2020**, *34*, e5725. [CrossRef]

67. Mirabedini, M.; Motamedi, E.; Kassaee, M.Z. Magnetic CuO Nanoparticles Supported on Graphene Oxide as an Efficient Catalyst for A^3-Coupling Synthesis of Propargylamines. *Chin. Chem. Lett.* **2015**, *26*, 1085–1090. [CrossRef]
68. Paioti, P.H.S.; Abboud, K.A.; Aponick, A. Incorporation of Axial Chirality into Phosphino-Imidazoline Ligands for Enantioselective Catalysis. *ACS Catal.* **2017**, *7*, 2133–2138. [CrossRef]
69. Cardoso, F.S.P.; Abboud, K.A.; Aponick, A. Design, Preparation, and Implementation of an Imidazole-Based Chiral Biaryl P,N-Ligand for Asymmetric Catalysis. *J. Am. Chem. Soc.* **2013**, *135*, 14548–14551. [CrossRef]
70. Dube, H.; Gommermann, N.; Knochel, P. Synthesis of Chiral α-Aminoalkylpyrimidines Using an Enantioselective Three-Component Reaction. *Synthesis* **2004**, *4*, 2015–2025. [CrossRef]
71. Rokade, B.V.; Guiry, P.J. Diastereofacial π-Stacking as an Approach to Access an Axially Chiral P,N-Ligand for Asymmetric Catalysis. *ACS Catal.* **2017**, *7*, 2334–2338. [CrossRef]
72. Zhao, C.; Seidel, D. Enantioselective A^3 Reactions of Secondary Amines with a Cu(I)/Acid-Thiourea Catalyst Combination. *J. Am. Chem. Soc.* **2015**, *137*, 4650–4653. [CrossRef]
73. Lauder, K.; Toscani, A.; Scalacci, N.; Castagnolo, D. Synthesis and Reactivity of Propargylamines in Organic Chemistry. *Chem. Rev.* **2017**, *117*, 14091–14200. [CrossRef] [PubMed]
74. Jesin, I.; Nandi, G.C. Recent Advances in the A^3 Coupling Reactions and Their Applications. *Eur. J. Org. Chem.* **2019**, *2019*, 2704–2720. [CrossRef]
75. Peshkov, V.A.; Pereshivko, O.P.; Van der Eycken, E.V. A Walk around the A^3-Coupling. *Chem. Soc. Rev.* **2012**, *41*, 3790–3807. [CrossRef] [PubMed]
76. Wei, C.; Li, Z.; Li, C.J. The Development of A^3-Coupling (Aldehyde-Alkyne-Amine) and AA^3-Coupling (Asymmetric Aldehyde-Alkyne-Amine). *Synlett* **2004**, *2004*, 1472–1483. [CrossRef]
77. Rokade, B.V.; Barker, J.; Guiry, P.J. Development of and Recent Advances in Asymmetric A^3 Coupling. *Chem. Soc. Rev.* **2019**, *48*, 4766–4790. [CrossRef]
78. Dong, K.; Liu, M.; Xu, X.; Dong, K.; Liu, M.; Xu, X. Recent Advances in Catalytic Alkyne Transformation via Copper Carbene Intermediates. *Molecules* **2022**, *27*, 3088. [CrossRef]
79. Shah, S.; Das, B.G.; Singh, V.K. Recent Advancement in Copper-Catalyzed Asymmetric Reactions of Alkynes. *Tetrahedron* **2021**, *93*, 132238. [CrossRef]
80. Syeda Huma, H.Z.; Halder, R.; Singh Kalra, S.; Das, J.; Iqbal, J. Cu(I)-Catalyzed Three Component Coupling Protocol for the Synthesis of Quinoline Derivatives. *Tetrahedron Lett.* **2002**, *43*, 6485–6488. [CrossRef]
81. Gurubrahamam, R.; Periasamy, M. Copper(I) Halide Promoted Diastereoselective Synthesis of Chiral Propargylamines and Chiral Allenes Using 2-Dialkylaminomethylpyrrolidine, Aldehydes, and 1-Alkynes. *J. Org. Chem.* **2013**, *78*, 1463–1470. [CrossRef]
82. Zhang, Y.; Feng, H.; Liu, X.; Huang, L. A Highly Chemoselective Synthesis of Cyclic Divalent Propargylamines by Copper-Catalyzed Annulation/Double A^3-Couplings. *Eur. J. Org. Chem.* **2018**, *2018*, 2039–2046. [CrossRef]
83. Feng, H.; Zhang, Y.; Zhang, Z.; Chen, F.; Huang, L. Copper-Catalyzed Annulation/A^3-Coupling Cascade: Diastereodivergent Synthesis of Sterically Hindered Monocyclic Oxazolidines Bearing Multiple Stereocenters. *Eur. J. Org. Chem.* **2019**, 1931–1939. [CrossRef]
84. Choi, Y.J.; Jang, H.Y. Copper-Catalyzed A^3-Coupling: Synthesis of 3-Amino-1,4-Diynes. *Eur. J. Org. Chem.* **2016**, *2016*, 3047–3050. [CrossRef]
85. Lim, J.; Park, K.; Byeun, A.; Lee, S. Copper-Catalyzed Decarboxylative Coupling Reactions for the Synthesis of Propargyl Amines. *Tetrahedron Lett.* **2014**, *55*, 4875–4878. [CrossRef]
86. Meyet, C.E.; Pierce, C.J.; Larsen, C.H. A Single Cu(II) Catalyst for the Three-Component Coupling of Diverse Nitrogen Sources with Aldehydes and Alkynes. *Org. Lett.* **2012**, *14*, 964–967. [CrossRef]
87. Martinez-Amezaga, M.; Giordano, R.A.; Prada Gori, D.N.; Permingeat Squizatto, C.; Giolito, M.V.; Scharovsky, O.G.; Rozados, V.R.; Rico, M.J.; Mata, E.G.; Delpiccolo, C.M.L. Synthesis of Propargylamines: Via the A^3 Multicomponent Reaction and Their Biological Evaluation as Potential Anticancer Agents. *Org. Biomol. Chem.* **2020**, *18*, 2475–2486. [CrossRef]
88. Huang, B.; Yao, X.; Li, C.J. Diastereoselective Synthesis of α-Oxyamines via Gold-, Silver- and Copper-Catalyzed, Three-Component Couplings of α-Oxyaldehydes, Alkynes, and Amines in Water. *Adv. Synth. Catal.* **2006**, *348*, 1528–1532. [CrossRef]
89. Zhang, X.; Corma, A. Supported Gold(III) Catalysts for Highly Efficient Three-Component Coupling Reactions. *Angew. Chem. Int. Ed.* **2008**, *47*, 4358–4361. [CrossRef]
90. Li, P.; Zhang, Y.; Wang, L. Iron-Catalyzed Ligand-Free Three-Component Coupling Reactions of Aldehydes, Terminal Alkynes, and Amines. *Chem. Eur. J.* **2009**, *15*, 2045–2049. [CrossRef]
91. Colombo, F.; Benaglia, M.; Orlandi, S.; Usuelli, F.; Celentano, G. Very Mild, Enantioselective Synthesis of Propargylamines Catalyzed by Copper(I)-Bisimine Complexes. *J. Org. Chem.* **2006**, *71*, 2064–2070. [CrossRef]
92. Benaglia, M.; Negri, D.; Dell'Anna, G. Enantioselective Addition of Phenyl and Alkyl Acetylenes to Imines Catalyzed by Chiral Cu(I) Complexes. *Tetrahedron Lett.* **2004**, *45*, 8705–8708. [CrossRef]
93. Hatano, M.; Asai, T.; Ishihara, K. Enantioselective Alkynylation to Aldimines Catalyzed by Chiral 2,2′-Di(2-Aminoaryloxy)-1,1′-Binaphthyl-Copper(I) Complexes. *Tetrahedron Lett.* **2008**, *49*, 379–382. [CrossRef]
94. Liu, J.; Liu, B.; Jia, X.; Li, X.; Chan, A.S.C. Asymmetric Addition of Alkynes to Imines in Water Catalyzed with a Recyclable Cu(I)-Bis(Oxazoline) and Stearic Acid System. *Tetrahedron Asymmetry* **2007**, *18*, 396–399. [CrossRef]

95. Bisai, A.; Singh, V.K. Enantioselective One-Pot Three-Component Synthesis of Propargylamines. *Org. Lett.* **2006**, *8*, 2405–2408. [CrossRef] [PubMed]
96. Irmak, M.; Boysen, M.M.K. A New Pyridyl Bis(Oxazoline) Ligand Prepared from D-Glucosamine for Asymmetric Alkynylation of Imines. *Adv. Synth. Catal.* **2008**, *350*, 403–405. [CrossRef]
97. Nakamura, S.; Ohara, M.; Nakamura, Y.; Shibata, N.; Toru, T. Copper-Catalyzed Enantioselective Three-Component Synthesis of Optically Active Propargylamines from Aldehydes, Amines, and Aliphatic Alkynes. *Chem. Eur. J.* **2010**, *16*, 2360–2362. [CrossRef] [PubMed]
98. Lu, Y.; Johnstone, T.C.; Arndtsen, B.A. Hydrogen-Bonding Asymmetric Metal Catalysis with α-Amino Acids: A Simple and Tunable Approach to High Enantioinduction. *J. Am. Chem. Soc.* **2009**, *131*, 11284–11285. [CrossRef] [PubMed]
99. Gommermann, N.; Koradin, C.; Polborn, K.; Knochel, P. Enantioselective, Copper(I)-Catalyzed Three-Component Reaction for the Preparation of Propargylamines. *Angew. Chem. Int. Ed.* **2003**, *42*, 5763–5766. [CrossRef]
100. Knoepfel, T.F.; Aschwanden, P.; Ichikawa, T.; Watanabe, T.; Carreira, E.M. Readily Available Biaryl P,N Ligands for Asymmetric Catalysis. *Angew. Chem. Int. Ed.* **2004**, *43*, 5971–5973. [CrossRef]
101. Aschwanden, P.; Stephenson, C.R.J.; Carreira, E.M. Highly Enantioselective Access to Primary Propargylamines: 4-Piperidinone as a Convenient Protecting Group. *Org. Lett.* **2006**, *8*, 2437–2440. [CrossRef]
102. Paioti, P.H.S.; Abboud, K.A.; Aponick, A. Catalytic Enantioselective Synthesis of Amino Skipped Diynes. *J. Am. Chem. Soc.* **2016**, *138*, 2150–2153. [CrossRef]
103. Rokade, B.V.; Guiry, P.J. Enantioselective Catalytic Asymmetric A^3 Coupling with Phosphino-Imidazoline Ligands. *J. Org. Chem.* **2019**, *84*, 5763–5772. [CrossRef]
104. Liu, Q.; Xu, H.; Li, Y.; Yao, Y.; Zhang, X.; Guo, Y.; Ma, S. Pyrinap Ligands for Enantioselective Syntheses of Amines. *Nat. Commun.* **2021**, *12*, 19. [CrossRef]
105. Lo, V.K.Y.; Liu, Y.; Wong, M.K.; Che, C.M. Gold(III) Salen Complex-Catalyzed Synthesis of Propargylamines via a Three-Component Coupling Reaction. *Org. Lett.* **2006**, *8*, 1529–1532. [CrossRef]
106. Liu, B.; Huang, L.; Liu, J.; Zhong, Y.; Li, X.; Chan, A.S.C. Chiral Cu(II) Complex Catalyzed Enantioselective Addition of Phenylacetylene to N-Aryl Arylimines. *Tetrahedron Asymmetry* **2007**, *18*, 2901–2904. [CrossRef]
107. Thakur, K.; Khare, N.K. Copper Mediated A^3-Coupling Reaction for the Preparation of Enantioselective Deoxy Sugar Based Chiral Propargylamines Using Bifunctional Ligand L-Proline. *Carbohydr. Res.* **2020**, *494*, 108053. [CrossRef]
108. Naeimi, H.; Moradian, M. Thioether-Based Copper(I) Schiff Base Complex as a Catalyst for a Direct and Asymmetric A^3-Coupling Reaction. *Tetrahedron Asymmetry* **2014**, *25*, 429–434. [CrossRef]
109. Hopkinson, M.N.; Richter, C.; Schedler, M.; Glorius, F. An Overview of N-Heterocyclic Carbenes. *Nature* **2014**, *510*, 485–496. [CrossRef]
110. Li, P.; Wang, L.; Zhang, Y.; Wang, M. Highly Efficient Three-Component (Aldehyde–Alkyne–Amine) Coupling Reactions Catalyzed by a Reusable PS-Supported NHC–Ag(I) under Solvent-Free Reaction Conditions. *Tetrahedron Lett.* **2008**, *49*, 6650–6654. [CrossRef]
111. Chen, M.-T.; Landers, B.; Navarro, O. Well-Defined (N-Heterocyclic Carbene)-Ag(i) Complexes as Catalysts for A^3 Reactions. *Org. Biomol. Chem.* **2012**, *10*, 2206–2208. [CrossRef]
112. Mariconda, A.; Sirignano, M.; Costabile, C.; Longo, P. New NHC- Silver and Gold Complexes Active in A^3-Coupling (Aldehyde-Alkyne-Amine) Reaction. *Mol. Catal.* **2020**, *480*, 110570. [CrossRef]
113. Li, Y.; Chen, X.; Song, Y.; Fang, L.; Zou, G. Well-Defined N-Heterocyclic Carbene Silver Halides of 1-Cyclohexyl-3- Arylmethylimidazolylidenes: Synthesis, Structure and Catalysis in A^3-Reaction of Aldehydes, Amines and Alkynes. *Dalt. Trans.* **2011**, *40*, 2046–2052. [CrossRef]
114. Zhao, Y.; Zhou, X.; Okamura, T.A.; Chen, M.; Lu, Y.; Sun, W.Y.; Yu, J.Q. Silver Supramolecule Catalyzed Multicomponent Reactions under Mild Conditions. *Dalton Trans.* **2012**, *41*, 5889–5896. [CrossRef]
115. Chen, H.-B.; Zhao, Y.; Liao, Y. Aldehyde-Alkyne-Amine (A^3) Coupling Catalyzed by a Highly Efficient Dicopper Complex. *RSC Adv.* **2015**, *5*, 37737–37741. [CrossRef]
116. Rosales, J.; Garcia, J.M.; Ávila, E.; González, T.; Coll, D.S.; Ocando-Mavárez, E. A Novel Tetramer Copper(I) Complex Containing Diallylphosphine Ligands: Synthesis, Characterization and Catalytic Application in A^3-Coupling (Aldehyde-Amine-Alkyne) Reactions. *Inorg. Chim. Acta* **2017**, *467*, 155–162. [CrossRef]
117. Alfonso, S.; González, S.; Higuera-Padilla, A.R.; Vidal, A.; Fernández, M.; Taylor, P.; Urdanibia, I.; Reiber, A.; Otero, Y.; Castro, W. A New Complex of Copper-Phosphole. Synthesis, Characterization and Evaluation of Biological Activity. *Inorg. Chim. Acta* **2016**, *453*, 538–546. [CrossRef]
118. Cammarata, J.R.; Rivera, R.; Fuentes, F.; Otero, Y.; Ocando-Mavárez, E.; Arce, A.; Garcia, J.M. Single and Double A^3-Coupling (Aldehyde-Amine-Alkyne) Reaction Catalyzed by an Air Stable Copper(I)-Phosphole Complex. *Tetrahedron Lett.* **2017**, *58*, 4078–4081. [CrossRef]
119. Prat, D.; Hayler, J.; Wells, A. A Survey of Solvent Selection Guides. *Green Chem.* **2014**, *16*, 4546–4551. [CrossRef]
120. Loukopoulos, E.; Abdul-Sada, A.; Viseux, E.M.E.; Lykakis, I.N.; Kostakis, G.E. Structural Diversity and Catalytic Properties in a Family of Ag(I)-Benzotriazole Based Coordination Compounds. *Cryst. Growth Des.* **2018**, *18*, 5638–5651. [CrossRef]

121. Peewasan, K.; Merkel, M.P.; Fuhr, O.; Anson, C.E.; Powell, A.K. A Multifunctional Use of Bis(Methylene)Bis(5-Bromo-2-Hydroxyl Salicyloylhydrazone): From Metal Sensing to Ambient Catalysis of A^3 Coupling Reactions. *RSC Adv.* **2020**, *10*, 40739–40744. [CrossRef] [PubMed]
122. Sampani, S.I.; Zdorichenko, V.; Danopoulou, M.; Leech, M.C.; Lam, K.; Abdul-Sada, A.; Cox, B.; Tizzard, G.J.; Coles, S.J.; Tsipis, A.; et al. Shedding Light on the Use of Cu(II)-Salen Complexes in the A^3 Coupling Reaction. *Dalton Trans.* **2020**, *49*, 289–299. [CrossRef] [PubMed]
123. Agrahari, B.; Layek, S.; Ganguly, R.; Pathak, D.D. Synthesis and Crystal Structures of Salen-Type Cu(II) and Ni(II) Schiff Base Complexes: Application in [3+2]-Cycloaddition and A^3-Coupling Reactions. *New J. Chem.* **2018**, *42*, 13754–13762. [CrossRef]
124. Singh, A.; Maji, A.; Mohanty, A.; Ghosh, K. Copper-Based Catalysts Derived from Salen-Type Ligands: Synthesis of 5-Substituted-1: H-Tetrazoles via [3+2] Cycloaddition and Propargylamines via A^3-Coupling Reactions. *New J. Chem.* **2020**, *44*, 18399–18418. [CrossRef]
125. Sampani, S.I.; Zdorichenko, V.; Devonport, J.; Rossini, G.; Leech, M.C.; Lam, K.; Cox, B.; Abdul-Sada, A.; Vargas, A.; Kostakis, G.E. Structural and Electronic Control of 1-(2-pyridyl)Benzotriazole Bidentate Ligand in Copper Chemistry with Application to Catalysis in the A^3 Coupling Reaction. *Chem. Eur. J.* **2021**, *27*, 4394–4400. [CrossRef]
126. Devonport, J.; Sully, L.; Boudalis, A.K.; Hassell-Hart, S.; Leech, M.C.; Lam, K.; Abdul-Sada, A.; Tizzard, G.J.; Coles, S.J.; Spencer, J.; et al. Room Temperature Cu(II) Radical-Triggered Alkyne C-H Activation. *JACS Au* **2021**, *1*, 1937–1948. [CrossRef]